Feasibility Of Using An Industrial Robot With The LODOX Technology

BY

Gregory Henry Flash

Submitted to the Faculty of Health Sciences at
the University of Cape Town in partial fulfillment of the requirements for the degree of
Master of Science in Medicine in Biomedical Engineering.

March 2002
Cape Town, South Africa

Declaration

Feasibility Of Using An Industrial Robot With The LODOX Technology:

I, GREGORY HENRY FLASH, hereby declare that:

(a) the above thesis is my own unaided work , both in concept and execution, and that apart from the normal guidance from my supervisor, I have received no assistance except as stated below:

(b) except as stated below, neither the substance nor any part of the above thesis has been submitted in the past, or is being, or is to be submitted for a degree at the University of Cape Town or any other university.

The thesis has been presented by me for examination for the degree of Master of Science in Medicine in Biomedical Engineering.

_____

Signature

_____

Date

Acknowledgements

I wish to thank the following people for their assistance and guidance:

Professor C.L. Vaughan, Hyman Goldberg Professor of Biomedical Engineering, University of Cape Town, for his constant guidance and encouragement as thesis supervisor.

African Medical Imaging for funding this project.

Mr Cuan Van Aswegen, Mr John Markus and Mr Jan Van Der Merwe, for building and designing many of the electrical and mechanical components needed to complete this project.

Mr Nick Schreeuder, for all his input concerning the robot at the National Accelerator Centre.

Mr Steffen Schanz, fellow student who assisted in many of the accuracy tests on the robot at the National Accelerator Centre.

Dr David Boonzaier, for his knowledge of medical robots and robotics.

Mr Paul Van Looy of De Beers, for his in-depth mechanical knowledge of the LODOX technology.

My fellow students in the Biomedical Engineering Department, for their innovative ideas and support.

Mr Jacob Lagendyk and Mr Ben Wright of African Medical Imaging, for their input in the risk analysis of the LODOX-LACT machine.

Ms Judy Sacks my partner and friend, for always supporting me in all my endeavours.

Abstract

DebTech Pty(LTD), a subsidiary of De Beers South Africa, has designed a low dosage digital X-ray machine called LODOX. This innovative machine has been commissioned in Groote Schuur Hospital in Cape Town, South Africa. It is capable of performing standard radiological scans, producing high quality images quickly and in a digital form.

It is planned that Computed Tomography (CT) and screening for Tuberculosis (TB) will be incorporated into future LODOX machines' capabilities. To this end the mechanics, electronics and software will have to be redesigned. This project was concerned only with the design of the mechanics of a future machine. An alternative option to redesigning the mechanics of the existing machine is to make use of an industrial robot such as the MOTOMAN SK150 instead. Motivations in favour of the robot included: the robot has many degrees-of-freedom, and hence any type of movement can be achieved; utilising an off-the-shelf industrial robot could be more cost effective than redesigning the mechanics of the existing machine; the robot conforms to international safety standards, and therefore certification of a LODOX machine incorporating such a robot may be relatively simple to achieve.

This project was therefore a feasibility study to determine the suitability of utilising an industrial robot to enhance the capabilities of future LODOX machines. The feasibility study incorporated the aspects of simulation, accuracy and safety to come to a conclusion.

Simulation software and a model of part of the existing LODOX machine were used to simulate the movements of different types of scans. From these simulations, important issues including the benefits of using simulation software, potential cabling (electrical and cooling) problems and the weight restrictions of the robot were discov-

ered. These issues would have a bearing on the design of such a machine in the future.

The accuracy of the robot was evaluated in terms of repetitive positioning, linear movement and constant velocity. This accuracy was compared to that of the present LODOX machine in an effort to determine if image quality would be compromised by using the robot. Various accuracy measurement techniques were used to achieve this. The results of the accuracy analysis revealed that on the whole, the robot was less accurate than LODOX. For the robot, the repetitive positioning accuracy was $< \pm 1\text{mm}$, while the linear movement accuracy was $\leq \pm 0.5\text{mm}$. Equivalent accuracies for LODOX were not determined, as it was assumed that due to the high quality images produced, these accuracies were perfect or very small. Constant velocity accuracy tests were conducted on both the robot and the LODOX machine using three different measurement techniques (with three different data capture rates). The values measured were inconsistent from one measurement technique to another. All that could be concluded was that LODOX had a more constant velocity accuracy than the robot.

The last aspect of the thesis concerned the issue of safety. The utilisation of an industrial robot in a medical environment raises many questions about the safety of clinicians and patients interacting with such a machine. This issue was investigated through looking at the literature on the subject, assessing relevant safety standards and performing a risk analysis of the present LODOX machine. The results of the safety assessment were a set of proposed safeguards and safety strategies that aimed to create a machine that was as safe as possible.

In conclusion, the incorporation of an industrial robot into a future LODOX machine was found to be feasible. However it is recommended that further accuracy measurements be made, a more in depth safety strategy be developed, and a detailed cost analysis be completed before such a machine enters the design stage of development.

Table Of Contents

List of Figures

List of Tables

Nomenclature

ANSI American National Standards Institute

CAD Computer Aided Design

CAS Computer Assisted Surgery

CCD Charged Coupled Device

CE European Union

CT Computed Tomography

CV Constant Velocity

EMI Electro Magnetic Interference

FDA United States Food and Drug Administration

FFT Fast Fourier Transform

FMEA Failure Mode and Effect Analysis

FMECA Failure Modes, Effects and Criticality Analysis

GPS Global Positioning System

GUI Graphical User Interface

ISO International Standards Organisation

LM Linear Movement

LODOX LOw DOsage X-ray

LODOX-LACT LOw DOsage X-ray - Limited Angle Computed Tomography

LODOX-MP LOw DOsage X-ray - Medical Prototype

LPC Local Positioning Console

LR LODOX-Robot

MIS Minimally Invasive Surgery

MRC Manual Robot Controller

MRI Magnetic Resonance Imaging

NAC National Accelerator Centre

NIST United States National Institute of Standards and Technology

OSHA Occupational Safety & Health Administration

PC Personal Computer

PLC Programmable Logic Controller

RCS Reference Co-ordinate System

RIA Robotic Industries Association

ROTSY Robot Off-line Teaching System of Yasakawa

RP Repetitive Positioning

SAE United States Society of Automobile Engineers

SCARA Selective Compliant Assembly Robot Arm

TB Tuberculosis

TCP Tool Centre Point

UPS Uninterruptable Power Supply

VI Virtual Instrument

Chapter 1

Introduction

DebTech Pty (Ltd), a subsidiary of De Beers South Africa, has developed a technique for producing high definition digital X-ray images with greatly reduced radiation dose. They designed, built and supplied the LOw DOsage X-ray - Medical Prototype (LODOX-MP) machine which was installed in the Trauma Unit of Groote Schuur Hospital Cape Town, in June 1999. A later model, LOw DOsage X-ray - Limited Angle Computed Tomography (LODOX-LACT) was commissioned in the Faculty of Health Sciences, University of Cape Town, during April 2001. A key feature of these machines is that they are able to produce high definition full body X-ray images in only 15 seconds, and at a significantly lower radiation dose to the patient (as compared to similar resolution images captured on standard X-ray machines).

The LOw DOsage X-ray (LODOX) machine consists of an *ionizing X-radiation emitting tube* and a *Charged Coupled Device (CCD) detector* mounted on a C-arm. This C-arm is connected via a support housing to a base frame, and the base frame is attached to the floor and/or ceiling. A patient trolley specially designed for the LODOX machine then docks with the base frame.

The LODOX machine takes an X-ray by emitting a fan beam while the C-arm moves along the length of the trolley. The image is captured by the detector using the technique of *Time Delayed Integration*. The images are then reconstructed by the Image Preprocessor computer and are displayed on the Diagnostic Viewing Station computer.

1.1 Definition of Problem

LODOX-MP is a X-ray machine capable of various conventional scans including: antero-posterior, lateral, Trendelenberg and erect chest. In order to capture these scans, the C-arm of the LODOX machine moves along the long axis of the trolley driven by a linear motor mounted on the back frame. For lateral and erect chest scans the C-arm rotates around the long axis of the trolley. This was initially achieved via a chain drive, which has been superseded by a belt drive for greater accuracy and smoother rotation. In addition, the trolley can be raised and lowered manually, giving the LODOX machine three degrees freedom of movement (Figure 1.1). To perform the Trendelenberg scan the trolley can be tilted by raising or lowering either end of the trolley, giving a limited fourth degree of freedom to the machine.

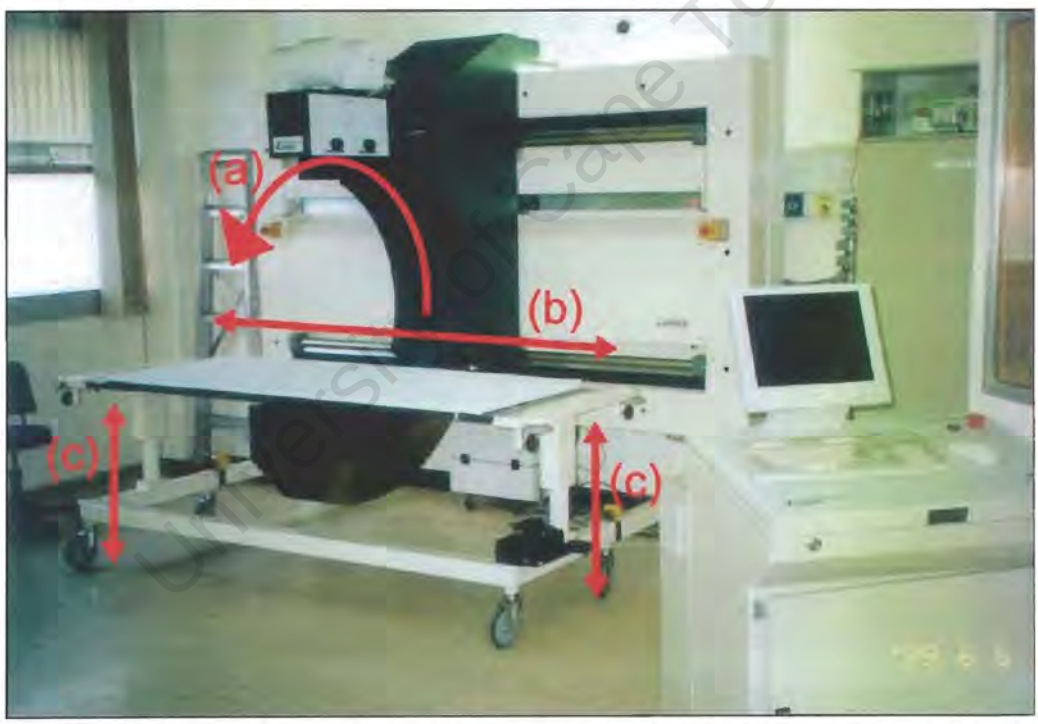

Figure 1.1: The three degrees freedom of movement of LODOX: (a) around the long axis of the trolley, (b) along the long axis of the trolley and (c) raising and lowering the ends of the trolley.

In order for the LODOX technology to be used for other applications such as Computed Tomography (CT) or Tuberculosis (TB) scanning, more degrees-of-freedom may be required, and hence the mechanics of the machine may have to be re-

designed. An alternative option is to use an industrial robot. Motivations for using such an industrial robot are threefold:

1. The robot under investigation, the MOTOMAN SK150, has six degrees of freedom (Figure 1.2). Hence almost any type of movements can be achieved, although only four degrees of freedom are probably all that would be required for most types of scanning.

2. The use of an off-the-shelf industrial robot would possibly alleviate the need for the lengthy and costly research and development process in redesigning the mechanics of the LODOX machine. The cost of the robot may be comparable to the cost of the mechanics of the present LODOX machines.

3. The robot is certified and conforms to standards of international regulatory bodies, and hence there may be a reduction in the time and cost of testing for safety.

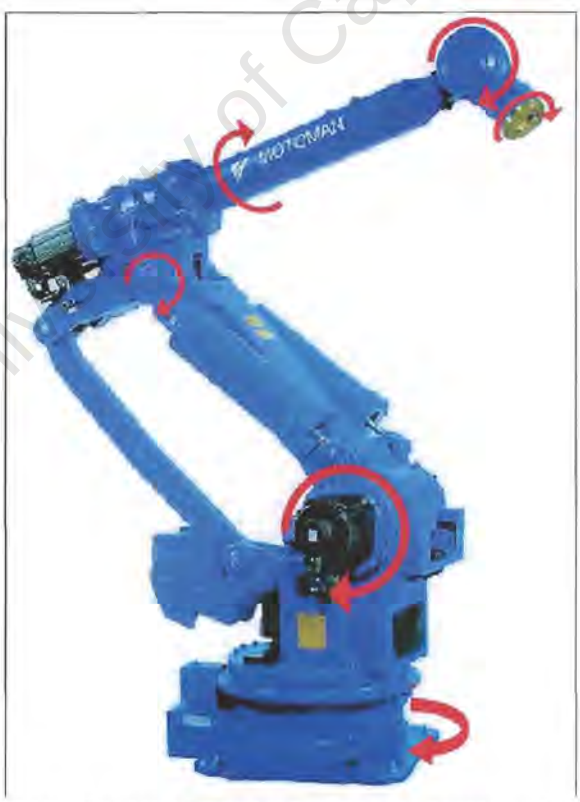

Figure 1.2: The MOTOMAN SK150 industrial robot. The six degrees-of-freedom are depicted by the arrows.

This thesis project was therefore a feasibility study. The purpose of the study was to determine if an industrial robot could replace the existing mechanics of the LODOX machine, in order to give greater freedom of movement, and hence allow other types of radiological scans to be performed.

This study involved three theoretical aspects:

1. the testing of a new hypothesis,
2. the gathering of data, and
3. the development of new technologies/techniques.

The *new hypothesis* was that the existing mechanics of the LODOX machines could be replaced by an off-the-shelf industrial robot such as the MOTOMAN SK150. This necessitates the accuracy of the robot to be the same or better than that of the existing mechanics of the LODOX machines.

Therefore the second aspect of the thesis, *the gathering of data* included taking measurements of accuracy of movement of both the LODOX machines, and the robot. Data were captured using optical, mechanical and vibrational techniques.

The *development of new technologies/techniques* part of the project consisted of designing a computer based simulation depicting the robot replacing the mechanics of the LODOX machines. In addition to the simulation, a full scale model of the C-arm was constructed and attached to the MOTOMAN SK150, and the movements of the LODOX machines were emulated. The MOTOMAN SK150 robot has six degrees of freedom, thus enabling far more complex movements to be accomplished. With this greater freedom, simulations of LODOX technology being used for CT and TB scanning were to be constructed.

Another area where the *development of new technologies/techniques* occurred was in the area of safety. Robots have been used in medicine for more than two decades, particularly in surgery (Davies, 2000). Regulatory bodies have set guidelines for the use of robots in surgery (Varley, 1999). For the most part these robots are custom designed for their specific purpose and the safety issue is part of the design from the beginning. The robot MOTOMAN SK150 is most commonly used for arc-welding in industries such as motor car manufacture and other industrial situations. The robot

is normally programmed for a specific job by the operator and then left to repeat the process continually. There is no human-robot interaction and hence little need for safety guidelines, other than fencing off the area within which the robot operates. To use an industrial robot in a hospital setting with all the equipment of a medical ward (monitors, intravenous drips, etc.), as well as the patient and the clinicians, the safety issue needed to be carefully addressed. A safety strategy and safety guidelines were therefore drawn up for a possible LODOX-Robot machine. Some of the methods that were considered included: collision control, out of bounds areas, cameras, touch sensitive surfaces and 'dead man's handles'. In addition a risk analysis tool called Failure Modes, Effects and Criticality Analysis (FMECA) was performed on the existing LODOX.

1.2 Objectives of the Study

The specific objectives of the feasibility study were therefore to:

1. Simulate the movements of the current LODOX using the MOTOMAN SK150. This included virtual simulations on a computer and real simulations with the robot.
2. Simulate other movements that are not possible with either LODOX machine. These movements included those needed for CT and TB scanning.
3. Determine the repetitive positioning, linear movement and constant velocity accuracy of the industrial robot MOTOMAN SK150 and the LODOX machines.
4. Investigate issues of safety when using an industrial robot in a medical setting, and draw up guidelines for a possible LODOX-Robot machine.

Chapter 2

Literature Review

This feasibility study required in-depth background research in the area of robots, in particularly industrial and medical robots. The issue of safety in robotic environments was researched, and a Risk Analysis engineering tool called Failure Modes, Effects and Criticality Analysis (FMECA) is also evaluated for possible use in the safety part of the project.

2.1 Robots

A definition of a robot is: *'a machine with a human appearance or functioning like a human; a machine capable of carrying out a complex series of actions automatically'* - The Concise Oxford Dictionary, Ninth Edition.

Robots are normally associated with artificially intelligent humanoids like R2D2 and C3PO of the Star Wars series of movies fame. These robots fall within the first part of the definition in that they have a human appearance and function and "think" like a human. However the second part of definition describes machines that are far more common in society. In essence it states that any machine that functions automatically and repetitively could be classed as a robot. Contrary to this, roboticists feel that the characteristics that make robots different from regular machinery are that robots usually function by themselves. In addition they are sensitive to their environment, they adapt to variations in the environment or to errors in prior performance. They are

also task-orientated and often have the ability to try different methods to accomplish a task. The earliest example of a robot comes from around 270 B.C. when the Greek engineer named Ctesibus made organs and water clocks with movable figures (ROver Ranch, 2001). The word "robot" was first introduced in a play in London written by Czechoslovakian Karel Capek. He introduced the word from the Czech "robota", which means a serf or one in subservient labour. However the Science fiction writer Isaac Asimov was the first to truly popularise the word "robot". Through his stories beginning in 1941 he coined the word "robotics" to describe the technology of robots and predicted the rise of a powerful robot industry (ROver Ranch, 2001).

Although there are many different types of robots, this chapter will concentrate on only industrial and medical robots, as they are the most relevant to the study.

2.1.1 Industrial Robots

The first industrial robots were designed in the 1950s and 1960s. The first robot company was Unimation which formed in 1954. Later in 1959, Planet Corporation marketed the first commercially available robot. The first industrial robot saw service in 1962 in a car factory run by General Motors in Trenton, New Jersey. The robot lifted hot pieces of metal from a die-casting machine and stacked them (DULLIER, 2002).

Typically industrial robots do jobs that are difficult, dangerous or repetitive. They lift heavy objects, paint, handle chemicals, weld and perform assembly work. They have high duty cycles while maintaining good levels of precision. Industrial robots can generally be broken up into six categories defined by mechanical structure and principle (Figure 2.1) (IFR, 2001):

Cartesian/Gantry Robot: Robot whose arm has three prismatic joints, whose axes are coincident with a Cartesian coordinator.

Cylindrical Robot: Robot whose axes form a cylindrical coordinate system.

Spherical Robot: Robot whose axes form a polar coordinate system.

Selective Compliant Assembly Robot Arm (SCARA) Robot: Robot which has two parallel rotary joints to provide compliance in a plane.

Articulated Robot: Robot whose arm has at least three rotary joints.

Parallel Robot: Robot whose arms have concurrent prismatic or rotary joints.

The MOTOMAN SK150 robot is an Articulated type robot as it has more than three rotary joints. Of the different types of industrial robots, all but Cartesian/Gantry and Parallel robots could be used for the proposed project. Cartesian/Gantry and Parallel robots could not be used for the project because their kinematic structure does not allow the movements needed. However, Parallel type robots are ideally suited to medical applications because of their high accuracy.

2.1.2 Medical Robots

Robots work in many areas of medicine, such as laboratories, hospitals, rehabilitation and surgery.

Laboratory Robots

Laboratory robots today are the third generation of laboratory systems which first appeared around the 1990's. Laboratory robots carry out hundreds of tests (blood testing for HIV, automated haematology, clinical chemistry, immunochemistry, coagulation and urinalysis) in parallel, saving time and freeing manpower for other purposes. They are used mainly because of their ability to perform repetitive tasks at high speeds, reliably and without fatigue. Hoffmann (1998) states that the latest generation of laboratory robots encompass two key concepts: consolidation and integration. Consolidation refers to combining different analytical technologies or strategies on one instrument or on one group of connected instruments. Integration refers to linking analytical instruments or groups of instruments with pre- and post- analytical devices. An example of such consolidation and integration is an automated coagulation workstation (Graves *et al.*, 1998). Graves *et al.* (1998) constructed a prototype workcell using a mobile robot, an articulated robotic arm, and a coagulation analytical system to automate the analysis of citrated whole blood for the diagnosis of haemostasis disorders.

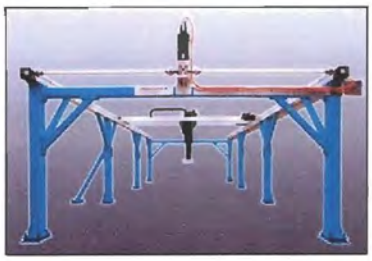

(a) Cartesian/Gantry Robot

(b) Cylindrical Robot

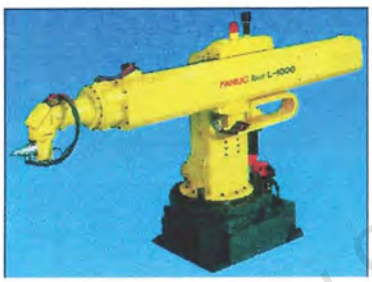

(c) Spherical Robot

(d) SCARA Robot

(e) Articulated Robot

(f) Parallel Robot

Figure 2.1: Robot Types reproduced from (IFR, 2001)

Because of their ability to perform repetitive tasks at high speeds, reliably and without fatigue, laboratory robots result in saving time, costs and freeing manpower for other purposes, while maintaining performance levels to that of a manual systems (Mifflin *et al.*, 2000; Prouskas and Oakman, 1996).

Hospital Robots

Hospital robots are essentially a broad group of service robots working in hospitals. They include mobile robots and are involved in such tasks as fetching and distributing medicine, carrying specimens and pharmaceuticals and even sometimes in patient handling (Lob, 1990). Prouskas and Oakman (1996) state that the use of robots in hospitals may be due to the short supply of hospital staff. An article by Deery (1997) concludes that the use of a robot to courier after-hours deliveries of meals and supplies, maintains high standards of patient care in the face of budget constraints by freeing support staff to focus on other tasks. Hospital robots also include robots used for cleaning. RoboKent and Dolphin are two such robots that scrub floors and vacuum and clean carpets in the hospital environment (Quayle, 1996).

Rehabilitation Robots

Rehabilitation robots are used as either an aid in the rehabilitation therapy process or as a permanent aid to the disabled. Robots used as permanent aids are either fixed in a position at a workstation or are mobile. Workstation rehabilitation robots usually perform simple tasks such as raising food to the mouth or turning a page in a book. The mobile robots consist of a mobile platform or a powered arm on the side of a motorised wheelchair (Prouskas and Oakman, 1996).

Permanent robot aids in development including DeVAR in the U.S., SPARTACUS and MASTER in France, HANDY1 in the UK, Neil Squire MOM in Canada, and so forth (Busnel and Cammoun, 1999). The MASTER system as described by Busnel and Cammoun (1999) is composed of a fixed robotised workstation that includes a six-axis SCARA robot mounted on a rail to allow horizontal movement and is equipped with tools for various tasks. This robot is aimed at aiding a functional person with

tetraplegia in tasks such as giving a drink, loading a floppy disk into a computer or grasping a phone receiver.

Many of the rehabilitation aid robots make use of off-the-shelf commercial and industrial robots which have been modified. This is due to the high cost, limited utility of the equipment, lack of reliability, frequency and technicality of maintenance, and difficulty in training people to use a particular system. Hence Regalbuto and Krouskop (1992) at Rice University and the Baylor College of Medicine are developing a simple, relatively inexpensive robotic system that can aid severely disabled persons by providing pick-and-place manipulative abilities to augment the functions of human or trained animal assistants. They are using an off-the-shelf modified HERO 2000 robot, a Macintosh SE host computer, and the X-10 Powerhouse household appliance controller.

In addition to giving mobility and independence to physically disabled people, robots can be used to develop skills. The PLAYBOT is one such system that assists disabled children in learning to play (Tsotsos *et al.*, 1998). The aim of this project is to develop a robot based on a motorised wheelchair on which the child sits. Mounted on the wheelchair is a robotic arm and hand, a stereo-colour vision robot head, and a control panel making use of the BLISS symbolic language. The robot is operated by the child choosing a sequence of pictorially represented actions that he or she wishes to perform with the toy. In essence the PLAYBOT is used to retrieve and "play" with the toy.

Robots used as rehabilitation therapy aids is a relatively new concept compared to robots being used as permanent aids to the disabled. A area where there in much activity is in robot aided neuro-rehabilitation, particularly for patients that have suffered a cerebrovascular accident or stroke. With the improvements in medicine and health care, resulting in an increase in human life expectancy, the incidence of stroke is becoming far more prevalent among older adults. Post-stroke therapy is labour-intensive, usually relying on one-on-one, manual interactions with therapists and with the constant demand for increased contact time and performance improvement at lower cost and in shorter time, robots have become a possible alternative (Krebs *et al.*, 2000; Dijkers and deBear, 1991). A second incentive for using robots for post-stroke therapy is that the quality of therapy can be improved. Robots can repeat the

same movement many times with a high level of precision as well as keep count and monitor patient treatment time in great detail (Dijkers and deBear, 1991).

Surgical Robots

Davies (2000), in a paper reviewing robotics in surgery, gives a definition of a surgical robot:

> "a powered computer controlled manipulator with artificial sensing that can be reprogrammed to move and position tools to carry out a range of surgical tasks".

He goes on further to distinguish between surgical robots and the related field, Computer Assisted Surgery (CAS). Surgical robots are moved by some motorised system, while CAS systems are generally powered manually by the surgeon. There are many reasons for using robots in surgery. Lueth and Bier (1999) describe the seven most important:

- Robots show the same power all the time and execute their tasks in a well-balanced manner.
- The behaviour of a robot is exactly known before execution, during execution and can be protocolled for documentation, evaluation and education after execution.
- Robots shake or vibrate much less than a human being.
- Robots can move much more precisely in space and time than a human being.
- Robots can react much faster than a human being.
- Robots can be controlled remotely.
- Robots and control systems can coordinate complex processes or events and are able to cooperate with other machines in the operating room within milliseconds.

The classification of surgical robots should be made according to their technology basis rather than for the tasks for which they were designed (Davies, 2000). The four categories of surgical robots that he describes are: *robots used as passive tool holders; active robots; synergistic systems; and master–slave 'telemanipulator' systems.*

Robots used as passive tool holders are just that. They are used to hold a tool in position during a procedure. They may be powered or un-powered. Active robots are used to actively interact with the patient during the procedure. Synergistic systems are robot systems in which the surgeon drives the robot with force control. This is a haptic system, in that there is active force feedback to the surgeon. Master–slave 'telemanipulator' systems are robots that are controlled remotely via some kind of 'joystick'.

Typical robotic surgery includes four stages: *surgical planning; registration of the robot to the patient; execution of the procedure; and evaluation of the procedure* (Prouskas and Oakman, 1996).

Surgical planning includes imaging the patient via X-ray, CT or Magnetic Resonance Imaging (MRI). A three-dimensional model is then created from the imaging data and the operation is rehearsed. The registration of the robot to the patient is the correlation of the robot's data about the patient with the actual patient, in terms of positioning. The execution of the procedure is monitored by the surgeon directly or remotely via monitor. Sensors on the robot are also monitored by the system in real-time. Lastly is the evaluation of the procedure. The surgeon evaluates the procedure and decides if it needs to be repeated by the robot again or manually by the surgeon themselves.

Minimally Invasive Surgery (MIS) came into development in the last twenty years. Its advantages are that due to the small size of incisions, the patient experiences less trauma and pain, and recovery time is decreased. The disadvantages of MIS are that the surgeon has less dexterity and restricted view because of the small size of the incision. These problems have partly been overcome by using a robotic application. As an example robots are used to position laparoscopes or directly manipulate the surgical instruments during laparoscopic surgery (Kwon *et al.*, 2001).

In addition to invasive surgery, robots are being used for non-invasive surgery. A similar study to the present project discusses the use of a FANUC Robotics computer

controlled robotic arm, which is used in radiosurgery Adler *et al.* (1999). The FANUC robot is an off-the-shelf industrial robot which is used to point a lightweight x-band linear accelerator in cranial radiosurgery. During the radiosurgery, an X-ray imaging system determines the location of the lesion and communicates the coordinates to the robot, which adjusts the pointing of the linear accelerator beam to maintain alignment with the target (Figure 2.2).

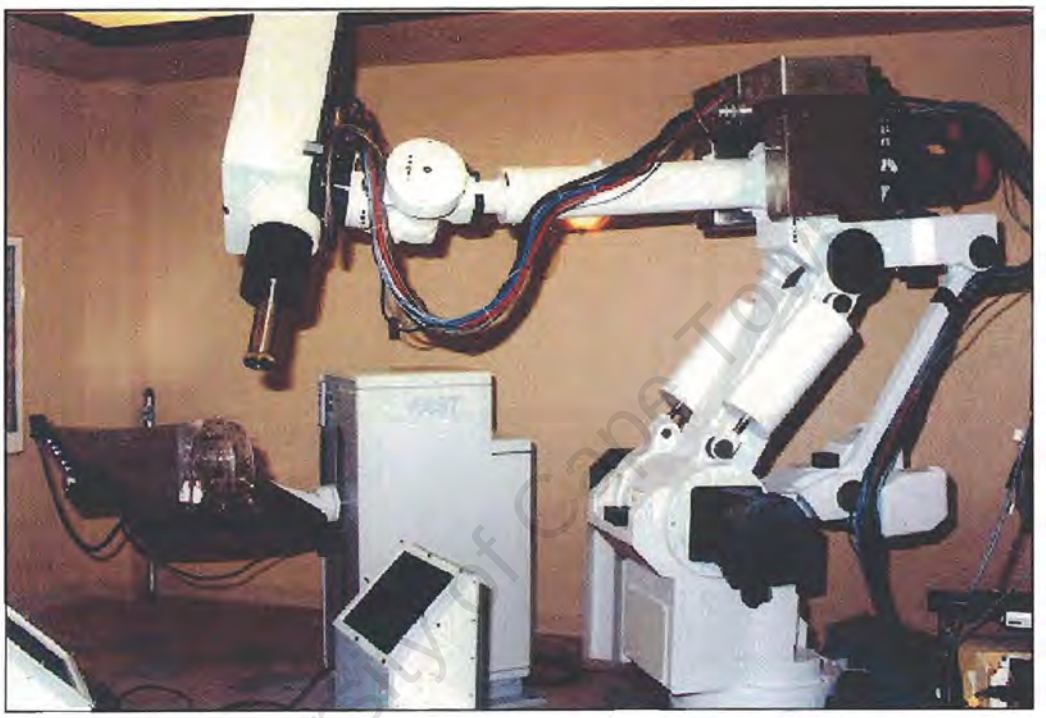

Figure 2.2: Image-guided radiosurgery using the ACCURAY CyberKnife® reproduced from Schweikard (1997)

2.2 Robot Safety

Safety considerations for personnel and equipment working in robotics environments differ depending on the application. Industrial robots have various standards dealing with such issues which are summarised in the following section. Medical robots through their close interaction with humans require further safety standards to that of industrial robots. Medical robot safety is therefore discussed in a separate section.

A risk assessment analysis technique entitled *FMECA* was used to analyse the existing LODOX system to identify issues for the proposed LODOX-Robot system. A

description of this technique is presented in the last section of this chapter, while the actual analysis is given in Chapter 5 - Safety.

2.2.1 Industrial Robots

Various safety standards for industrial robots exist. These include standards from the International Standards Organisation (ISO), the American National Standards Institute (ANSI) and the European Union (CE). Robotic Industries Association (RIA) is the industry leader for all robotic issues. The *ANSI/RIA R15.06-1999 Safety Requirements for Industrial Robots and Robot Systems* standard (American National Standards Institute/Robotic Industries Association, 1999) is 'the' safety standard for industrial robots. Although it is not law in the United States, more and more users require compliance with this standard in their contract specifications. In addition, for use in the United States manufacturers are required to comply with the Occupational Safety & Health Administration (OSHA) directives that include the ANSI/RIA R15.06-1999 standard by reference.

The ANSI/RIA R15.06-1999 standard includes sections on:

- manufacture, remanufacture and rebuild of robots
- design and manufacture of safety devices
- installation of robots and robot systems
- safeguarding of personnel (risk assessment)
- safeguarding of devices
- maintenance of robots and robot systems
- testing and safety training of personnel

Most industrial robots do not interact with humans other than during teaching or programming. Hence safety considerations are relatively simple and require only that the robot operate inside a cage away from people, and that the robot is only powered up when all personnel are excluded from the robot's working area (Davies, 2000).

2.2.2 Medical Robots

Many international standards provide guidelines and directives for medical electrical equipment, although there are currently no specific standard safety guidelines for medical robots (Baowei *et al.*, 2001; Davies, 2000). Prouskas and Oakman (1996) have suggested three reasons for this fact: the definition of safety depends largely on the application; there are no clear boundaries to the extent of the surgeon's and the manufacturer's responsibility in case of a fault; and manufacturers are reluctant to make all design specifications available to medical safety committees.

There is a great need for such a "Medical Robotics Standard" with many groups working toward this end. As recently as September 2001 a workshop sponsored by the United States National Institute of Standards and Technology (NIST), the United States Food and Drug Administration (FDA) and the RIA was convened to identify the metrology and standards needs of medical robots in order to allow the medical robot market to grow safely and rapidly. Issues identified for further analysis included: fail-safety, failure mode analysis, redundancy, review of existing standards applicable to medical robots, issues in taking industrial robots into the medical field, ergonomics, the man/machine interface and others.

Three factors present designers of medical robot systems with more complicated safety problems than their counterparts designing industrial robots (Prouskas and Oakman, 1996).

The first is the human presence. In the industrial sector there are no humans present in the application environment. Should humans enter the robot's workspace, safety regulations stipulate that the robot be de-activated. In the medical sector the robot often acts as an assistant, and hence it works in close proximity to humans. As the medical robot may work in a chaotic, time-varying environment such as an operating room, it is required to have great sensory capabilities.

The second factor is fault consequence. If safety strategies are followed, a fault in the industrial sector would result at worst in the loss of physical equipment, while the worst case scenario in the medical sector would be the loss of human life.

The third factor concerns the type of task that the robot is required to perform. In the industrial sector the tasks are normally repetitive and the series of movements are

performed in a pre-defined order. Not so in the medical field where the robot may be required to take account of the differences on an object-to-object basis. Hence testing is required for the many different scenarios that may occur.

Other safety strategies that must be employed in medical robot design include redundancy, limited operation and the idea that in the event of failure, the robot must fail-safely. These topics are discussed in Chapter 5 as safety strategies that could be employed in the proposed LODOX-Robot system.

2.2.3 Failure Modes, Effects and Criticality Analysis (FMECA)

Failure Mode and Effect Analysis (FMEA) is a tool which was originated by the United States Society of Automobile Engineers (SAE) and is used extensively by risk analysis engineers in many different fields of engineering design. It is an essential function in design from concept through development (United States Department of Defense, 1980). It analyses the potential effects caused by system elements ceasing to behave as intended (Mohr, 1994). FMEA can find the weaknesses in designs before the design is realised, either in prototype or production, hence saving time and money. It can also inherently add to the safety of a design.

FMEA is a qualitative reasoning approach best suited for reviews of mechanical and electrical hardware systems. The FMEA technique firstly considers how the failure modes of each system component can result in system performance problems. Secondly it ensures that appropriate safeguards against such problems are in place. Failure Modes, Effects and Criticality Analysis (FMECA) is known as the quantitative version of FMEA, in that a numerical value is assigned to how critical the failure mode is perceived to be (United States Coast Guard, 2002).

The process of a FMEA/FMECA consists of the following steps:

1. Define the *system to be analysed* and obtain all necessary drawings, charts and descriptions, diagrams and component lists. Clearly define the *boundaries of the system*, what is and what isn't included in the study.
2. Break the system down into convenient and logical *elements or sections*.

3. Choose the type of FMEA/FMECA approach for the study. Either *functional/top-down*—according to what the system elements do, or *geographic/bottom-up*—according to where the system elements are, or a hybrid of the two.
4. Establish a *coding system* to identify system elements.
5. Identify the potential *failure modes* for each system element.
6. Identify the potential *failure effects* for each failure mode.
7. Perform a quantitative evaluation (Criticality Analysis) of each of the failure effects by assigning a value according to probability and severity (FMECA).
8. Continue the analysis up (geographic approach) or down (functional approach) a level.
9. Document the analysis and use the results in modification of the design.

While designs continue to be upgraded or modified, the FMECA study never completes, hence the documentation should always be updated.

Chapter 3

Simulation

3.1 Introduction

The first objective of this project was to simulate the movements of the LODOX machines using the MOTOMAN SK150 robot, both virtually on a Personal Computer (PC) and physically using a phantom. The second objective was to simulate other movements not possible with the present mechanics of LODOX. These were to include movements required for CT and TB scanning.

3.2 Materials and Methods

3.2.1 Description of the MOTOMAN SK150 Industrial Robot

The MOTOMAN SK150 industrial robot is designed for assembly, material handling, material removal, spot welding and surface finishing tasks in an industrial environment. It is an *articulated robot* as designated by the IFR (2001) because it has at least three rotary joints.

An industrial robot system includes the power supply, controller and remote controls as well as the robot itself. The MOTOMAN SK150 consists of the manipulator or robotic arm, the Manual Robot Controller (MRC), the programming pendant (Fig-

(a) The robot arm or manipulator

(b) The Manual Robot Controller (MRC) and the programming pendant

Figure 3.1: The MOTOMAN SK150 Industrial Robot Located at the National Accelerator Centre (NAC), Faure, South Africa

ure 3.1), and the power supply. The robot has six joints that can be individually controlled, giving it six degrees-of-freedom and an extensive working range/envelope, which can be seen in Figure 3.2. The basic specifications of the MOTOMAN SK150 are given in Table 3.1, while the complete data sheet is reproduced in Appendix A.

The robot can be positioned using both joint and rectangular co-ordinates. When positioned using joint co-ordinates, the robot is moved by assigning an angle to each of the six joints. However, when using rectangular co-ordinates, both a linear distance and an angle of rotation are assigned to each of the three axes. The velocity can also be described in rectangular and joint co-ordinates over time, as (m/s) and (rad/s) respectively.

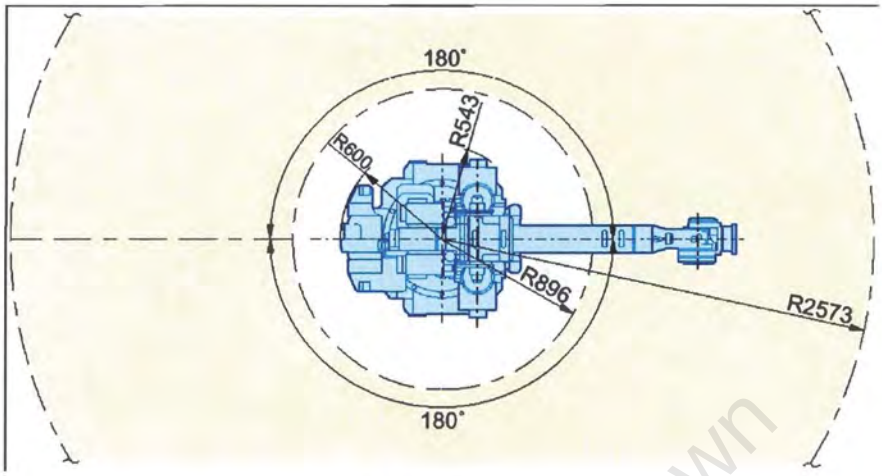

(a) Top View

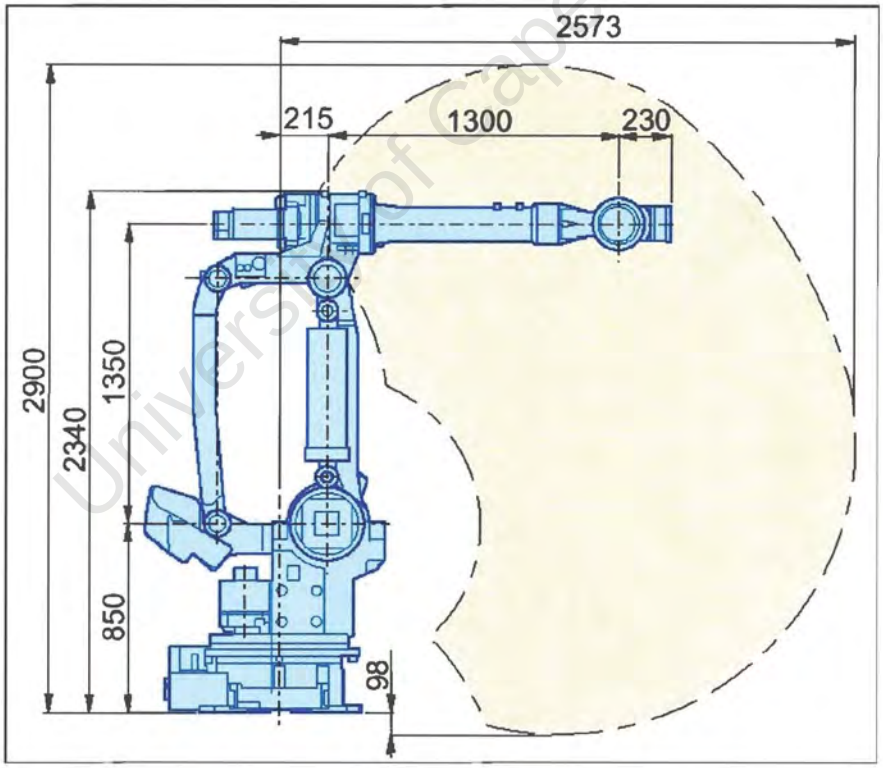

(b) Side View

Figure 3.2: The Working Range of the MOTOMAN SK150

Table 3.1: Basic Specifications of the MOTOMAN SK150 Industrial Robot.

Controlled Axes	6
Payload	150kgs
Repetitive Positioning Accuracy	±0.4mm
Weight	1500kgs
Power Supply	22kVA
Ambient Temperature	0–45°C
Ambient Relative Humidity	20–80% RH
Ambient Vibration	0.5G or less

The position of the robot is defined by both a Reference Co-ordinate System (RCS) and a Tool Centre Point (TCP). The RCS defines an origin from which the position of the robot TCP is measured from. The default TCP is the centre of the flange of the robot wrist. When a tool is attached to the wrist, a new TCP must be assigned to the "working" point of the tool.

The location of the TCP is given as co-ordinates measured from the origin of the RCS. There are three different RCSs: BASE, ROBOT and USER. The origin of the BASE RCS is defined as a point which is common to all robots within a specified area. This could be a corner of the room, or a mark on the floor, etc. If the BASE RCS is used when there are multiple robots within an area, all TCPs of robots within such an area are measured from the same BASE origin. The ROBOT RCS is defined as having an origin in the centre of the robot base. All TCP co-ordinates are measured from this ROBOT origin. The third RCS is the USER RCS. It is a defined by a user-defined origin which is only applicable to specific robot jobs (applications). There can be up to twenty-four different USER RCSs programmed and stored on the MRC.

The MOTOMAN SK150 used for this project is located in a operating room of the Faure Hospital at the National Accelerator Centre (NAC) (recently renamed iThemba LABS), in Faure, South Africa. The robot was commissioned for another project at NAC but was available for use on the current project.

3.2.2 Virtual Simulation

In industrial situations where most robots are used, robots can be programmed or taught in two ways, either *on-line* using a programming pendant or remote control, or *off-line* using simulation software.

On-line programming of MOTOMAN robots entails moving the TCP from point to point in space using the programming pendant. This is done in the *teach* mode of the MRC. At each point the coordinates are stored in a *job-file* together with the speed that the TCP should move to those coordinates. Once all coordinates are programmed, the MRC is changed to *play* mode and the programmed job-file can be run.

Off-line programming of robots requires simulation software. MOTOMAN's own proprietary simulation software is Robot Off-line Teaching System of Yasakawa (ROTSY). It is a graphically intensive off-line teaching system for Motoman robots using MRC controllers. The features of ROTSY as stated in the manual (Motoman, 1996) include: Import Capabilities (Faro Arm data, 3-D Computer Aided Design (CAD), ROTSY MDL, and many other file formats), TriSpectives Technical (a fully functional 3-D CAD package from 3D/EYE, Inc.), External Teach Capability (utilising a 6-degree-of- freedom positioning device), Accurate Job Cycle Time Calculation, Off-line Programming, Collision Detection (between the robot and other objects), Virtual Programming Pendant (resembling the Programming Pendant on the MRC), Full-control Cameras (to view the robot model from any point in space), Automatic Job Creation (attaches jobs to parts instead of robots), Trace (displays each update point as a path while the robot program executes; the points can be copied to the clipboard in a spreadsheet format), OLE (allows other programs to share information with ROTSY).

The ROTSY software is normally purchased with the robot, although in the case of NAC's robot the software was never supplied. For this project the local suppliers for MOTOMAN kindly loaned us a copy together with the required "dongle" or computer hardware-key. Much time was spent waiting for this software and during this time other manual ways of programming the robot off-line were investigated, but were found to be too laborious.

The simulation of the LODOX movements using the robot were created using the ROTSY software in the following stages:

1. The correct model of robot was chosen from the list available. This was confusing as there were five robot models called SK150, the only apparent difference being their different colours. The default model was chosen for the simulation. The robot was placed in the workspace with sufficient room for the other parts of the simulated environment.

2. The dimensions of the LODOX trolley were measured and a scaled model of the trolley was constructed in the program.

3. A model of a 1.8m person was found in the sample files of the ROTSY software and placed on the trolley in a suitable position.

4. The C-arm of the LODOX machine was then created. Because of its more complex shape than that of the trolley and even the human model it was decided to make use of a CAD package to design the C-arm. Although the features of the ROTSY software indicate that the TriSpectives Technical 3D CAD package is installed with ROTSY, it was found to be not so. The package was then borrowed from the local Motoman agents in Johannesburg. The C-arm was then designed in this package and an attempt to export the model to ROTSY was made. After little success it was concluded that this was not possible as our ROTSY version was not compatible with the TriSpectives Technical software. The C-arm was then designed using two other CAD packages, AutoCAD and ProEngineer. The models were exported as formats supposedly recognised by ROTSY according the manual (Motoman, 1996). Once again the models could not be imported. The C-arm was finally constructed in ROTSY directly. This was particularly tedious and resulted in a model inferior to those created in the CAD package, as ROTSY has limited design capability. Once the C-arm model was finished, it was attached to the wrist of the virtual robot.

5. A model of a partition was then created to hide the view of the virtual robot from the virtual patient lying on the trolley model.

6. All the various models of the simulation were moved into the correct positions, while keeping the area of floor space taken up by the virtual robot, trolley, human and C-arm to a minimum.

7. The movements of the robot and C-arm were then programmed in ROTSY, and different configurations were tried until a movement similar to LODOX was found recorded.

3.2.3 Physical Simulation

The physical simulation entailed three stages:

1. A phantom C-arm was designed and built according to measurements taken from the original LODOX assembly drawings. It was built from plywood in the departmental workshop by Mr John Marcus.
2. The phantom C-arm and a spare trolley from the Groote Schuur LODOX machine were then transported out to the NAC. The C-arm was attached to the robot, and the trolley was placed before the robot as depicted in the simulation.
3. The ROTSY simulations of the LODOX movements were then converted into job files and uploaded to the MRC. These job-files were then run on the robot with the phantom C-arm attached, and a subject lying on the trolley.

3.2.4 Simulation of CT, TB and Other Movements

Unfortunately the hardware key that was on loan from the South African supplier of the ROTSY software had to be returned before the any further simulations could be performed.

3.3 Results

3.3.1 Results of Virtual Simulation

The different simulations created in ROTSY and are difficult to display in print. They are depicted in a frame-by-frame form and must be "read" from top left to bottom

right. The actual simulations are given as .avi files on the CD-ROM attached to this document.

Figure 3.3 is the frame-by-frame simulation of LODOX conducting an antero-posterior scan, while Figure 3.4 is the frame-by-frame simulation of LODOX conducting a lateral scan. Note that the lateral scan simulation has a simplified C-arm.

3.3.2 Results of Physical Simulation

Figure 3.5 depicts the phantom C-arm attached to the robot "scanning" the subject lying on the trolley. A video of this is also given on the attached CD-ROM.

3.4 Discussion

Off-line programming using simulation software like ROTSY is more advantageous than on-line programming for a number of reasons:

Safety There is no chance of collisions when using simulation software, and there is also automatic collision detection built into the software. In addition, no-go areas can be defined to isolate the work area of the robot.

Speed Programming with simulation software is also faster, because of the above reason. There is no need to worry about hitting anything or going too fast while working out robot jobs. However, when programming on-line, the robot arm is moved slowly for safety reasons, and instructions have to be constantly confirmed, making the process much slower.

Ease of use Conceptualising the work environment is easier in simulation, and different views are available at the touch of a button.

The simulation of the LODOX movements in ROTSY was sufficient to give a simple conceptual idea to the feasibility study. With the physical simulation, potential problems and other issues were identified, including:

- The location of the attachment of the C-arm to the robot was chosen for simplicity in the simulations, although the attachment location would not be suitable for a real machine for two reasons. Firstly, the present attachment is at the location of the X-ray tube. Secondly, the attachment site is not suitable when considering the large cantilever effect the C-arm would produce at this point. A more suitable site would be further down the C-arm closer to the centre-of-mass.

- The actual connection between the robot and the C-arm would have to be investigated. The surface area of the connection would have to be increased to reduce vibration on acceleration and deceleration, due to the inertia of the C-arm.

- Although the robot was programmed to move linearly in the ROTSY simulation, there were periods in the physical simulations when this did not occur. What was simulated in ROTSY was not what was always simulated physically. The reason for this is not totally understood, but may be due to the wrong robot model being used in ROTSY. Also, the version of the ROTSY software is quite old, and this issue may have been rectified in a later version. The correct co-ordinate system may also not have been used.

- There are thick cables running between the C-arm and the base frame of LODOX (electrical cables and cooling pipes for the X-ray tube). These cables have not been included in the simulation and would be difficult to model in ROTSY because of their flexibility. Issues with said cables have occurred on the LODOX-MP machine during its commissioning. Brackets had to be fitted to stop the cables catching on the base frame and parts of the C-arm. For the robot, the cable issue is far more complex due to its greater freedom of movement. Tangling and twisting of the cables would be a major concern. The weight of the cables would also have to be taken into consideration.

- The weight of the phantom C-arm was only a few kilograms, compared to that of the real C-arm which weighs over three hundred kilograms. The robot is certified to a maximum load of one hundred and fifty kilograms, and hence the C-arm would have to be redesigned to be significantly lighter. However, the general shape of the C-arm would not have to be restricted to the status quo. All that is required is that the clearance volume, support for the same size and

weight components (i.e. the detector, tube and mirror/collimator assembly), and the stiffness qualities between the tube and source, have to remain constant.

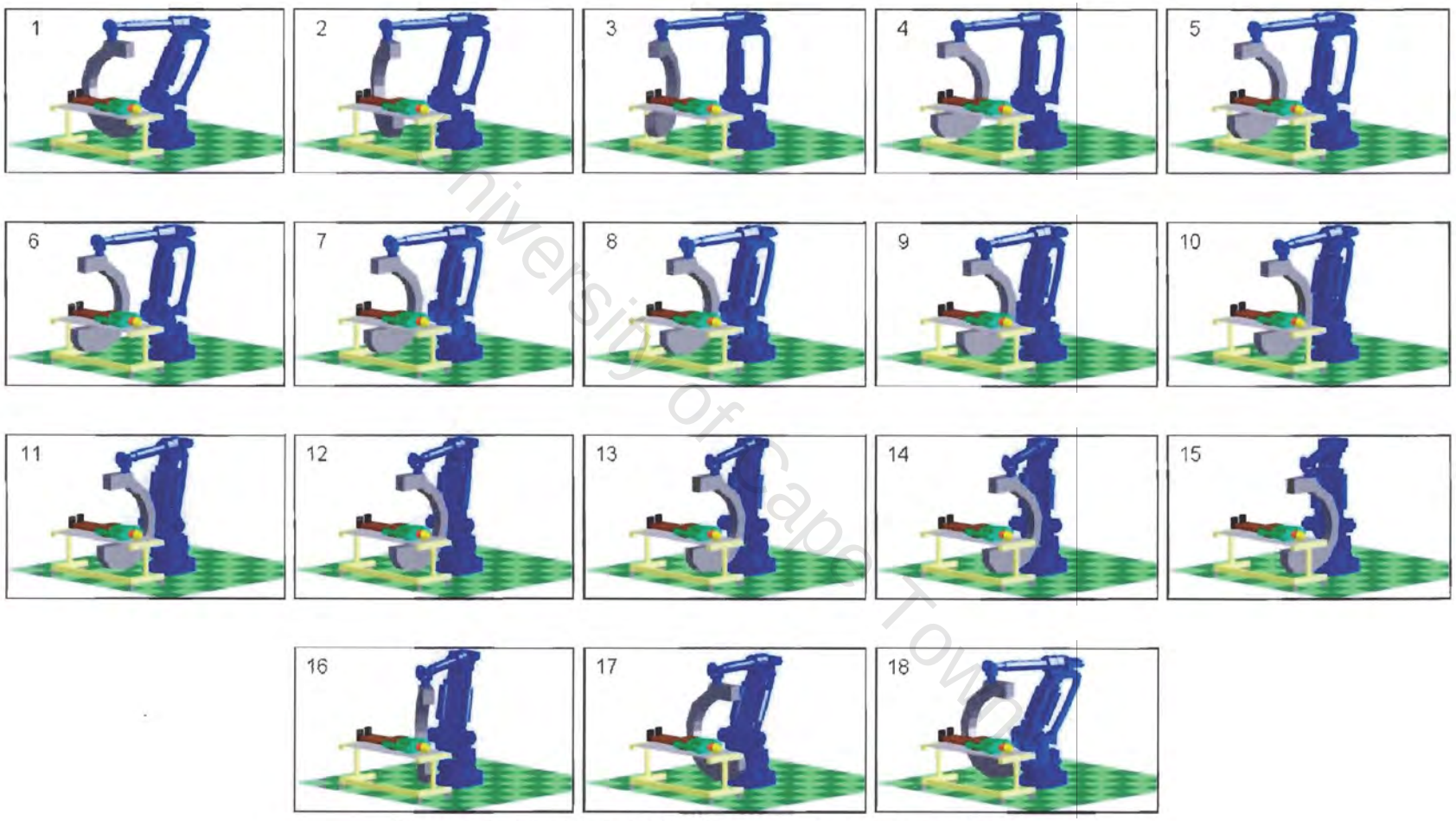

Figure 3.3: Simulation of LODOX conducting an antero-posterior scan

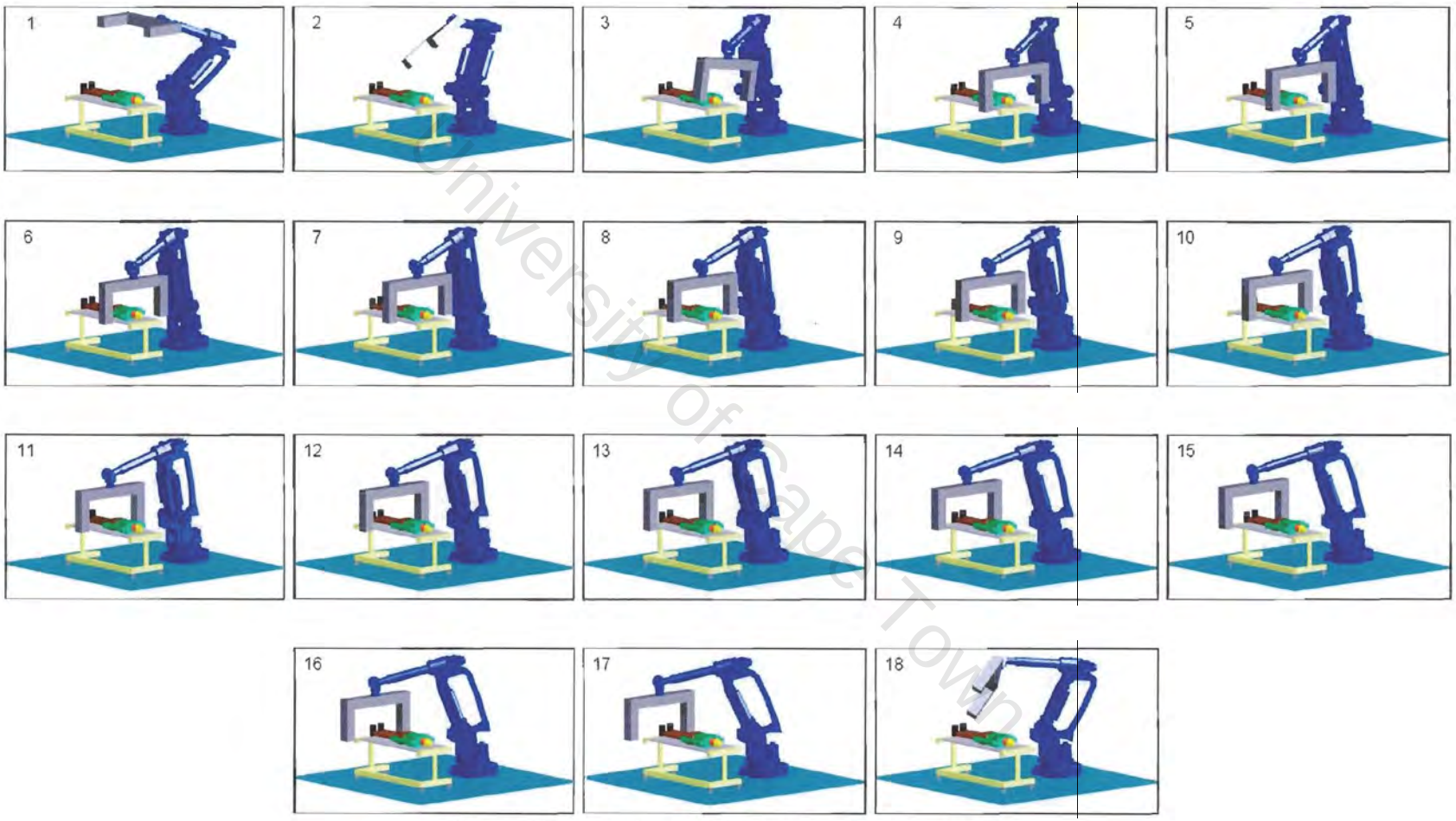

Figure 3.4: Simulation of LODOX conducting a lateral scan

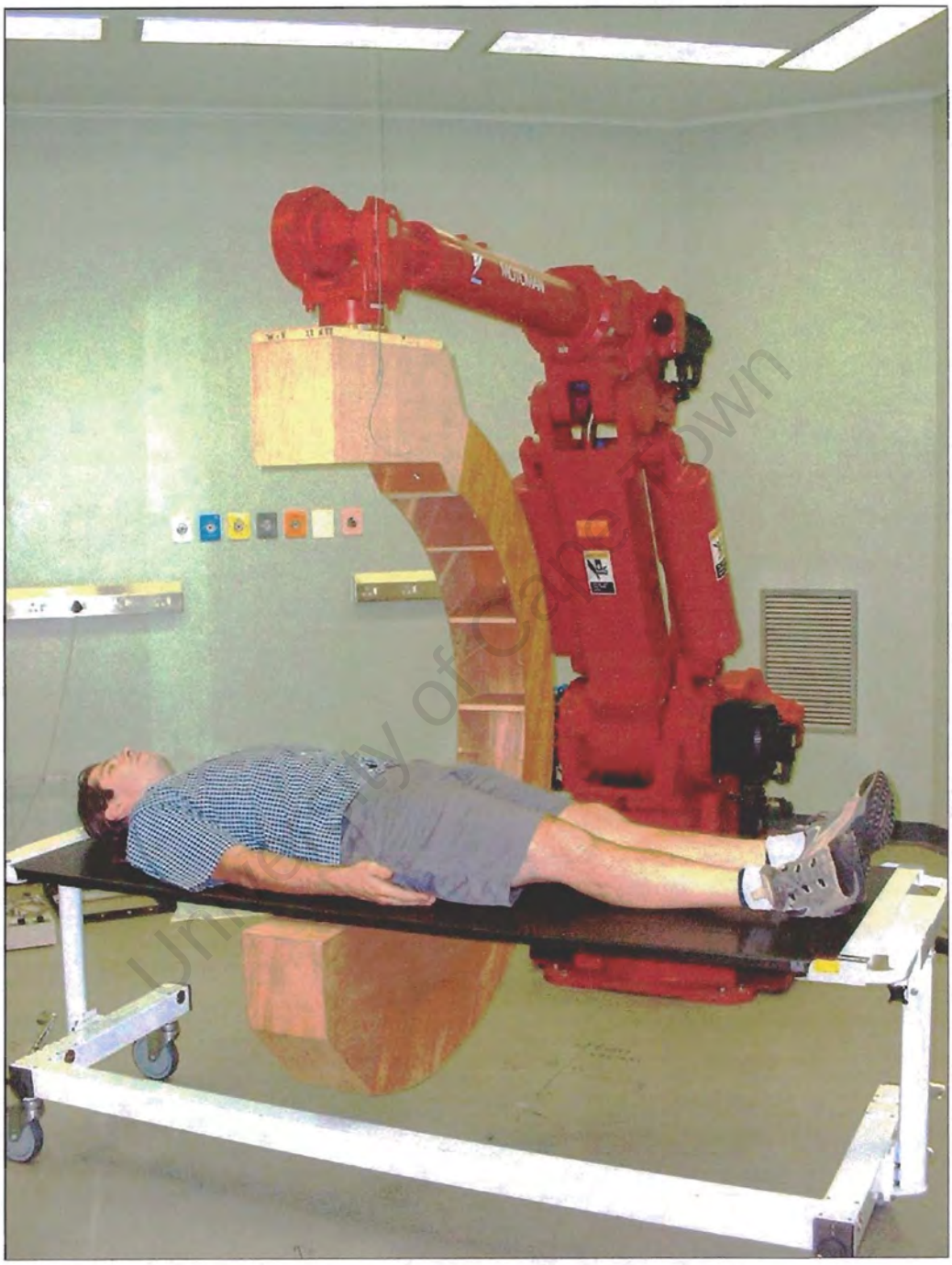

Figure 3.5: Scanning a patient using the phantom C-arm mounted on the robot

Chapter 4

Accuracy

4.1 Introduction

The effect of vibrational movement on the image quality of the LODOX system is not precisely known and was felt to be not part of this feasibility study (another student is conducting such a study for their Master's dissertation). However it was assumed that as long as the robot's movements were equal to or more precise than that of the LODOX machine, image quality would not be compromised. Hence the second aspect of this project was to determine the Repetitive Positioning (RP), Linear Movement (LM), and Constant Velocity (CV) accuracies of the industrial robot MOTOMAN SK150 and compare them to that of the LODOX machine values.

4.2 Materials and Methods

4.2.1 Repetitive Positioning Accuracy Tests

The RP accuracy is defined as the accuracy to which the TCP can repetitively return to the same position in three dimensional space. Motoman maintain a figure of < 0.4mm with the maximum recommended payload of 150kg (Table 3.1).

(a) Point seen through the viewfinder of the theodolite

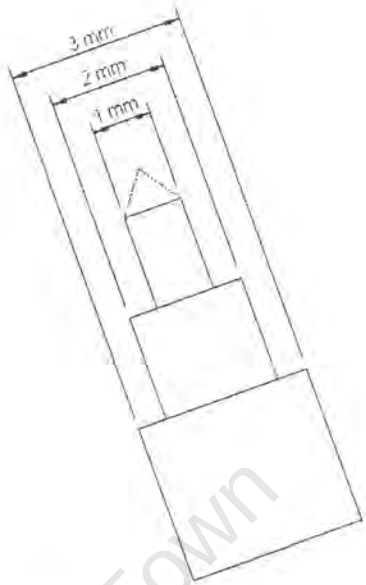

(b) Schematic of the point

Figure 4.1: The point used for RP accuracy and LM accuracy tests

To confirm this value, independent tests were conducted on the robot at the NAC. These tests were undertaken by Steffen Schanz, a undergraduate mechanical engineering student working on a similar project at the NAC. He used a theodolite and two precision machined rods attached to the wrist of the robot to measure the repetitive accuracy.

The rods used were machined from stainless steel to lengths of 0.1m (Rod 1) and 1m (Rod 2). A precision point was machined that could be attached to both rods. This point (Figure 4.1) was accurately machined to three stepped diameters: 3mm, 2mm and 1mm and then a point. The reason for these stepped diameters was for the linear accuracy tests, which are described in Section 4.2.2.

Two tests were conducted, both with Rod 2 connected to the robot and the point attached to the end of the rod. The TCP was assigned to the point of the rod, and the robot was then taught two different jobs. The first job was a simple movement through two co-ordinates and then it returned to the initial co-ordinate, while the second job moved the TCP through four co-ordinates before again returning it to the initial position (Figure 4.2).

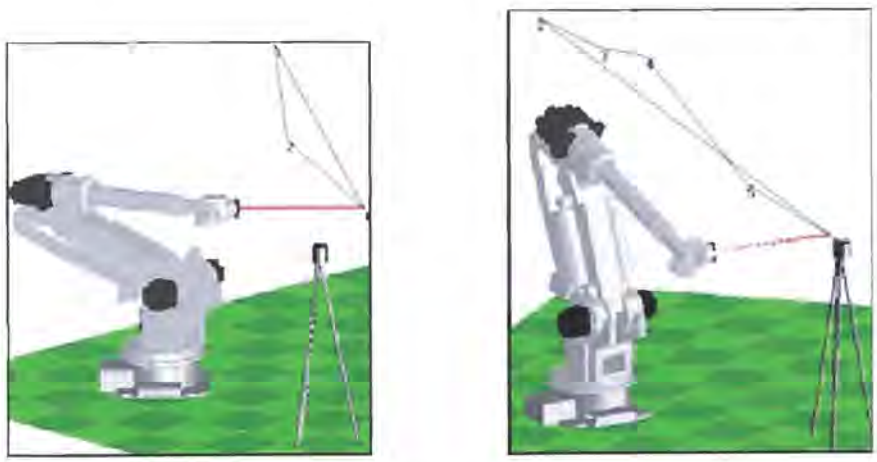

(a) Simple two co-ordinate job

(b) Complex four co-ordinate job

Figure 4.2: The two repetitive accuracy tests depicted in Robot Off-line Teaching System of Yasakawa (ROTSY) simulations

Before the jobs were run, the theodolite was set up with the cross-hairs of the viewfinder focused on the point attached to the end of the rod. The jobs were then subsequently run and the robot moved through the programmed co-ordinates ending at the initial position. The change in position of the point from the initial co-ordinate to the final co-ordinate was measured from the graduations in the viewfinder of the theodolite.

4.2.2 Linear Movement Accuracy Tests

Testing for LM accuracy involved determining how far off a straight line the robot TCP deviated when it was programmed to move linearly (using rectangular co-ordinates) between two points. The deviation from this line could occur in one or both of the planes tangential to the plane of movement. This deviation was measured using the theodolite.

Six one metre, two position robot jobs were programmed, three with each rod attached. The TCP was assigned to the point when attached to each rod. The theodolite was set up in such a way that the beginning and end positions of each of the jobs were perfectly in line with the cross-hair of the viewfinder. Thus on running each job, the TCP should not have moved when viewed through the viewfinder of the theodo-

lite. Deviations from the linear line could be measured by noting the position of the cross-hairs in reference to the stepped diameters. Images from ROTSY simulations of each of the tests are given in Figure 4.3 and Figure 4.4 respectively.

4.2.3 Constant Velocity Accuracy Tests

Calculating CV accuracy involved determining the velocity deviation from a preprogrammed linear velocity. Such a deviation can be measured directly by conducting velocity tests. The deviation can also be measured indirectly by conducting acceleration or displacement tests, which can then be integrated and differentiated respectively, to give a velocity. The constant velocity accuracy tests were conducted on both the robot and the LODOX machines. Three different testing regimes were employed using: *digital cameras (optical technique), a rotary encoder (mechanical technique)* and an *accelerometer system (vibrational technique)*.

Digital Cameras

A digital camera system normally used for human movement analysis was employed to track the movement of both the robot and LODOX machines. This testing regime directly measured velocity. The digital camera system comprised: the Vicon 370, 6 camera motion analysis system and the Vicon Workstation 3.0 motion analysis software from Oxford Metrics, and the Rdata2 conversion program from Motion Lab Systems. The principle of this testing regime was to track retro-reflective markers which were attached separately to the robot and the LODOX-MP machine, by synchronously strobing infra-red light (from light emitting diodes) on the markers and capturing the position of the markers with the digital cameras.

In conducting the tests, the tripod mounted digital cameras were arranged around each of the subjects as far back from the subject as possible and the camera's fields of view were focussed and aligned to capture the full range of movement of the subjects. For all tests conducted, only three of the six cameras of the system were utilised, and the strobe rate of the diodes and capture rate of the cameras were both set to the maximum, 120Hz. A single passive retro-reflective marker was placed on each of the subjects: the default TCP of the robot—the centre of the flange of the robot wrist, and

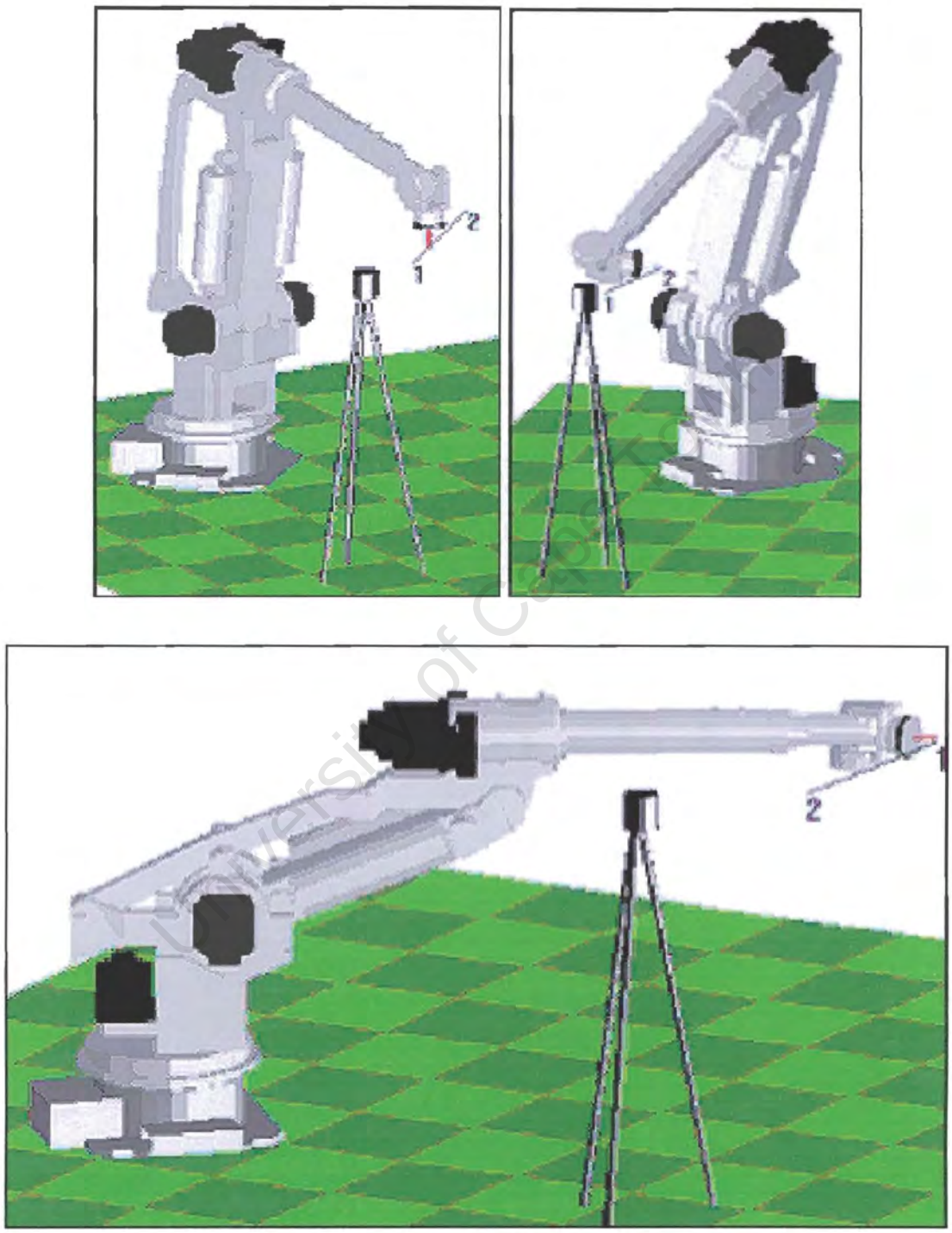

Figure 4.3: LM accuracy tests using the short rod, Rod 1

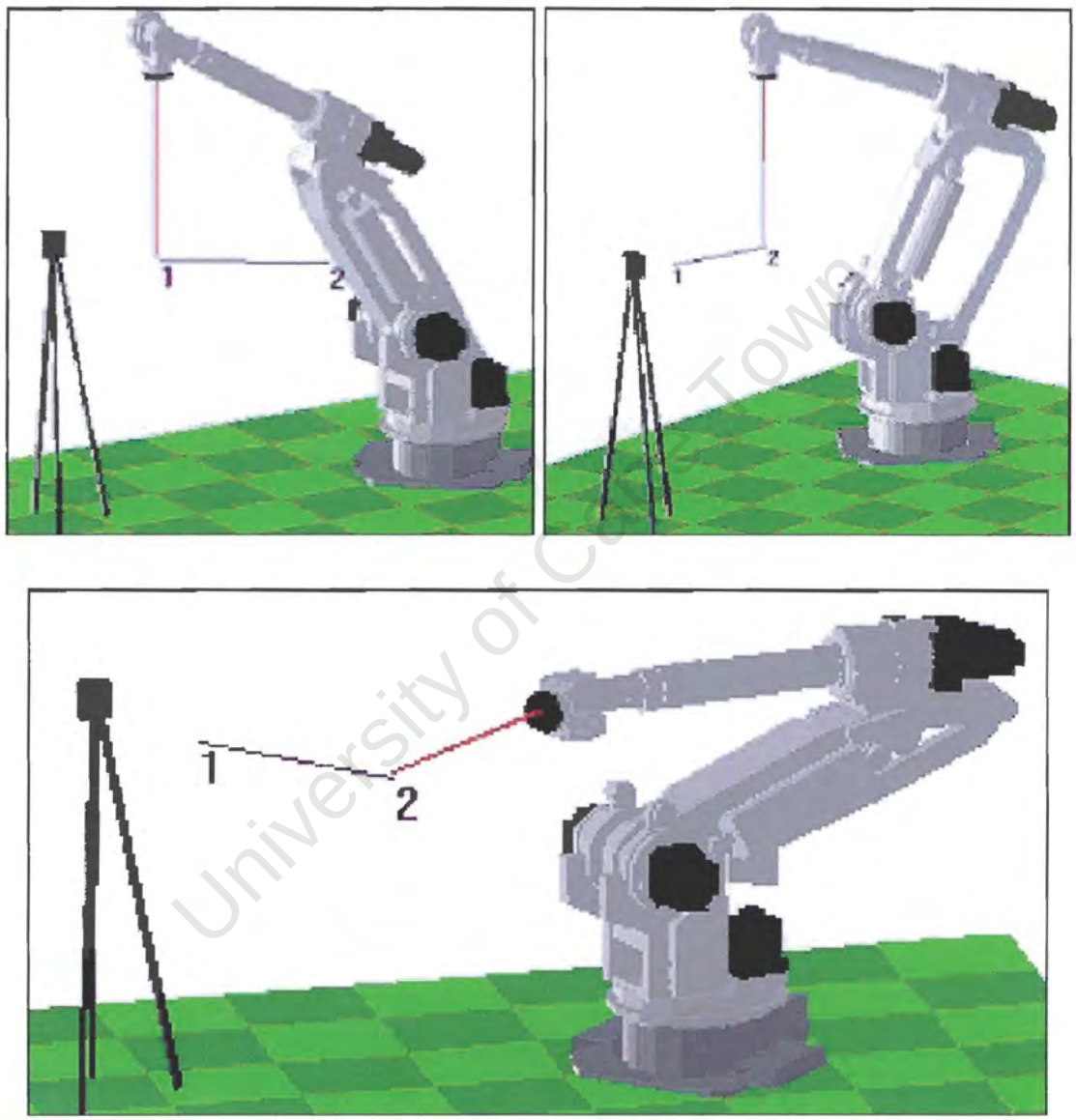

Figure 4.4: LM accuracy tests using the long rod, Rod 2

(a) On the TCP of the robot wrist

(b) On the collimator cover of the C-arm

Figure 4.5: The placement of the retro-reflective markers.

on the front of the collimator cover on the LODOX C-arm (Figure 4.5). Infra-red light was then strobed on the markers by the infra-red light emitting diodes which surround each of the lenses of the cameras. The reflections of the markers were then captured by the cameras. The images were processed by the Vicon Workstation 3.0 motion analysis software and converted by the Rdata2 conversion program into ASCII files.

Simple two-position jobs were programmed for the robot tests. One each in the vertical, horizontal and diagonal planes, all at a speed of 1000mm/s and over a distance of 1m.

For the LODOX machine, six tests were conducted. The distance of the tests was roughly two metres and the speed was the full speed of a normal LODOX scan, approximately 140mm/s. Four tests were conducted with the C-arm in its open position (antero-posterior scans) and two tests in the extended position (lateral and erect chest scans).

Rotary Encoder

The second method for testing CV accuracy consisted of using a rotary encoder to measure the velocity. The testing rig consisted of a pulley, a rotary encoder, a length of video tape and a PC.

The pulley was machined to a circumference of 25mm with two walls to act as guides for the tape running over it. It was then mounted on the shaft of the rotary encoder, which itself was mounted on a fixed surface like a wall, exactly horizontal to the plane of movement of the subject. The length of video tape was then placed on the pulley, with the one end attached to the subject and the other to a counter-weight. The length of tape from the pulley to the subject was therefore directly orthogonal to the wall, while the length of tape from the pulley to the weight hung vertically downwards. As the subject moved, the tape was pulled over the pulley and pulses were generated by the rotary encoder. The encoder is a 500 pulse per revolution rotary encoder which was attached to the serial port of the PC. A specially designed program written by Jan Van Der Merwe at the NAC captured the pulses and outputted them to .txt files.

A ROTSY picture of the testing rig attached to the robot's TCP is given in Figure 4.6. A similar setup was used for testing the LODOX machine, where the tape was attached to the collimator housing on the C-arm.

Figure 4.6: Testing for CV accuracy with the rotary encoder rig

Because the circumference of the pulley was 25mm and the encoder produced a maximum of 500 pulses per revolution, a pulse was produced by every 0.05mm of tape that passed over the pulley. The capture program on the PC could be set to

different step sizes, 0.05mm – 2mm. A step size of 2mm used every fortieth pulse, while a step size of 0.5mm used every pulse.

The tests on the LODOX were made with both wide (8mm) and narrow (4mm) video tape, half of each moving towards the pulley and half away. Tests were also made with different sample steps. A total of thirty-two tests were conducted on the LODOX machine. All tests on the LODOX machine were conducted over a distance of approximately one metre and at the maximum speed of 140mm/s.

Many tests were conducted on the robot at speeds of 100, 200mm/s, 500mm/s and 1000mm/s. The distance of movement was approximately 1m and the tests were conducted both towards and away from the robot. Various step sizes from 0.05mm – 2mm were also used.

Accelerometer System

The third method for measuring CV accuracy was by using a system of miniature accelerometers to measure the acceleration of the subjects. This acceleration was then integrated to give a velocity.

The accelerometer used was the Analog Devices ADXL105 . The ADXL105 is a high performance, high accuracy single axis accelerometer. It can measure both dynamic accelerations typical of vibration, and static accelerations such as inertial force, gravity or tilt. It has a full scale range of ±5g and a resolution of 2mg. The full data sheet for the ADXL105 can be found in Appendix B.

As the ADXL105 accelerometer measures only a single axis, three accelerometers were needed to measure in the three planes. The output of the accelerometer is an analogue voltage nominally 250mV/g. A major concern with using accelerometers is increasing the signal-to-noise ratio. An R-C low-pass filter was therefore added between the V_{dd} pin and the supply. In addition to further reduce noise on the supply, common mode rejection was employed, and the voltage was outputted in a differential mode. A schematic of the aforementioned circuit is given in Figure 4.7. Although the ADXL105 has both an uncommitted amplifier for setting the output scale factor, and a ratiometric voltage-output-temperature sensor for optional calibration of the accelerometer over temperature, neither of these were used. The capture card was

rather used for scaling the output and the temperature sensor was not needed as the temperature of the subjects was essentially constant.

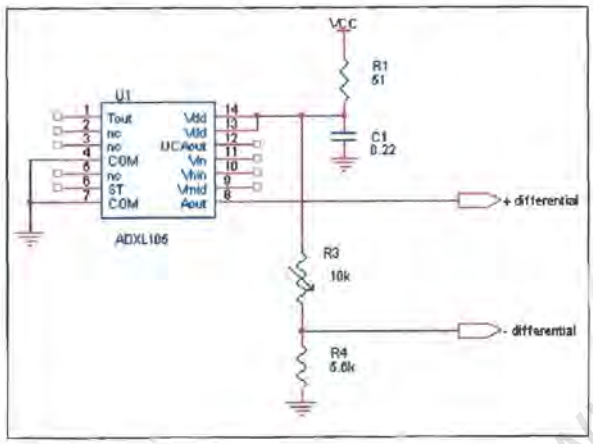

Figure 4.7: The schematic of the accelerometer circuit (for one plane)

The accelerometers were mounted orthogonal to each other on a machined nylon block (Figure 4.8). The accelerometers were bonded to the block with epoxy, with their legs facing outwards. This was to reduce vibrations of the electronic components from affecting the accelerometer itself.

Figure 4.8: The three accelerometers mounted orthogonally on the nylon block

The ADXL105 is designed so that Electro Magnetic Interference (EMI) or magnetic fields do not normally affect it, although the other electrical components of the test rig are affected by EMI which was experienced in initial testing. The unshielded 8-core cable was therefore replaced with a shielded cable and ferrite cores were attached to either end of the cable. The nylon block was also encased in a grounded metal box (Figure 4.9). These precautions together with the low-pass filter on the supply voltage and a differential output voltage helped to produce useful signals from the tests.The signals captured with this shielding were then able to be used.

Figure 4.9: The shielding of the accelerometers

The capture card used to interface with the accelerometers was the Eagle Technology PC30FA. The PC30FA is a 12bit ISA-bus multifunction analogue and digital I/O board. It accommodates the following signals: 16 single ended or 8 differential lines of analogue input; 4 lines of analogue output; 24 digital I/O lines; external trigger and clock; ± 12V power supply, with limited current output, as well as an optional $+5$V supply. The card also has a programmable gain of 10, 100 or 1000. The data sheet for the PC30FA card can be found in Appendix C.

As the output of the accelerometers was a differential analogue voltage, three single ended and three differential analogue inputs on the capture card were used, as well as the $+5$V supply and ground. The PC30FA has a capture rate of 100kHz per channel when capturing two or more channels, and 333kHz when capturing a single channel.

The program that was used to capture the data was Wave View. This software was supplied with the capture card from Eagle Technology. Wave View is a DOS based capture and analysis program which can handle multiple channels and boards simultaneously. In addition it can control the gain for each channel independently. The analysis part of the program can produce Fast Fourier Transforms (FFTs) of any captured signal. All captured data can be printed directly from the program or can be outputted as text files.

The captured data consisted of three tab-delimited columns, one for each of the planes of movement. The output of the accelerometers is a voltage representing an acceleration. Conversion of these voltages into meaningful velocities in m/s, required the use of other applications. The functions that were required to be implemented in these applications were as follows:

1. The captured data file must be loaded into memory.
2. The calibration files must be loaded into memory.
3. The scale factor for the conversion of voltage (V) to acceleration (m/s^2) must be calculated from the calibration files, and must be applied to the data file.
4. The acceleration must be low-pass filtered.
5. The velocity must be calculated by integrating the acceleration (raw and filtered).
6. The displacement must be calculated by integrating the velocity (raw and filtered).
7. The acceleration, velocity and displacement curves must be plotted (raw and filtered).

Initially MATLAB code was written to implement the aforementioned functions. This code can be found in Appendix D. In addition, the same functions were implemented in code written for the National Instruments LabVIEW package. LabVIEW allows the user to create a Virtual Instrument (VI) which represents a standard laboratory instrument on a PC. Signals are directly input into the PC via a capture card, or are loaded from text files. VIs are extremely customisable with highly configurable Graphical User Interfaces (GUIs). This was the reason for using LabVIEW as well as MATLAB to analyse the sampled data.

A VI was designed for the analysis of the captured data, using many built-in functions. This VI applied the aforementioned functions to the outputted text files from LabVIEW. The GUI of this VI has two pages: the first depicting the acceleration in volts, both raw and filtered; and the second depicting the scaled and filtered acceleration, and the integrated velocity (integrated from the raw acceleration)(Figure 4.10). The "circuit diagram" of this VI is given in Appendix E, together with a legend of some of the built-in functions used. In addition to the designed VI, a VI supplied by Eagle Technology for their PC30FA capture card was used for monitoring the output of the accelerometers in real-time. This VI was used to calibrate the zero-offset of each of the accelerometers by adjusting the variable resistors for each plane of movement.

The CV accuracy tests using the accelerometers were run with the capture card set to its maximum sampling rate of 333kHz. At this rate each plane of movement had to

be captured individually. Five tests each per plane of movement were made on the LODOX machine with the C-arm moving at the default speed of 0.14m/s. The same was also conducted on the robot. Moreover each set of five tests were conducted in three different areas of the robot's working envelope. These different areas of movement are depicted in Figure 4.11.

The placement of the accelerometer rig on LODOX-LACT and the robot are shown in Figure 4.12.

4.3 Results

4.3.1 Results of the Repetitive Positioning Accuracy Tests

For the two tests conducted on the robot, the deviations were smaller than the resolution of the theodolite (0.1mm), hence actual values can not be given.

4.3.2 Results of the Linear Movement Accuracy Tests

For all six tests conducted, in both orthogonal directions to the axis of movement, the deviation was observed to be less than 5 millimetres. Once again actual values can not be given, as the movement was "watched" through the viewfinder of the theodolite and the deviation was constantly varying.

4.3.3 Results of the Constant Velocity Accuracy Tests

Digital Cameras

Three dimensional displacement data were outputted from the Vicon system. The data were then filtered and the first and second derivatives in the time domain were calculated using first-order finite differences. The above process was all done automatically in software called GGPSA developed by Giannis Giakas (Giakas and Balt-

Table 4.1: Results of the Constant Velocity accuracy tests on LODOX using the digital cameras.

(mm/s)	OpenLR1	Open RL1	Open LR2	OpenRL2	Closed RL	Closed LR
Mean	135.8	135.8	135.8	135.8	136.0	136.0
Std.Dev.	0.6	0.5	0.7	0.7	1.6	1.2

zopoulos, 1997a,b; Giakas, 2001). The data were filtered by the software using a second-order Butterworth low-pass filter. The cut-off frequency was determined by the software through assessing the power spectrum of the raw displacement data.

It was difficult to align the co-ordinate system of the digital cameras with both the robot and the LODOX co-ordinate systems. Hence it could be seen in the displacement data that there appeared to be gross movement on all axes, when there should have been only movement along one or perhaps two axes (depending on the job). This problem was worst for the tests on the robot as can be seen in Figure 4.13. The blue line (X) depicts displacement in the horizontal plane, which is correct, although movement in the other two planes is evident from the not-zero gradient of the purple (Y) and red (Z) lines, which is incorrect. To resolve this problem, resultant velocities were calculated from each set of co-ordinates using pythagoras in three dimensions.

Both sets of tests (robot and LODOX) captured data which included acceleration up to and deceleration from the programmed velocity. As only the period of constant velocity was of interest, each test was cropped. A standard deviation and mean for each of these cropped tests was then calculated for LODOX (Table 4.1) and the robot (Table 4.2).

Table 4.2: Results of the CV accuracy tests on the robot using the digital cameras.

(mm/s)	V1000	H1000	D1000
Mean	235.2	331.3	495.9
Std.Dev.	0.7	2.2	1.1

In Table 4.1, OpenLR1 refers to the first test with the C-arm of LODOX in its normal position moving from the left to the right, ClosedRL2 similarly refers to the second

test with the C-arm of LODOX in its extended position moving from the right to left. In Table 4.2, V1000 refers to the vertical test with the speed set at 1000mm/s, similarly H1000 and D1000 are for the horizontal and diagonal tests respectively at 1000mm/s.

Rotary Encoder

The pulses outputted from the rotary encoder were captured by a PC. The data were then differentiated and outputted as text files. No filtering occurred prior to differentiation.

The tests performed on the LODOX machine with the rotary encoder totalled thirty-two, eight tests each for step sizes ranging from 0.1mm – 2mm. Unfortunately the tests with the 0.1mm step size were corrupted by the capture PC. Only tests with a velocity of 100mm/s were considered for the robot, as this was the speed closest to that of LODOX.

The results of the tests on LODOX and the robot are given in Table 4.3 and Table 4.4 respectively. For each test, test number, tape width, distance between pulses, equivalent sample rate at constant velocity, direction of test (away from—A, towards—T encoder), standard deviation and mean are given. Again all tests were cropped, to remove the acceleration to and deceleration from the programmed constant velocity, this before calculation of mean and standard deviation.

Accelerometers

The results of the CV accuracy tests using the accelerometer block are given in Table 4.5. Tests 1-45 are concerned with the robot, and 46-60 with the LODOX machine. The tests on the robot are divided into three sets, each one for a different area of movement in the robot's working envelope (Figure 4.11). For each test, a mean and a standard deviation are given. As five tests were conducted for each axis and position, an average mean and standard deviation for the five tests are also given.

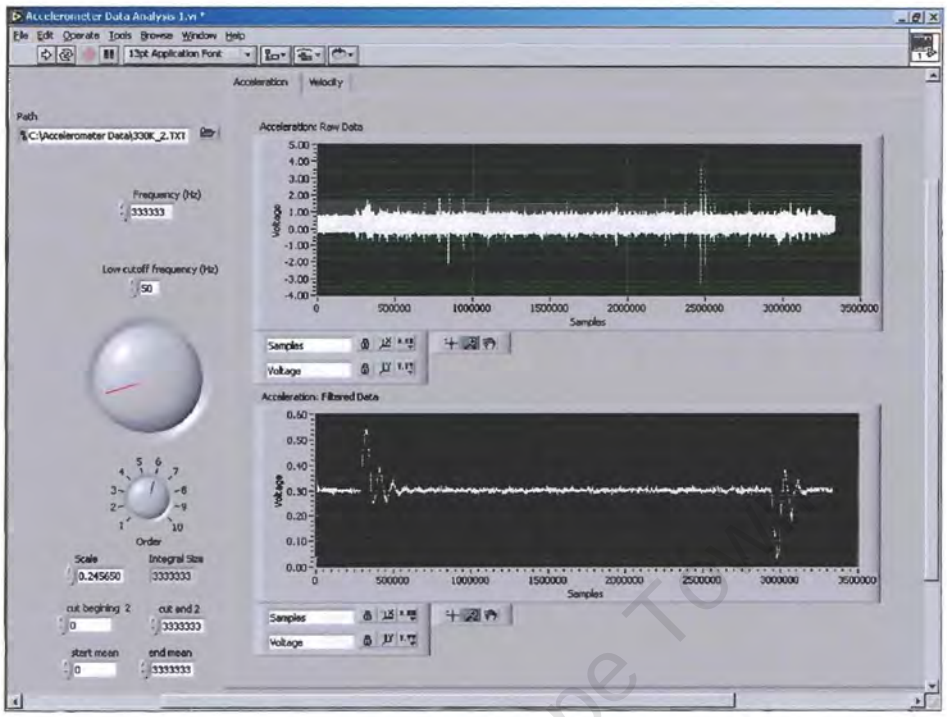

(a) The raw and filtered acceleration in volts.

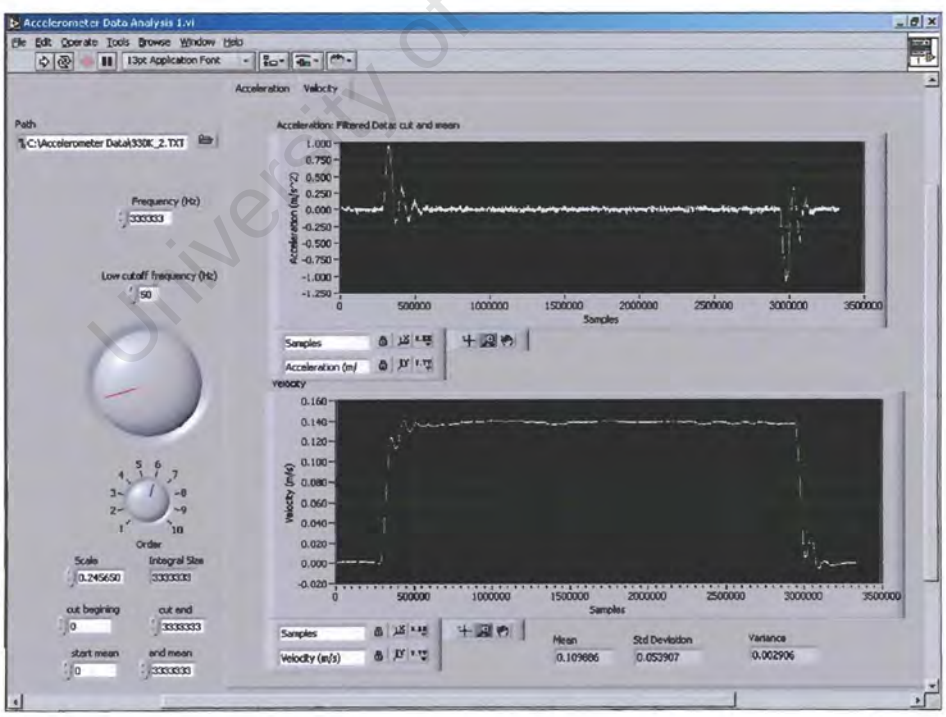

(b) The filtered and scaled acceleration (in m/s) and the raw velocity (in m/s^2)

Figure 4.10: The graphical-user-interface of the Accelerometer Data Analysis VI.

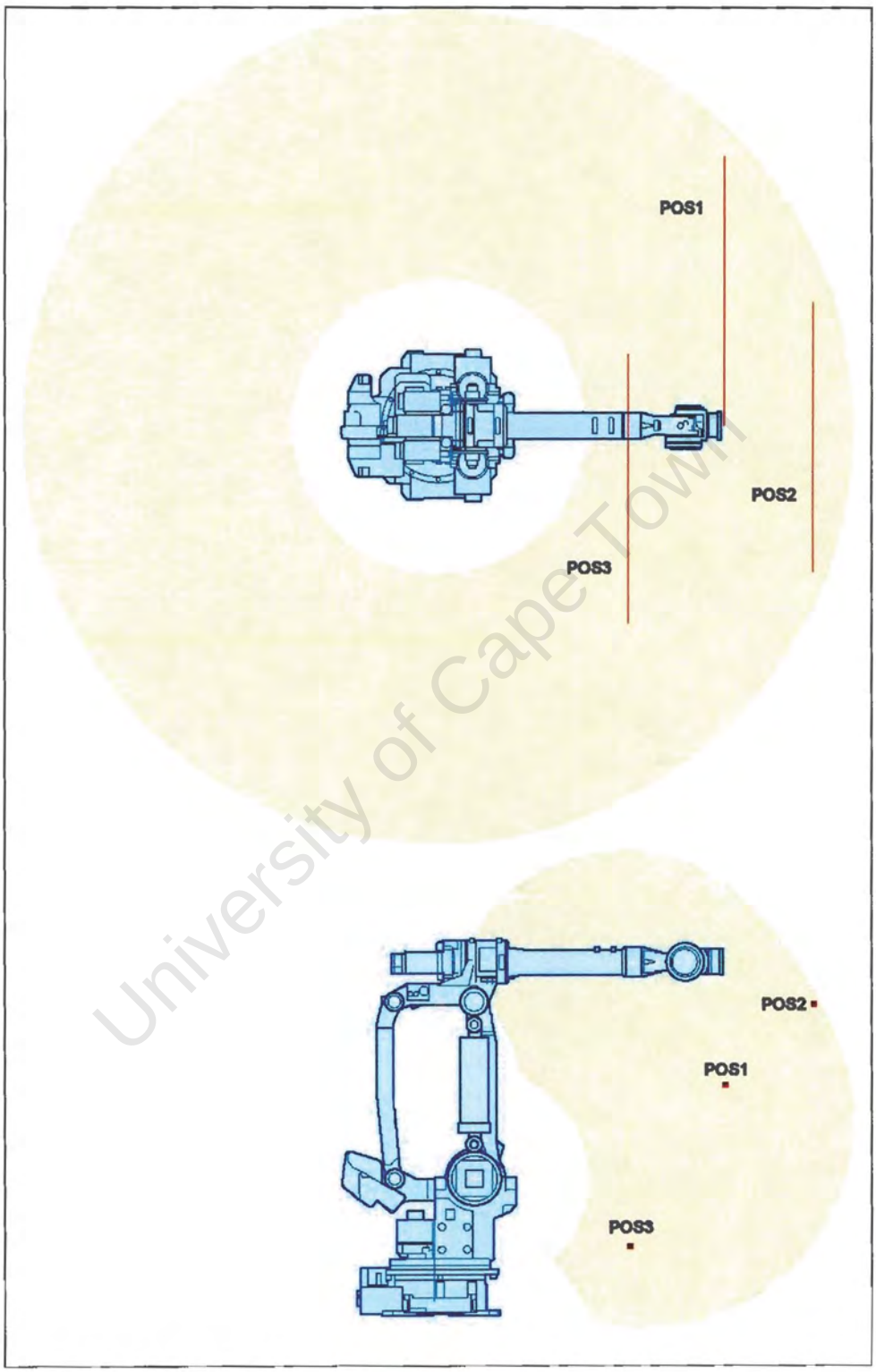

Figure 4.11: The location of the three sets of CV accuracy tests (using accelerometers) conducted on the robot.

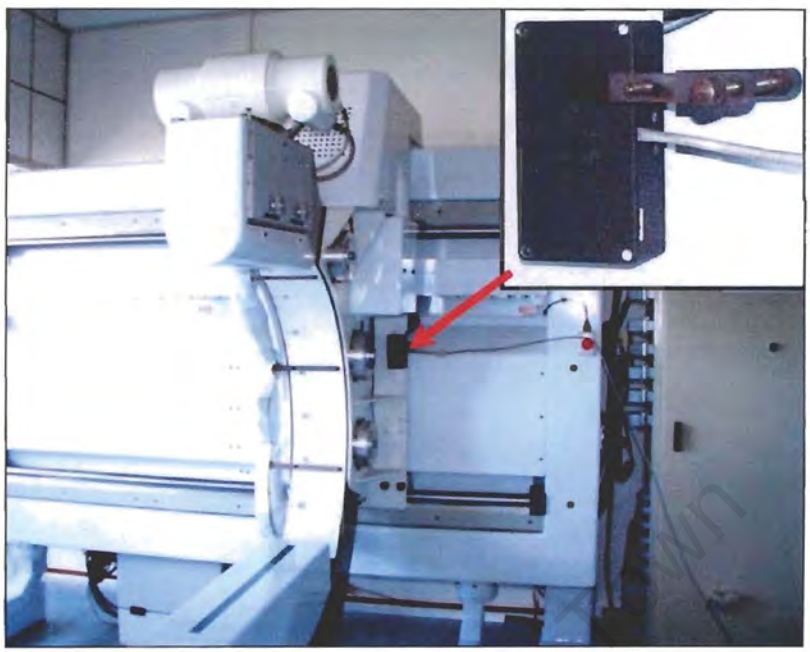

(a) On LODOX-LACT.

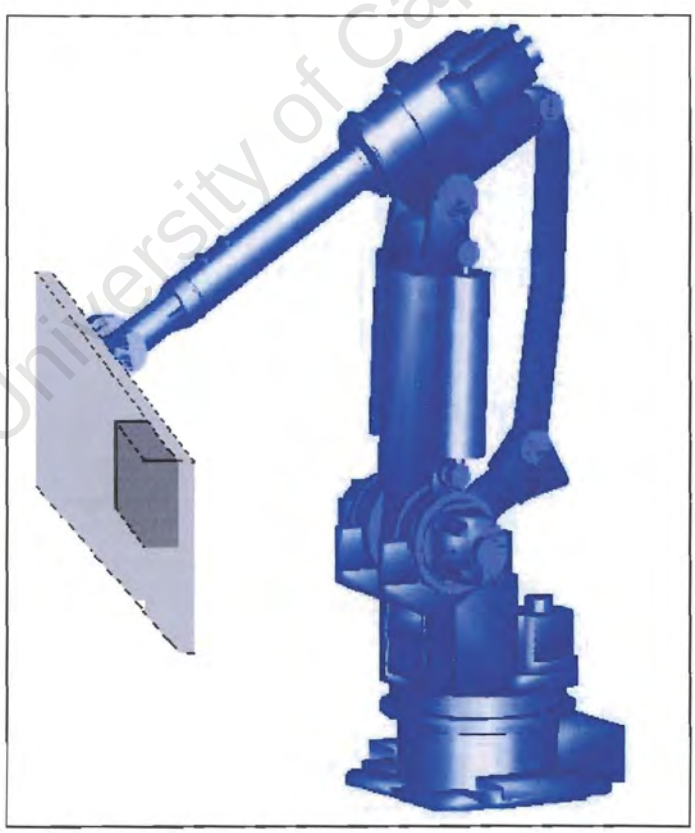

(b) On the robot.

Figure 4.12: The placement of the accelerometer rig.

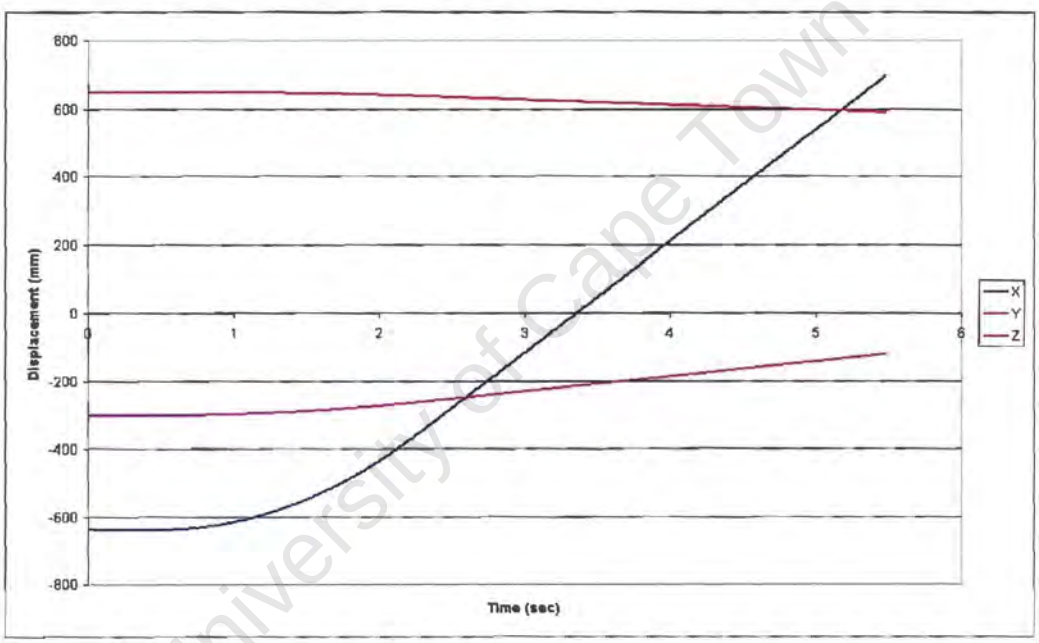

Figure 4.13: A displacement vs. time graph of the robot Tool Centre Point moving ±1.4m horizontally.

Table 4.3: Results of the CV accuracy tests on LODOX using the rotary encoder.

Broad Tape												
Test Number	1	2	3	4	5	6	7	8	9	10	11	12
Pulse Distance(mm)	1	1	1	1	2	2	2	2	0.2	0.2	0.2	0.2
Equiv.Sample Rate(Hz)	140	140	140	140	70	70	70	70	700	700	700	700
Direction	A	A	T	T	A	T	A	T	A	T	A	T
Mean(mm/s)	139.5	139.5	139.5	139.5	139.5	139.5	139.5	139.5	139.5	139.5	139.5	139.4
Std.Dev(mm/s)	1.0	1.1	1.0	1.0	0.8	0.8	0.8	0.8	2.2	2.4	2.2	2.8
Narrow Tape												
Test Number	21	22	23	24	25	26	27	28	29	30	31	32
Pulse Distance(mm)	0.2	0.2	0.2	0.2	1	1	1	1	2	2	2	2
Equiv.Sample Rate(Hz)	700	700	700	700	140	140	140	140	70	70	70	70
Direction	A	T	A	T	A	T	A	T	A	T	A	T
Mean(mm/s)	139.5	139.5	139.6	139.5	139.5	139.5	139.5	139.5	139.6	139.5	139.5	139.5
Std.Dev(mm/s)	2.0	1.9	2.1	1.9	1.3	1.3	1.3	1.3	8.5	0.7	0.7	0.6

Table 4.4: Results of the CV accuracy tests on the robot using the rotary encoder.

	Broad Tape		Narrow Tape	
Test Number	BT1	BT2	NT1	NT2
Pulse Distance(mm)	0.1	0.2	0.1	0.2
Equiv.Sample Rate(Hz)	1000	500	1000	500
Direction	A	T	T	A
Mean(mm/s)	100.0	100.0	100.0	100.0
Std.Dev(mm/s)	3.0	3.0	2.9	2.9

Table 4.5: Results of the CV accuracy tests on the robot and LODOX using the accelerometer block.

ROBOT POS1				ROBOT POS2			ROBOT POS3			LODOX		
Axis	Test	Mean	Std.Dev.	Test	Mean	Std.Dev.	Test	Mean	Std.Dev.	Test	Mean	Std.Dev.
0	1	164.9	4.4	16	156.8	3.3	31	194.0	4.6	46	134.5	4.5
0	2	154.4	5.1	17	143.4	3.5	32	181.7	4.6	47	143.7	2.3
0	3	161.0	4.9	18	160.2	3.3	33	182.0	4.2	48	142.5	3.6
0	4	154.5	5.5	19	161.6	4.1	34	176.7	5.1	49	148.0	2.5
0	5	163.6	5.5	20	164.6	3.3	35	180.4	3.5	50	147.7	4.6
Ave.		159.7	5.1		157.3	3.5		183.0	4.4		143.3	3.5
1	6	-3.1	3.0	21	-0.3	1.9	36	3.6	2.5	51	3.5	2.7
1	7	-10.8	3.0	22	-9.9	3.9	37	-14.5	6.2	52	-0.6	1.2
1	8	-3.4	3.4	23	5.5	3.3	38	4.4	3.4	53	-10.3	2.1
1	9	-8.7	3.3	24	5.5	3.3	39	-1.8	4.7	54	-7.4	1.6
1	10	5.4	2.0	25	21.3	7.7	40	-1.6	3.2	55	10.0	8.2
Ave.		-4.1	2.9		4.4	4.0		-2.0	4.0		-1.0	3.2
2	11	-7.9	4.3	26	-13.0	3.5	41	8.8	5.9	56	-8.9	2.3
2	12	3.1	1.5	27	0.4	2.1	42	-2.0	3.2	57	-0.8	3.1
2	13	0.2	1.5	28	2.2	5.2	43	-0.4	4.2	58	3.8	1.6
2	14	-10.3	1.6	29	8.6	3.0	44	5.8	2.8	59	-17.5	6.8
2	15	-10.3	1.6	30	8.6	3.0	45	-4.7	2.5	60	0.1	1.4
Ave.		-5.0	2.1		1.4	3.4		1.5	3.7		-4.7	3.0

4.4 Discussion

The high definition images that are produced by the LODOX technology are due to the algorithm used to capture the images, the high quality CCD cameras which actually capture the images and the accuracy of the mechanics of the machine itself. The first two issues are not relevant to this project, although the last is most important. When assessing the mechanics of the LODOX machine, a conclusion may be easily drawn that the whole machine is very strong structurally, the aim being to keep the machine very stiff to reduce vibrations. Vibrations of the machine would affect image quality, in particular vibrations of the C-arm and between the two ends of the C-arm. There are only two degrees-of-freedom in the present LODOX machines, with the other degrees being provided by the trolley. It follows that with the more degrees of freedom a machine has, the more chance that vibration problems would occur. Hence with a six degree-of-freedom robot arm, vibration is far more of an issue. In addition, repeatability is also more likely to be affected by higher degrees-of-freedom.

In addition to image quality being affected by vibration, X-ray dosage to the body would be affected to a lesser extent. The movement of the C-arm must be constant and smooth, so that each part of the body gets the same dose of X-rays. Although non-constant movement would probably only minutely affect the evenness of dosage to the patient, this may be a stumbling block when applying for FDA or CE certification.

Hence the testing of accuracy of the robot and LODOX was an integral part of this project, which consumed more than half of the time allocated to the project. The major problem in assessing the accuracy of the two machines, was that there was no quantifiable evidence of how or what type (frequency, amplitude, etc.) of vibration affected the image quality of the LODOX images. Therefore the frequency bandwidth of the accuracy tests had to be as wide as possible, which resulted in large and cumbersome files. Also to filter out noise was very difficult as the frequency of the signal and of the noise was not known.

4.4.1 Repetitive Positioning Accuracy Tests

The RP accuracy tests were only conducted with Rod 2 as it is the longer of the two rods and any deviation by the robot would be more accentuated with the longer rod. The results of the RP accuracy tests on the robot revealed no detectable deviation (smaller than resolution of theodolite—$< \pm 1$mm) , and therefore this confirmed MOTOMAN's statement of an RP accuracy of ≤ 4mm. However the independent tests conducted at the NAC were with the robot unloaded, while MOTOMAN's were at full load of 150kg. Hence further tests were conducted with a load of 90kg. Again no deviation was detected. But the conditions under which both machines were tested were still not the same. The RP tests by MOTOMAN were conducted at full load, as well as full speed. Although there was a difference in load between MOTOMAN's and the NAC tests, it was felt that as there was no difference in the measured RP accuracy between the unloaded and the 90kg loaded test, the extra 60kg would still have no effect on RP accuracy. The reason for using lower than the full load was for safety reasons and for convenience. In addition, the speed of MOTOMAN's tests and ours were not the same. This is because the robot at the NAC has had its acceleration retarded for safety reasons. Hence the maximum speed attained was not that which MOTOMAN tested their robot at.

All in all, the RP tests were satisfactory, as this type of accuracy is the least important for the plane x-rays that LODOX produces. It does not really affect the image quality, as where a scan actually starts and stops, does affect the image quality. On the other hand, for possible CT scanning this type of accuracy would be more critical, as the alignment of CT slices would rely on RP accuracy. Also it may be required to know the accuracy of the RP down to a matter of microns.

4.4.2 Linear Movement Accuracy Tests

The LM accuracy tests were carried out using the theodolite. Once again the results were mostly qualitative, although some quantitative results were also recorded. The LM accuracy was seen (through the theodolite) to be $\leq \pm 0.5$mm in both possible planes of movement. This figure was achieved by the use of the machined point which was attached to each rod. The cross-hairs of the theodolite could be seen to move

less than the step between the different diameters, which is 0.5mm. The deviation from the perfect linear movement was not repetitive or regular. By duplicating a test, it could again be seen that the inaccuracies were not in the same place. A problem which occurred with using a theodolite to measure this LM accuracy, was that the view finder had to be continually focussed as the distance to the point constantly changed. This therefore enforced the LM tests to be done at low velocities. LM accuracy may be seen as part of the CV accuracy. Essentially if the LM is totally accurate, the velocity tangentially to the line of movement is constant and zero. Hence the LM accuracy can be compared to the the other constant velocity tests.

Both the RP and LM test results were mostly qualitative rather than quantitative, due to the type of testing instrument. Also the resolution of the theodolite is only a tenth of a millimetre, whereas accuracies of microns may be required. Possible test equipment which could produce more quantitative results and have a finer resolution are that of laser displacement testing devices. These devices should be used in any further testing of the RP and LM accuracies.

It was assumed that the RP and LM accuracies of the LODOX machines were perfect, or accurate enough to produce high quality images, hence these accuracy tests were only conducted on the robot. This assumption may not be true, and further RP and LM may be needed to be conducted on the LODOX machines. Accuracy tests for constant velocity however were conducted on both the robot and LODOX, as accuracy of this sort was felt to be the most critical to image quality.

4.4.3 Constant Velocity Accuracy Tests

Three different testing methods were used to test CV accuracy for the robot and the LODOX machine. The reason for this was that the early results of first two testing regimes were initially not felt to be suitable, as their resolutions were not high enough. Also the sample rates of the first two methods were felt not to be high enough to capture any high frequency vibration that may be present on the two machines. However the results of each of the regimes will be discussed separately and then will be compared.

The tests using the digital cameras yielded good results at first glance. The mean velocity was essentially constant at 135.8mm/s with a standard deviation of 0.5mm/s-0.7mm/s for LODOX in the normal position, and a mean of 136.0mm/s and a standard deviation of 1.2mm/s – 1.6mm/s in the extended position. This is just a range of 0.4% – 1.1% standard deviation from the mean. The increased standard deviation for the extended position can be attributed the greater lever-arm when the LODOX is extended, hence greater vibration.

Although the standard deviation for the three CV tests with the digital cameras on the robot were very good with values of 0.7mm/s – 2.2mm/s, a range of 0.2% – 0.7% standard deviation from the mean, the means varied greatly from 235.2mm/s – 495.9mm/s. The velocity was programmed to be 1000mm/s for all three tests, although due to the acceleration retarding that is built into the NAC robot for safety reasons, this velocity was never reached. The question may be asked then, why were the attained velocities not the same? The reason is that depending on the type of movement and where exactly the TCP of the robot is in its working envelope, affects its maximum acceleration. The robot has six different joints and moves according to these joints. To achieve a linear movement requires constantly varying angular velocities for each of the joints. The retardation of the acceleration is not on linear acceleration but rather on angular acceleration. Further tests should be conducted with the programmed velocity being that of LODOX and nothing else, then a proper comparison could be made between the two machines.

When applying Butterworth low pass filters to the displacement data captured by the digital cameras, it is important to choose the correct cut-off frequency. There are many semi and automatic filtering algorithms which can perform this.

On further consideration, the results from the cameras were found to be not accurate enough. The reasons for this was that it was felt that the sample rate of the digital cameras was not high enough to capture possible high frequency vibrations, and the resolution of the cameras was also insufficient. The cameras sampled at only 120Hz, hence only 60Hz of the signal was able to be used because of Nyquist. In addition the GGPSA program filtered the displacement data to frequencies below 10Hz to reduce large errors occurring in the first differential-velocity plots. The resolution of the camera system was also estimated to be only 3mm which is much larger than the standard deviations achieved.

Hence another testing method was employed with a higher resolution and sample rate, this was by making use of a rotary encoder. The encoder produces 500 pulses per rotation, hence with the 25mm circumference pulley, the encoder has a maximum resolution of 0.05mm. The sample rate for rotary encoders is dependant on the linear speed of what is being measured. For the tests on LODOX and the robot, the resolutions were 0.2mm and 0.1mm respectively. Both the resolutions were supposed to be at the maximum of 0.05mm, but the capture PC and software could not handle the size of the files. As can be seen from Table 4.3 the mean was essentially constant a 139.5mm/s. However the standard deviation varied for the different resolutions from 0.6mm/s – 2.4mm/s (test 29 should be ignored as part of the data were corrupted). Generally the standard deviations were lower for the tests conducted with the narrow tape. This was because the narrow tape did not touch the sides of the pulley as much as the wider tape. Hence the narrower tape produced less noise. Also the standard deviations were greater for the tests at higher resolutions. This implies that the tests conducted with larger pulse distances were essentially low-pass filtered. The best data captured by the rotary encoder on LODOX were therefore at an equivalent sample rate of 700Hz and yielded a standard deviation of 1.4% of the mean velocity.

The CV tests with the rotary encoder conducted on the robot yielded slightly higher standard deviations. Although a slightly higher equivalent sample rate was achieved of 1000Hz, the standard deviation was 2.9% of the mean velocity. This was with the narrow tape and with a pulse distance of 0.1mm. The tests were not run at the same speed as LODOX, because these tests were run independently for another project at the NAC, and 100mm/s was more relevant to the NAC project, than for the robot.

It is clear from this testing method that the CV accuracy of the robot is half of that of LODOX, remembering that the rotary encoder could only capture in the line of movement, and therefore did not take into account the movements in the other two planes.

Once again the sample rate (or equivalent sample rate) of the chosen method—the rotary encoder—was not felt to be sufficient for measuring the possible high frequency vibrations that may occur in the robot and LODOX. The use of accelerometers was then considered. Rather than measuring displacement, from which velocity profiles were calculated by differentiation, the velocity profiles were instead formed by integrating the accelerometer data. Displacement data which are to be differentiated for

velocity profiles always have to be filtered first, or gross noise artifacts may be generated. Capturing the acceleration directly, essentially gives an idea of the vibrations directly. Also the capture rate of the accelerometers used is much higher than that of the digital cameras and the rotary encoder.

Although the PC30FA card can capture multiple signals at a maximum of 100kHz simultaneously, it was found that capturing at 333kHz yielded better results. This is because aliasing is reduced by sampling at higher frequencies. As a result of the high sample rate, enormous data files were produced which were cumbersome to handle and their analysis took some time to compute.

An analysis of the results of the tests conducted on the robot and the LODOX machine (Table 4.5) yields three important issues.

Firstly, the set of tests conducted at positions 1 and 2 yielded different results compared to those measured at position 3. The mean velocities in the plane of motion (Axis 1) measured at position 3 were significantly higher than those measured at position 1 and 2. This illustrates that the linear movement of the robot differs depending on where in the robot's workspace it occurs. It was expected that the vibration (amplitude and frequency) of the robot would differ at different points in the robot's workspace, due to the different positions of the six joints. This is illustrated, as the two planes tangential to the line of movement (Axis 1 and 2) for position 3 showed a mean generally lower than that of position 1 and 2. Hence from the above it can be concluded that linear movement of the robot is subject to where in the robot's envelope this movement occurs.

Secondly, while the robot was programmed to move at 140mm/s, the actual mean velocities of the different robot tests varied significantly from this, and from each other ($143.4\text{mm/s} - 194.0\text{mm/s}$). The mean velocity of the tests conducted on the LODOX machine also varied from the stipulated value of 140mm/s, ($134.5\text{mm/s} - 148.0\text{mm/s}$), but to a lesser degree. The average standard deviation of the means of the LODOX machine was also lower than that for the robot. It can be concluded that there is less deviation (vibration) from the constant velocity of 140mm/s by the LODOX machine compared to the robot, and therefore the LODOX appears to have a more constant velocity than the robot. Furthermore, it could be detected from some of the data

displayed in LabVIEW that there was regular vibration present in the signal of the robot, while it was not present in any of the signals of the LODOX machine.

Thirdly, there appears to be a problem with the accelerometer data. The manufacturer of the linear motor, KOLMORGEN claims that the motor is capable of a constant velocity with an accuracy of 0.01%. This is significantly less than the values that the accelerometer produced. The means of the velocity in the direction of movement for the LODOX machine varied by 9.6%, significantly more than that stated by the manufacturer. Although there may be other factors that affect the speed of the C-arm of LODOX (encoder feedback, misalignment, etc.), it is difficult to believe that they would have such an effect. From further research into velocity and position applications of accelerometers, it was found that accelerometers tend to produce "random walk drift". This means that minute changes in temperature and attitude of an accelerometer are exaggerated greatly when integrated once for velocity or twice for displacement (Hague *et al.*, 2000). Although accelerometers are still used for position and velocity measurement, such systems use other dead reckoning sensors such as Global Positioning Systems (GPSs) to reset the accelerometers on a regular basis. Such measures are not suitable for the current project, and hence the data from the accelerometers were also not sufficient to assist in making a definitive judgement of the accuracy of the robot and of the LODOX machine.

Chapter 5

Safety

5.1 Introduction

The Three Laws of Robotics (Asimov, 1942) state:

1. A robot may not injure a human being, or, through inaction allow a human being to come to harm.
2. A robot must obey the orders given it by human beings except where such orders would conflict with the First Law.
3. A robot must protect its own existence as long as such protection does not conflict with the First or Second Law.

Isaac Asimov's famous three robot laws continue to apply to all areas of safety in all fields of robot design. The first law is the most important and is the primary focus of all safety standards. The second and third laws in turn follow the first and are indirectly implemented by following safety standards and good design principles. Risk management in robotics is discussed by Clarke (1994) in an article entitled: *Asimov's Laws of Robotics—Implications for Information Technology.* In the article he states:

> Whether or not subjected to intrinsic laws or design guidelines, robotics embodies risks to property as well as to humans. These risks must be managed; appropriate forms of risk avoidance and diminution need to be

applied, and regimes for fallback, recovery, and retribution must be established. Controls are needed to ensure that intrinsic laws, if any, are operational at all times and that guidelines for design, development, testing, use, and maintenance are applied.

This chapter therefore documents the development, and the actual laws needed to ensure safety of both people and equipment through the safe design of the proposed LODOX-Robot (LR) machine. It begins by describing the existing safeguards in place for LODOX and for the robot. Following this a Failure Modes Effects and Criticality Analysis performed on LODOX is discussed. Finally a safety strategy for the LR system is proposed taking into account the results of the FMECA studies described above, relevant safety standards, and the literature on industrial and medical robot safety.

5.2 Existing Safety Strategies

Safety strategies that are described here concern safety of humans and not equipment, although they are often not mutually exclusive.

5.2.1 LODOX

There are three sources of hazards to humans who come into contact with the LODOX machine, be they patients, clinicians or others. These are from radiation, physical motion and electrical discharge.

Safeguards against irradiation of the operator and other persons in the vicinity of the LODOX machine (not the patient) include lead shielded walls, floors and ceilings where necessary. In some cases lead is not required as the concrete of the walls, floors and ceilings may provide sufficient shielding from the scattered radiation. Between the operator and the machine is a lead lined partition which includes a shielded window. A red line on the floor demarcates an area around the machine outside of which it is safe to stand during a scan. Any persons (other than the patient) residing

within this area during a scan are required to wear lead lined aprons. Radiation warning lights are present at the entrance to the room as well as on the operator console and the Local Positioning Console (LPC). These glow red while a scan is in progress.

Touch sensitive covers on both the detector housing (attached to the bottom of the C-arm) and the C-arm extension (attached to the top of the C-arm) act as safeguards against collision of the C-arm with anything in its path. The only other direct protection from possible hazards pertaining to the physical motion of the machine is a safety feature built into the linear and rotary motors. If a force of a certain amount is applied on the C-arm, either the linear motor drive or the rotary motor drive or both will trip and the system will halt immediately. The size of the force is programmed to be less than that which would cause a moderate injury. Emergency-stop buttons on the LPC, the operator console and on the base frame of the machine serve as indirect protection from possible hazards due to physical motion. In addition, the scan lever on the operator console is of the "dead man's handle" type, therefore scans cannot be run without an operator being in control of the machine. The emergency-stop buttons and the scan lever also help indirectly to protect against unwanted radiation exposure.

Potential hazards from electrical discharge are prevented by correct insulation of conductors and the presence of earth leakage circuits as stipulated in safety standards for electrical medical devices. The floor is also shielded against electro-static discharge.

5.2.2 MOTOMAN-SK150

There are two main sources of hazards to humans from industrial robots like the MOTOMAN-SK150. These are from physical motion and electrical discharge.

The safeguards against hazards caused by physical motion in place on the robot at NAC are only the limitation of the robot's acceleration and the emergency stop buttons. The robot has been limited to one hundredth of its maximum acceleration. Hence its maximum speed is greatly reduced. This helps to reduce the risk of the operator losing control of the robot during a teaching or programming phase. The emergency stop buttons are located on the MRC and the local positioning pendant.

There is no "dead-man's-handle", an operator is only required to begin a robot job, but not be present while it is running.

Safeguards against electrical discharge exist only through the principles of good manufacturing practice for all wiring and insulation. These are laid down in various standards on the design of industrial electrical equipment (American National Standards Institute/Robotic Industries Association, 1999; U.S. Department of Labor, Occupational Safety & Health Administration, 1981).

As the source of most hazards are from the physical motion of the robot, most safeguards are therefore concerned with this. These safeguards are designed to restrict access of persons from the robot's working area, and to shut the robot down (or not allow it to begin moving) if access is gained to its working area. The robot at the NAC was purchased to work in the medical sector and hence with clinicians and patients very near and sometimes in direct contact with it. Therefore the many safeguards used normally for this type of robot in an industrial environment are nonsensical, because their specific aim is to restrict persons from the robot working area. The robot at the NAC is hence potentially very dangerous, as it can damage equipment and harm people, without the system even detecting any problem.

5.3 Failure Mode Effects and Criticality Analyses

The Failure Modes, Effects and Criticality Analysis (FMECA) technique was described in Section 2.2.3. This section describes the results of the FMECA on LODOX and the reason for not conducting one on the robot.

5.3.1 LODOX

At the time of this project, Lodox Systems (PTY) LTD had made their first submission to the FDA for 510k approval. One of the procedures that they followed to get to this point was to have a risk assessment undertaken by an outside company (DEBTECH, 2002). This risk assessment was conducted at a very macro level (systems), it was therefore decided to conduct an FMECA at more of a micro level (systems, subsys-

tems, assemblies, subassemblies). The data gathered in the previous risk analysis were incorporated and expanded (in some cases) in the FMECA.

At the time of the project there were three distinct versions of the LODOX machine in existence. Firstly the oldest, LODOX-MP, the machine in Groote Schuur Hospital; secondly LODOX-LACT, the development model located in the Biomedical Engineering Department of the University of Cape Town; and thirdly LODOX 3, the model being built at DebTech in Johannesburg for commercial sale. It was decided to conduct the FMECA on the LODOX-LACT machine as this was the most convenient, and it was also the machine that had been worked on the most by the LODOX team who were the main source of information for the analysis.

The boundaries of the study were defined as the machine and the surrounding environment required for radiological equipment. This included shielded walls, floors and ceilings. Access control and radiation warning lights were also within the boundaries of the study. Air-conditioning and dust protection mechanisms were also included, as ambient environment conditions are required for the machine to work at its optimum level. Power supply to the machine as a whole was not within the boundaries, but a Uninterruptable Power Supply (UPS) were included. The communication network between the various computers and the Programmable Logic Controller (PLC) of the system was included, but not the network to the outside world (computers not part of the scanning or viewing system).

The LODOX-LACT machine and everything within the boundaries of the study was broken up in to systems, subsystems, assemblies and subassemblies. Because the systems and subsystems described functional elements, while the assemblies and subassemblies described geographical elements, it was decided to conduct the hybrid type of FMECA. All the elements of the machine were then coded logically according to their level.

The actual analysis of the whole system was then conducted. Initially data from the previous risk analysis were converted into a form suitable for the FMECA. Following this, through many hours of consultation with the LODOX team, failure modes and effects were determined for the elements of the machine. In addition quantitative assessments of the criticality of many of the failure effects were recorded. Finally recommendations for the reduction of risk of failure for each element were discussed.

All of the these steps were recorded in spreadsheets allowing for further analysis as an FMECA is never actually completed.

The results of the FMECA concerning safety indicated that the machine was generally safe for operators and patients. Radiation safety was sufficient, however restricting access to the LODOX room during scans needed to be implemented. Patient and operator safety issues were acceptable, but a few issues with the trolley design needed to be addressed, many of which were subsequently fixed on the trolley for the LODOX 3 machine.

As an example, part of the FMECA conducted on the LODOX-LACT machine concerning the patient interface (includes trolley and its location with the machine) is given in Appendix F. Legends for the various codes in the FMECA are also presented.

5.3.2 MOTOMAN-SK150

An analysis of the robot was not conducted. Firstly the author had little success in gathering in-depth data/specifications for the robot from the manufacturer in Sweden or the local agents in South Africa. One reason for this is that many robot manufacturers are uninterested in a medical projects, as liabilities from potential failures are too great. In comparison, all data on the LODOX system were readily available. In addition it was possible to speak directly with the designers at DebTech and hence gain insights into aspects of the machine that had not been documented.

Secondly, an FMECA should ideally be undertaken during development. The MOTOMAN SK150 robot has many years of past development as it is now a discontinued model. The reason for the use of a discontinued robot is that it was simply the only robot available. It is felt that the conclusions drawn from this study will be as attributable to newer robot models as they are to this discontinued model.

Thirdly the robot has been built according to international quality and safety standards. As the SK150 robot has been discontinued, if the LR system was found to be feasible, then another robot would have to be selected. Presently all of MOTOMAN's (and many other manufacturers') robots conform to the ANSI/RIA R15.06-1999 standard, therefore risk analyses on the robot in its (industrial) environment are not re-

quired as these analyses have been conducted already by the manufacturer during development.

5.4 Safety Strategy For A LODOX-Robot System

Due to the fact that the design of the proposed LR system is little more than a concept, it is difficult to specify safety measures for such a system. Rather strategies and general measures are proposed from the existing safeguards in both LODOX and the robot, results of the FMECA study described above, relevant safety standards and the literature on industrial and medical robot safety.

5.4.1 Classification Of The Proposed LODOX-Robot System

Before laying down a safety strategy for the proposed LR system, the system had to be categorised within the various medical robot types as described in Section 2.1.2. The LR machine fits best into the surgical category. This is despite the fact that surgical robots assist or do actual surgery, while the LR system is only a diagnostic tool. The other feature which defines surgical robots different to the other categories is that surgical robots can only be operated with a person present and in control. All other types of medical robots need not have a clinician present. Even some rehabilitation robots can be operated by the patient alone. The proposed LR system will require human control to operate (a "dead man's handle"). For this reason the LR system is categorised a surgical robot.

An example of a similar machine which falls in the surgical robot category is the Accuray CyberKnife system (Adler *et al.*, 1999). Just like LR it also cannot be operated without an operator being present, but although it does not ever make contact with the patient during normal operation, it is unlike LR in that it is a true surgical robot, be it of the non-invasive type. However the Accuray CyberKnife is still the closest type of medical robot to LR on the market. This is for two reasons: it carries a radiological source and it makes use of a large industrial robot. For these two reasons it was most interesting to the author for safety issues.

5.4.2 Possible Hazards From The Proposed LODOX-Robot System

Of the three sources of possible hazards to the patients and clinicians from the current LODOX machine, physical motion hazards are the most difficult to protect against. Therefore in the proposed LR system, physical motion hazards are of even greater importance to protect against, as the robot increases the kinetic energy greatly over that of the existing LODOX machine.

The safeguards against radiation and electrical discharge hazards in the proposed LR system can be taken from the existing LODOX machine because nothing in these two areas would change significantly.

The hazards due to physical movement can be broken up into three subsections: hazards from mass, hazards from speed, and hazards from power (Figure 5.1).

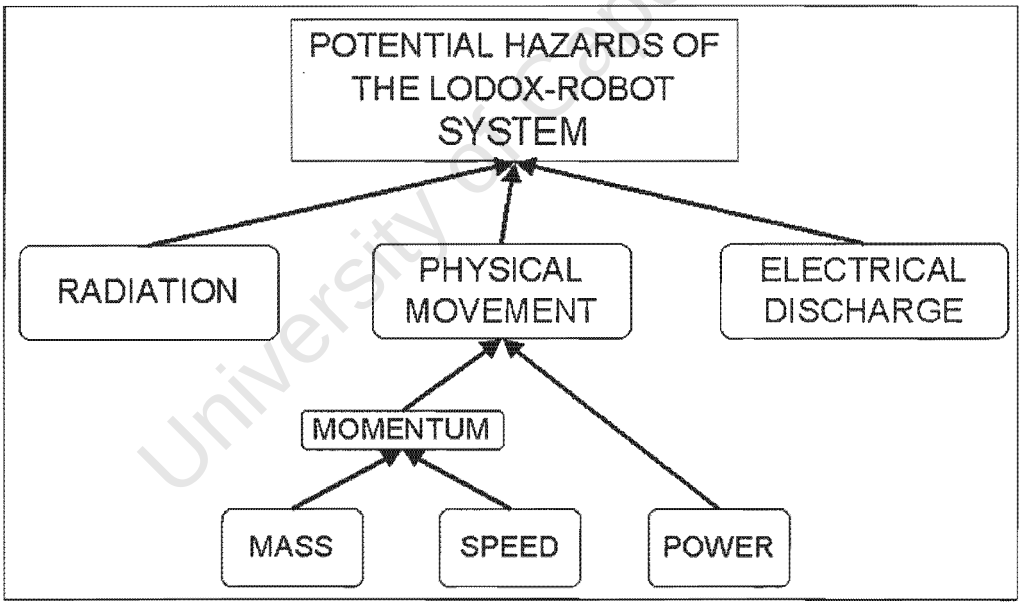

Figure 5.1: Potential hazards of the proposed LODOX-Robot system

Hazards From Mass

Due to the large mass of the C-arm, a heavy duty industrial robot is required to move it around. The C-arm including both the X-ray tube assembly and the detector

assembly weigh more than 300 kilograms. The MOTOMAN SK150 is actually only certified to carry a maximum of 150 kilograms. It is unclear in the robot specifications if this weight limit is due to a static (zero acceleration) or dynamic (maximum acceleration) stress limit. Therefore for a real LR system to be built, an even stronger and potentially more dangerous robot may possibly be required. However if the C-arm could be redesigned to optimise for a minimum mass, possibly a smaller robot could be utilised. Nevertheless the weight of the X-ray tube assembly and the detector assembly (together they weigh approximately 110 kilograms) cannot be reduced without major redesign of the core of the LODOX system. Therefore a medium to large industrial robot is still required.

The main possible hazard attributed to the mass of the LR system is its momentum. All surgical robots that the author has encountered, other than the Accuray CyberKnife, make use of small desktop-type robots with maximum load bearing capacities of less than 10 kilograms. This is mainly because the tools which the robots are manipulating are relatively small and light. Small robots are also used to reduce momentum, hence making it easier and quicker to bring the tool attached to the robot to a halt in both normal working conditions and in emergencies. A mitigating factor in the LR system's favour is that the system never makes contact with the person during normal operation, therefore there is a margin of area for the system to come to a stop safely before colliding with anything.

Hazards From Speed

Three issues relating to the speed of the robot have implications on possible hazards. Firstly the robot is capable of high speeds, secondly momentum is directly proportional to speed, and thirdly the distance travelled during a fault is determined by the velocity of the robot.

The maximum speed of the present LODOX machine in any direction is 0.14 metres per second, while the robot can reach speeds of 1.5 metres per second under some conditions. Hence the maximum speed of the robot could be reduced to something similar to that of the existing LODOX machine. However one of the main reasons for this feasibility study is to enable the machine to perform other types of scans,

in particular CT. For CT, faster speeds may be required particularly in rotation, the maximum speed may therefore not be able to be reduced as much as was hoped for.

Hazards from momentum were discussed in the previous section. As speed is directly proportional to momentum, it is important to reduce the speed as much as possible to reduce momentum and its related hazards.

Equipment damage and injuries resulting from a fault are limited by the velocity of the robot. This is because the displacement travelled is limited by the velocity.

Hazards From Power And Torque

One of the problems with using industrial robots in medical environments is that the robots are not "intrinsically safe". What this means is that all the failures of the robot should be predictable and all the faults should be handled online (Pierrot *et al.*, 1999). Such robots are designed from the ground up with safety as a priority. The main aspect which make these robots intrinsically safe is that they are designed with low installed power. The motors and joints used in these types of robots provide the minimum amount of power required for the task, thereby ensuring that in the event of a fault such as a collision with a person, as small an injury as possible is inflicted. In the development of a robotic system to assist doctors in monitoring arteries for cardiovascular disease prevention, Pierrot *et al.* (1999) conducted a feasibility study with an industrial robot to validate the concept. However the group had to abandon the industrial robot as the system was not considered safe enough for human testing. The actuators at the joints were too powerful and hence an intrinsically safe robot was rather designed—the Hippocrate robot.

According to the specifications of the MOTOMAN SK150, its weakest joint (T-axis) can impart a torque of 441 Newton metres, while its strongest joint (L-axis) can impart greater than 3600 Newton metres. The power of the robot is therefore easily sufficient to cause a major injury or fatality. An example of the power of the robot was made evident on one occasion when the author inadvertently drove the robot into the ceiling (at low speed). A 15mm mild steel plate was bolted onto the robot's TCP at the time and this plate was bent easily without any warning or alarm being issued from the system (no damage was done to ceiling or the robot in this collision).

5.4.3 Recommended Safeguards For The Proposed LODOX-Robot System

Safety strategies cannot prevent a machine from ever failing, but they can lower the probability of failures occurring. However only one failure in a thousand or a million is more than can be tolerated when such a failure could cause injury or death. Hence a system must be designed with the knowledge that it will fail at some time, and this failure must be detected and controlled. This concept is called "failing safely". In the case of surgical robots this usually involves shutting the robot down and removing it from the patient (Prouskas and Oakman, 1996).

Hence the safety strategy of the LR system should be to firstly *prevent* failure using safeguards, secondly if a failure occurs it must be *detected* using sensors, and thirdly once the failure is detected it must be *controlled* to minimise damage or injury through the use of intelligent control systems. Preventing, detecting or controlling potential failures that involve radiation and electrical discharge hazards will not be discussed here as the mechanisms in place on the existing LODOX machine are sufficient and should be included on the proposed LR machine. Only potential failures concerning physical movement hazards are discussed in the following sections.

Preventing Potential Failures

To prevent physical movement hazards attributed to the momentum of the robot and the C-arm, requires the reduction of the mass and speed of the moving part of the machine. Reducing the mass involves reducing the the mass of the C-arm either by using different materials or by totally redesigning the assembly in such a way that it is lighter. All that is required is that the detector assembly and the X-ray tube assembly be held in the same orientation and distance from each other as they are on the LODOX machine. The mass of the aforementioned assemblies can only be reduced by reducing the mass of their housings, and nothing else. The reduction of mass of the C-arm must not compromise the structural stiffness of the C-arm or this will impact badly on the image quality of the machine. By reducing the mass of the C-arm and the two assemblies attached to it, in essence the load of the robot is lessened and hence a smaller robot can be used, which in turn results in lower total momentum.

The maximum speed that the robot can reach is determined by the acceleration. This acceleration as mentioned before in Section 5.2.2 can be limited by the MRC. The maximum total linear and angular velocities need therefore to be determined for the movements involved in the scans that the LR machine would perform. Then the acceleration constant could be determined and programmed in the PLC. In addition it should be determined if the deceleration constant would also be affected, as keeping the deceleration constant as high as possible is preferential for safety reasons (emergency stops).

Preventing hazards due to the power and torque of the robot is difficult as the power of the robot is proportional to the load it is required to bear, and the momentum it is required to overcome. The best way to limit the power is to limit the size of the robot. Another way of limiting the power would be to use mechanical torque limiting devices which could be incorporated into each joint of the robot (Pierrot *et al.*, 1999). However this would require redesigning the robot itself, which defeats the purpose of using an off-the-shelf robot.

There are many other preventative strategies that could be employed on the LR machine, the most important two being redundancy and motion restriction (Kassel *et al.*, 1997; Pierrot *et al.*, 1999).

Redundancy of all safety critical systems is needed. There is obviously an increased cost but this should not amount to much in comparison to legal costs if a person is injured or killed and and the manufacturer is blamed for the accident. Redundant position and velocity sensors on the robot must be installed as the encoders on each motor of the robot may fail and there may be a loss of mechanical motion between the sensor and the actual output it is supposed to measure (Ng and Tan, 1996). All redundant sensors should be connected to a separate dedicated safety controller, with a separate UPS. This controller must be able to override the normal control of the machine and disable it at any time.

The range of motion of the proposed LR system is significantly more complicated than that of the existing LODOX machine because of the greater degrees-of-freedom of movement, hence there is a higher probability of movement error for the LR system over the LODOX system. To further reduce the chance of hazards from physical motion, the range of movement of the robot must be restricted. This motion restriction

is described in terms of restriction of working volume or axes limiting and issues of singularity (Kassel *et al.*, 1997; Fryman, 2002).

The working volume can be restricted by disabling some of the degrees of freedom of the system that are not needed. The robot can be restricted from a certain area by software as well as by hardware. Axes limiting is performed by providing adjustable mechanical stops which would physically prevent the robot from rotating further on a certain axis. The use of such mechanical methods are preferential to electrical or software methods in preventing hazards as they are found to be more reliable (Ng and Tan, 1996).

Singularity which is unique to robotics, is a condition caused by the collinear alignment of two or more robot axes resulting in unpredictable robot motion and velocities (Fryman, 2002). In other words a singularity is a point in space that a robotic arm reaches that presents it with many different, but correct routes for it to follow from its present position to the next position in space. Hence its motion is unpredictable and may result in a hazard. Such singularities are encountered first during "teaching" or programming, the risk of such a hazard occurring is therefore for the programmer and not the end users (clinicians and patients). The programmer must adjust the route to avoid the singularity when one is encountered and check the robot job runs correctly.

A "dead-man's-handle" device and emergency stop devices are the two safeguards which guard against all potential hazards (radiation, electrical discharge and physical movement) which must be implemented on the proposed LR machine. Both are found on the LODOX machine, while the former is not present on the robot. The dead-man's-handle on the LODOX machine is sufficient for the LR system, but can be improved. Recent studies have shown that such a device should not be a simple off-on device, but an off-on-off device (Fryman, 2002). People often react to emergencies by initially clenching their hand rather than releasing it, thereby not stopping the machine immediately. By having the three position handle this is alleviated.

Emergency stops are found on almost all large machines. They act to totally override and shut down the system. Although this is important, operators of such equipment try not to use these emergency stops or even try to "short-cut" the devices (Fryman, 2002). This is because of the loss of productivity and time wasted from having to restart the system after an emergency-stop button has been hit. Injuries can and have

occurred due to this reason. To combat this there should be two types of machine stops, a emergency-stop and a safety-stop. The emergency-stop should act normally and shut the whole system down, while the safety-stop should only disable the local part of the system, thereby alleviating the need to totally restart the system. The safety-stop may also be a passive stop and be triggered by another hazard preventing safeguard.

From the use of the FMECA technique in analysing the LODOX machine it is recommended that the technique be used if the LR machine were to enter the design and manufacture stage. This is ratified by the use of FMECA in every step of the development of the Hippocrate robot (Pierrot *et al.*, 1999) which acts to assist doctors in early detection of heart disease through the use of ultrasonic probes. Other risk assessment techniques may also be used during development.

Detecting Potential Failures

Before failures can be controlled, they must first be detected. The LODOX system has many "watchdog" devices to detect potential failures that may lead to hazards. These include the touch sensitive covers which detect collisions as well as a limit switch on the shutter in the X-ray assembly which reports that the shutter is open and x-rays may be emitted. All of the existing devices on the LODOX machine should be implemented on a future LR machine. In addition, further external sensors such as cameras and accelerometers should be used to help detect erratic movement and/or collisions. These external sensors should be connected to the same dedicated safety controller which the redundancy sensors are connected to. The mechanical limiting devices mentioned earlier should also be able to detect, and hence warn the system of a failure, and not just physically prevent one.

Controlling Potential Failures

Once a failure has been detected it must be controlled to ensure that the LR "fails safely". This means that the robot must shut down, and all danger to the patient and/or clinicians be removed. An example of a system where a robot does not "fail safely" is if during robotic surgery the robot (surgeon) falls onto the patient because

the holding torque of the joints is removed due to a power failure. This system should have mechanical breaking on the joints of the robot which activate automatically when the power is off.

Hence for the LR machine, all possible failure scenarios should be determined and be accounted for in the control system, particularly in the case of power failures, the safety and emergency-stop buttons being hit, and fire. In the event of power failure the robot is locked in position mechanically by its gearboxes. This is advantages in that the robot cannot ever fall onto somebody when the power is removed, however in the case that the robot has pinned a person or a limb, it is impossible to move the robot without power. To plan for this, there must always be sufficient battery backup power to move the robot.

Fail-safety concerning electrical discharge and radiation are sufficient on the LODOX machine and conform to safety standards, therefore nothing further is required for the LR machine in these respects.

In conclusion, a summary of the recommended safety strategy for the LODOX-Robot machine follows:

- Reduce the momentum of the machine by limiting the speed and the mass of the machine.
- Reduce the power of the robot through the use of a less powerful robot which is still suitable for the system, and investigate torque limiting devices being retro-fitted to the robot.
- Install redundant position and velocity sensors which are monitored by a separate dedicated safety controller. The controller must be able to disable the system at any time safely.
- Reduce the range of motion of the machine as much as possible through the use of mechanical and electrical limiting devices.
- Eradicate all singularities from all possible movements during the programming of the system. Particular vigilance must be taken by the programmer in this regard as they are the most at risk.
- Upgrade the "dead man's handle" to an off-on-off type of device.

- Design and install safety-stops as well as emergency-stops.
- Conduct and update an FMECA for the whole duration of the design and development of the machine.
- Implement all "watchdog sensors" present on the LODOX machine, on the LR machine.
- Install further external sensors such as cameras and accelerometers to detect erratic movement and collisions. These sensors must be monitored by the dedicated safety controller.
- Ensure the machine "fails safely" by anticipating all possible failure scenarios, in particular during a power failure, deactivation of the machine by an emergency-stop and fire.

Chapter 6

Summary

The LODOX machine is an unconventional X-ray system capable of performing conventional radiological scans. It produces high quality full-body images in a digital format and at a lower radiation dosage than conventional X-ray systems. Possibilities exist that the machine may be adapted in order to perform addition types of scans such as Computed Tomography (CT) or scanning for TB. In order for these scans to be possible, the mechanics, electronics and software would need to be upgraded. This project was concerned only with the mechanics of such a machine and how they would have to be redesigned.

Two options exist: first, the mechanics could be redesigned in order to facilitate the required movements of these additional scans; or second, an off-the-shelf industrial robot could become the mechanics of such a system. This project was a feasibility study to assess the suitability of such an option. Three aspects had to be assessed:

- Could an industrial robot physically do the job required? This was addressed through virtual and real simulations.
- Would an industrial robot have accurate enough movements for the proposed system? This was assessed by comparing accuracies of the robot with that of the existing LODOX machine.
- How can an industrial robot be made safe enough to work in a medical environment? Standards, research and risk analysis techniques were studied and/or performed in an attempt to answer this question.

6.1 Cost Implications

A brief investigation into the cost of a LODOX-Robot machine was conducted. The MOTOMAN SK150 robot is discontinued and has been replaced by the MOTOMAN UP165 robot. This model has all the features of the older robot, but with greater Repetitive Positioning accuracy, a larger working envelope, and a larger load carrying capacity (165 kilograms). The cost is R650 000 per robot, with a discount of up to 15% for larger quantities. There would also be further costs for the added safety features required and development of the machine.

In comparison, the mechanical development of the LODOX-LACT machine cost R1 200 000. In addition the price of the mechanics is R420 000 per machine, but larger quantities (50 manufactured per year) would bring the cost price down by half.

6.2 Conclusions

The simulation part of the project was conducted by using MOTOMAN's proprietary simulation software ROTSY, and by constructing a phantom C-arm which was attached to the robot for real simulations. The benefits of off-line simulation compared to on-line programming were noted through the use of the software. In programming a robot job, off-line software was found to be safer, faster and easier to use than on-line programming.

The virtual and physical simulations were very helpful in identifying potential problems of the proposed LODOX-Robot system. These included: the site for attachment to the C-arm would have to be carefully assessed to balance the mass and not obstruct any components; the actual connection between the robot and the C-arm would have to be investigated to reduce possible vibration; the implementation of the off-line program did not always produce the expected movements, this may have been a software or configuration problem; the cabling and tubing on the LODOX machine were not modelled in the simulation software, this issue would have to be addressed for the proposed machine; the weight of the existing C-arm is in excess of what the robot can handle, the C-arm may need to be redesigned to reduce the weight.

In assessing the accuracy of the robot compared to the existing LODOX machine, three types of accuracies were measured: Repetitive Positioning (RP) accuracy, Linear Movement (LM) accuracy and Constant Velocity (CV) accuracy. RP and LM accuracy were measured manually using a theodolite. These two accuracy tests were only conducted on the robot, as it was assumed that the LODOX machine's RP and LM accuracies were perfect. Although the results of the tests to establish RP and LM accuracies of the robot were not accurately quantifiable, they did indicate that the robot was quite accurate in these two respects. However RP accuracy and LM accuracy are of lesser importance than that of CV accuracy, as image quality is negatively affected most by vibration.

CV accuracy was calculated for both the robot and the LODOX machine. This was the most difficult accuracy to measure. Three different methods were undertaken utilising digital cameras, a rotary encoder and accelerometers. The tests run with the accelerometers produced the best results. This was due to the higher resolution and higher sample rate of this method compared to the other two methods. The results of the CV tests undertaken with the accelerometers indicated that there was greater vibration in the movements of the robot. This had been expected, as the robot has more degrees-of-freedom than the LODOX machine, and it is intuitive that with more degrees-of-freedom, there should be greater possibility of error.

The actual values for CV accuracy for the robot and particularly for the LODOX machine were not believable because the linear motor driving the C-arm of the LODOX machine has an accuracy far better than the actual values measured by the accelerometers. This was concluded from the values given for the mean velocity of the C-arm during a normal full-speed scan, which were found to be significantly different to the predicted value. The difference between the measured and the predicted value was many orders of magnitude greater than what the manufacturer of the linear motor in the LODOX machine claimed. Later investigation and research suggested that accelerometers experience drift, which is magnified when integrated to get velocity and position data. Hence the measurements of CV accuracy calculated using the accelerometers were not as informative as was hoped.

In assessing the safety of using an industrial robot such as the MOTOMAN SK150 in a medical environment, many safeguards and safety strategies were suggested. These included: reducing the momentum of the machine, by reducing speed and

mass; reducing the physical power of the robot; installing redundant sensors and control systems; reducing the range of motion of the machine; eradicating dangerous singularities from all robot jobs; upgrading/redesigning the "dead man's handle" and the emergency stop buttons; conducting risk analysis studies such as FMECA throughout the design process of the proposed system; install sensors to detect possible failures; and ensuring that in the event of failure, the machine would always "fail-safely".

The cost of a LODOX-Robot machine would appear to be higher than that of the LODOX-LACT machine. The LODOX-LACT machine is already capable of CT type movements, but it is still fairly restricted in its overall movements. Therefore the higher cost of the LODOX-Robot machine could only be justified by the added flexibility in movements (allowing further types of scans) that it would provide.

6.3 Recommendations

Unfortunately the simulations of CT and TB movements that a possible LODOX-Robot machine may be required to perform were not created. This was due to the loaned hardware key for the ROTSY software being returned to the MOTOMAN agents before all simulations could be completed. If further simulations are to be made, then the software should be purchased from MOTOMAN, or other simulation software should be utilised. Simulation is crucial when working with robots. For the proposed LODOX-Robot machine, the simulation software would be required by the design engineers of the system, and possibly by the clinicians who would run the machine. The design engineers would use the software in many areas of the design process, particulary the safety aspects. It is envisioned that the clinicians using the machine would choose from a database of standard scans, or use the software to design specific scans.

The accuracy of the LODOX machine and the robot need to be further assessed before any proposed LODOX-Robot machine can be designed. This feasibility study could only show that the robot was less accurate than the LODOX machine, but quantitative values could not be calculated because of the testing methods used. In measuring CV accuracy in particular, another testing method must be found that is more accurate and less suspectable to noise than the methods previously used. Perhaps

a purely optical method such as laser-interferometry would be suitable. However, no matter what method is chosen, the effect of vibration (including the type, magnitude and frequency) on the image quality of the LODOX machine must be quantifiably determined and measured. Without this, the CV accuracy is extremely difficult to measure as the range of frequencies recorded has to be as large as possible to include all possible vibrations, which causes subsequent problems when computing the resulting gigantic data files.

The safety of a machine in a medical environment is of paramount importance. If a machine is not totally safe, it will never be approved by the various regulatory bodies. Further work must be done to optimise the safety strategy of using an industrial robot in a medical environment. The strategy must guarantee total fail-safety. Other robot manufacturers who design their robots for medical applications should be approached. In addition the designers of the ACCURAY CyberKnife® should be approached in an effort to ascertain how they made their system safe enough to get FDA approval, as the CyberKnife® is the closest system to the proposed LODOX-Robot system in existence.

A detailed cost analysis of the proposed LODOX-Robot machine should be made. The added value due to the further flexibility of utilising a robot, should be compared to the increased cost of such a system.

This feasibility study found that the use of an industrial robot to be part of a future LODOX machine is possible. However, much more information is needed concerning the accuracy required from such a system, as well as determining which, and what type of industrial robot would be most suitable. The safety issue must also be further investigated and a safety strategy must be further developed. In addition the cost benefits should be thoroughly assessed before the project proceeds any further.

Appendix A

The MOTOMAN-SK150 Industrial Robot

Industrial Robot

MOTOMAN-SK120
MOTOMAN-SK120-150

MOTOMAN-SK120 • MOTOMAN-SK120-150

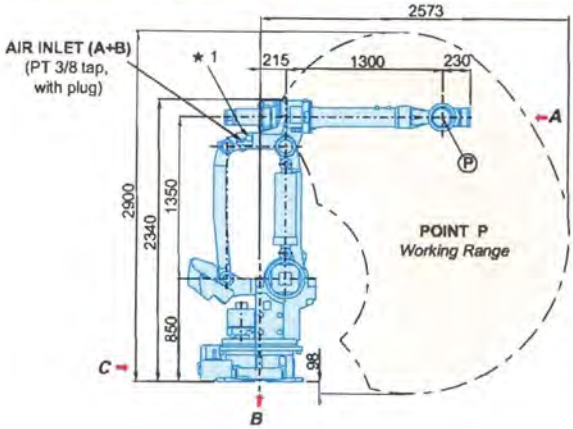

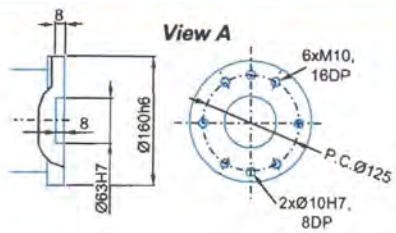

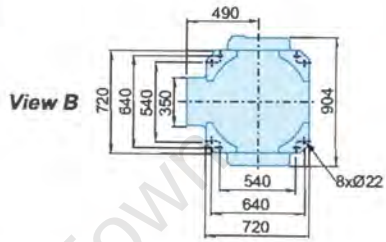

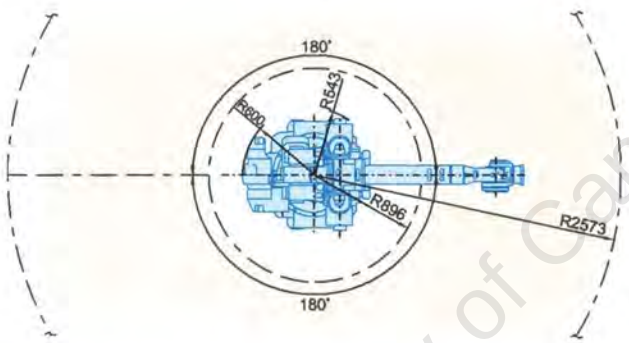

★	Connector type	Plug type (not included)
1	JL05-2A24-28SC	JL05-5A24-28P
2	JL05-2A24-28PC	JL05-6A24-28S

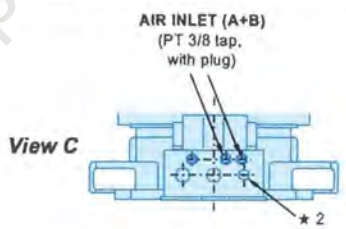

Specifications

		SK-120	SK120-150
Controlled Axes		6	6
Payload		120 kgs	150 kgs
Repetitive Positioning Accuracy		±0.4mm	±0.4mm
Motion Range	S-axis (turning)	±180°	±180°
	L-axis (lower arm)	±70°	±70°
	U-axis (upper arm)	+35°, -115°	+35°, -115°
	R-axis (wrist roll)	±350°	±350°
	B-axis (wrist pitch)	±130°	±130°
	T-axis (wrist twist)	±355°	±355°
Maximum Speed	S-axis	110°/s	100°/s
	L-axis	125°/s	100°/s
	U-axis	125°/s	100°/s
	R-axis	150°/s	125°/s
	B-axis	150°/s	125°/s
	T-axis	250°/s	200°/s

		SK-120	SK120-150
Weight		1500 kgs	1500 kgs
Power Supply		22 kVA	22 kVA
Allowable Moment	R-axis	686Nm (70kgf•m)	833Nm (85kgf•m)
	B-axis	686Nm (70kgf•m)	833Nm (85kgf•m)
	T-axis	392Nm (40kgf•m)	441Nm (45kgf•m)
Allowable Inertia GD²/4	R-axis	42kg•m²	49kg•m²
	B-axis	42kg•m²	49kg•m²
	T-axis	14.5kg•m²	14.5kg•m²
Ambient Conditions	Temperature	0 to 45°C	
	Rel. Humidity	20 to 80% RH	
	Vibration	0.5G or less	
	Others	• IP65 (wrist unit)	
		• Free from excessive electrical noise.	
		• Free from corrosive gas or liquid, or explosive gas.	

Headquarters:
MOTOMAN ROBOTICS AB
Box 504 • S-385 25 Torsås • Sweden
Tel +46-486-10575 • Fax +46-486-41410

Subsidiaries:
MOTOMAN ROBOTICS (UK) LTD
1 Swan Industrial Estate • Banbury • Oxon OX16 8DJ • England
Tel +44-1295 272755 • Fax +44-1295 267127

MOTOMAN ROBOTICS ITALIA s.r.l.
Via Emilia est 1420/16 • I-41100 Modena • Italy
Tel +39-59 280496 • Fax +39-59 280602

MOTOMAN ROBOTICS FRANCE S.A.
Rue Nungesser et Coli • D2A Nantes-Atlantique •
F-44860 St-Aignan-de-Grand-Lieu • France
Tel +33-40 84 09 29 • Fax +33-40 75 41 47

Reg. TF-01-05-94GB

Appendix B

The ANALOG DEVICES ADXL105 Accelerometer

High Accuracy ±1 *g* to ±5 *g* Single Axis *i*MEMS® Accelerometer with Analog Input

ADXL105*

FEATURES
Monolithic IC Chip
2 m*g* Resolution
10 kHz Bandwidth
Flat Amplitude Response (±1%) to 5 kHz
Low Bias and Sensitivity Drift
Low Power 2 mA
Output Ratiometric to Supply
User Scalable *g* Range
On-Board Temperature Sensor
Uncommitted Amplifier
Surface Mount Package
+2.7 V to +5.25 V Single Supply Operation
1000 *g* Shock Survival

APPLICATIONS
Automotive
Accurate Tilt Sensing with Fast Response
Machine Health and Vibration Measurement
Affordable Inertial Sensing of Velocity and Position
Seismic Sensing
Rotational Acceleration

FUNCTIONAL BLOCK DIAGRAM

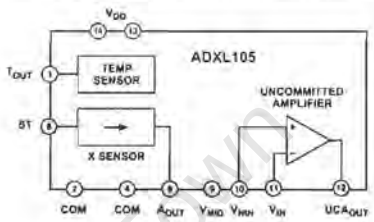

GENERAL DESCRIPTION
The ADXL105 is a high performance, high accuracy and complete single-axis acceleration measurement system on a single monolithic IC. The ADXL105 offers significantly increased bandwidth and reduced noise versus previously available micromachined devices. The ADXL105 measures acceleration with a full-scale range up to ±5 *g* and produces an analog voltage output. Typical noise floor is 225 $\mu g/\sqrt{Hz}$ allowing signals below 2 m*g* to be resolved. A 10 kHz wide frequency response enables vibration measurement applications. The product exhibits significant reduction in offset and sensitivity drift over temperature compared to the ADXL05.

The ADXL105 can measure both dynamic accelerations, (typical of vibration) or static accelerations (such as inertial force, gravity or tilt).

Output scale factors from 250 mV/*g* to 1.5 V/*g* are set using the on-board uncommitted amplifier and external resistors. The device features an on-board temperature sensor with an output of 8 mV/°C for optional temperature compensation of offset vs. temperature for high accuracy application.

The ADXL105 is available in a hermetic 14-lead surface mount Cerpak with versions specified for the 0°C to +70°C, and –40°C to +85°C temperature ranges.

*Patent Pending.
*i*MEMS is a registered trademark of Analog Devices, Inc.

REV. A

One Technology Way, P.O. Box 9106, Norwood, MA 02062-9106, U.S.A.
Tel: 781/329-4700 World Wide Web Site: http://www.analog.com
Fax: 781/326-8703

ADXL105–SPECIFICATIONS ($T_A = T_{MIN}$ to T_{MAX}, T_A = +25°C for J Grade Only, V_S = +5 V, @ Acceleration = 0 *g*, unless otherwise noted)

Parameter	Conditions	ADXL105JJA Min	Typ	Max	Units
SENSOR INPUT					
Measurement Range[1]		±5	±7		*g*
Nonlinearity	Best Fit Straight Line		0.2		% of FS
Alignment Error[2]			±1		Degrees
Cross Axis Sensitivity[3]	Z Axis, @ +25°C		±1	±5	%
SENSITIVITY[4] (Ratiometric)	At A_{OUT}				
Initial		225	250	275	mV/*g*
	V_S = 2.7 V	80	105	120	mV/*g*
vs. Temperature[5, 6]			±0.5		%
ZERO *g* BIAS LEVEL[5] (Ratiometric)	At A_{OUT}				
Zero *g* Offset Error	From +2.5 V Nominal	–625		+625	mV
vs. Supply		–20		+20	mV/V_{DD}/V
vs. Temperature[5, 7]			50		mV
NOISE PERFORMANCE					
Voltage Density[7]	@ +25°C		225	325	$\mu g/\sqrt{Hz}$
Noise in 100 Hz Bandwidth			2.25		mg rms
FREQUENCY RESPONSE					
3 dB Bandwidth		10	12		kHz
Sensor Resonant Frequency		13	18		kHz
TEMP SENSOR[4] (Ratiometric)					
Output Error at +25°C	From +2.5 V Nominal	–100		+100	mV
Nominal Scale Factor			8		mV/°C
Output Impedance			10		kΩ
V_{MID}[4] (Ratiometric)					
Output Error	From +2.5 V Nominal	–15		+15	mV
Output Impedance			10		kΩ
SELF-TEST (Proportional to V_{DD})					
Voltage Delta at A_{OUT}	Self-Test "0" to "1"	100		500	mV
Input Impedance[8]		30	50		kΩ
A_{OUT}					
Output Drive	I = ±50 µA	0.50		V_S – 0.5	V
Capacitive Load Drive		1000			pF
UNCOMMITTED AMPLIFIER					
Initial Offset		–25		+25	mV
Initial Offset vs. Temperature			5		µV/°C
Common-Mode Range		1.0		4.0	V
Input Bias Current[9]			25		nA
Open Loop Gain			100		V/mV
Output Drive	I = ±100 µA	0.25		V_S – 0.25	V
Capacitive Load Drive		1000			pF
POWER SUPPLY					
Operating Voltage Range		2.70		5.25	V
Quiescent Supply Current	At 5.0 V		1.9	2.6	mA
	At 2.7 V		1.3	2.0	mA
Turn-On Time			700		µs
TEMPERATURE RANGE					
Operating Range J		0		+70	°C
Specified Performance A		–40		+85	°C

NOTES

[1]Guaranteed by tests of zero *g* bias, sensitivity and output swing.

[2]Alignment of the X axis is with respect to the long edge of the bottom half of the Cerpak package.

[3]Cross axis sensitivity is measured with an applied acceleration in the Z axis of the device.

[4]This parameter is ratiometric to the supply voltage V_{DD}. Specification is shown with a 5.0 V V_{DD}. To calculate approximate values at another V_{DD}, multiply the specification by V_{DD}/5 V.

[5]Specification refers to the maximum change in parameter from its initial value at +25°C to its worst case value at T_{MIN} to T_{MAX}.

[6]See Figure 3.

[7]See Figure 2.

[8]CMOS and TTL Compatible.

[9]UCA input bias current is tested at final test.

All min and max specifications are guaranteed. Typical specifications are not tested or guaranteed.
Specifications subject to change without notice.

ABSOLUTE MAXIMUM RATINGS*

Acceleration (Any Axis, Unpowered for 0.5 ms) . . . . . 1000 *g*
Acceleration (Any Axis, Powered for 0.5 ms) . . . . . 500 *g*
$+V_S$ . . . . . –0.3 V to +7.0 V
Output Short Circuit Duration
(Any Pin to Common) . . . . . Indefinite
Operating Temperature . . . . . –55°C to +125°C
Storage Temperature . . . . . –65°C to +150°C

*Stresses above those listed under Absolute Maximum Ratings may cause permanent damage to the device. This is a stress rating only; the functional operation of the device at these or any other conditions above those indicated in the operational sections of this specification is not implied. Exposure to absolute maximum rating conditions for extended periods may affect device reliability.

Package Characteristics

Package	θ_{JA}	θ_{JC}	Device Weight
14-Lead Cerpak	110°C/W	30°C/W	<2 Grams

ORDERING GUIDE

Model	Temperature Range	Package Option
ADXL105JQC	0°C to +70°C	QC-14
ADXL105AQC	–40°C to +85°C	QC-14

CAUTION

ESD (electrostatic discharge) sensitive device. Electrostatic charges as high as 4000 V readily accumulate on the human body and test equipment and can discharge without detection. Although the ADXL105 features proprietary ESD protection circuitry, permanent damage may occur on devices subjected to high energy electrostatic discharges. Therefore, proper ESD precautions are recommended to avoid performance degradation or loss of functionality.

Drops onto hard surfaces can cause shocks of greater than 1000 *g* and exceed the absolute maximum rating of the device. Care should be exercised in handling to avoid damage.

PIN FUNCTION DESCRIPTIONS

Pin No.	Name	Description
1	T_{OUT}	Temperature Sensor Output
2, 3, 5	NC	No Connect
4	COM	Common
6	ST	Self-Test
7	COM	Common (Substrate)
8	A_{OUT}	Accelerometer Output
9	V_{MID}	$V_{DD}/2$ Reference Voltage
10	V_{NIN}	Uncommitted Amp Noninverting Input
11	V_{IN}	Uncommitted Amp Inverting Input
12	UCA_{OUT}	Uncommitted Amp Output
13, 14	V_{DD}	Power Supply Voltage

PIN CONFIGURATION

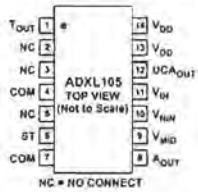

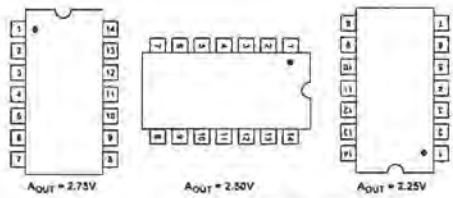

Figure 1. ADXL105 Response Due to Gravity

ADXL105–Typical Performance Characteristics

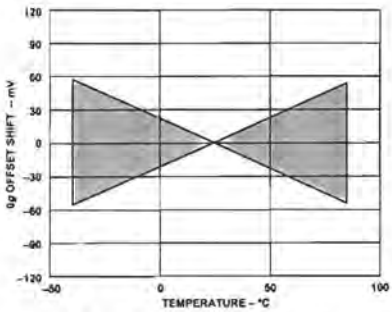

Figure 2. Typical 0 g Shift vs. Temperature*

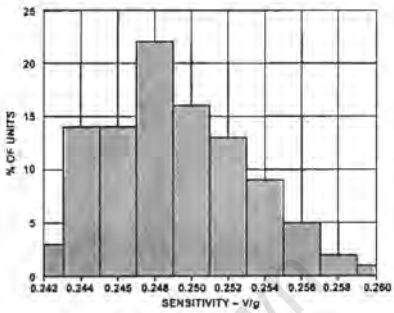

Figure 5. Sensitivity Distribution*

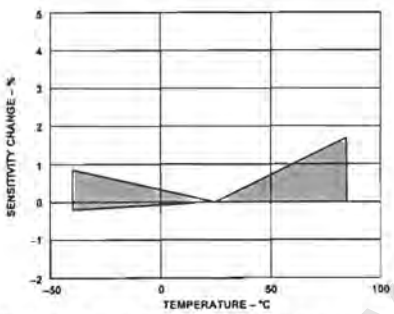

Figure 3. Typical Sensitivity Shift vs. Temperature*

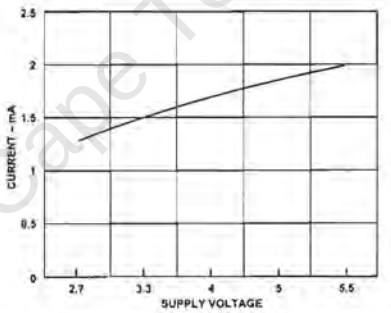

Figure 6. Typical Supply Current vs. Supply Voltage

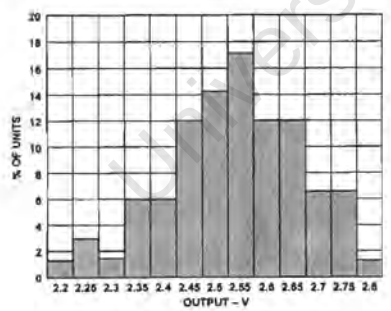

Figure 4. 0 g Output Distribution*

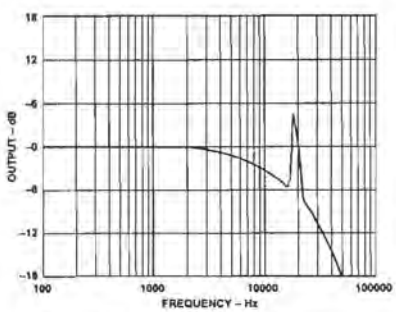

Figure 7. Noise Graph

*Data from several characterization lots.

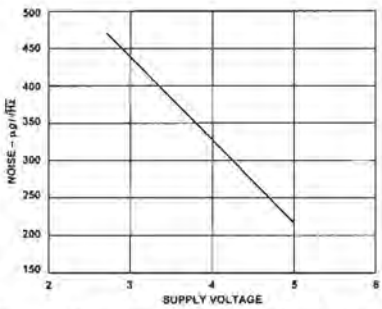

Figure 8. Typical Noise Density vs. Supply Voltage

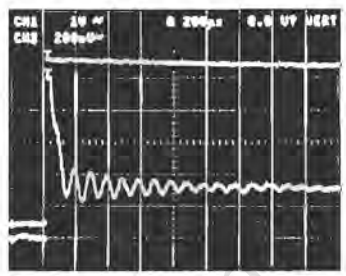

Figure 11. Typical Self-Test Response at V_{DD} = 5 V

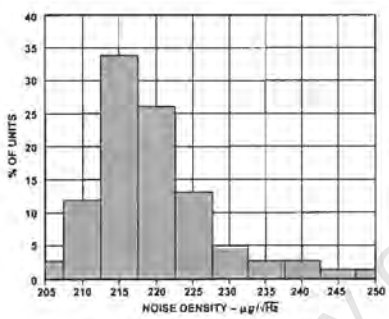

Figure 9. Noise Distribution*

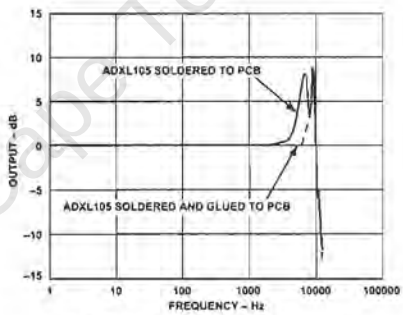

Figure 12. Frequency Response

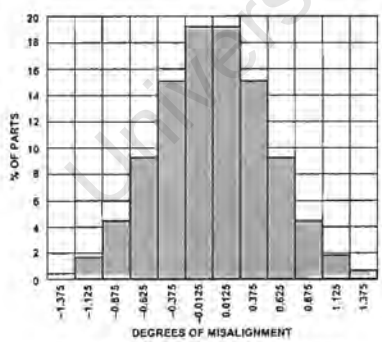

Figure 10. Rotational Die Alignment*

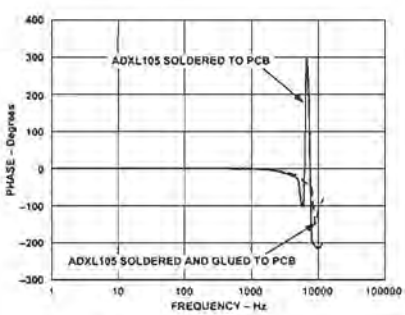

Figure 13. Phase Response

*Data from several characterization lots.

THEORY OF OPERATION

The ADXL105 is a complete acceleration measurement system on a single monolithic IC. It contains a polysilicon surface-micromachined sensor and BiMOS signal conditioning circuitry to implement an open loop acceleration measurement architecture. The ADXL105 is capable of measuring both positive and negative accelerations to a maximum level of ±5 *g*. The accelerometer also measures static acceleration such as gravity, allowing it to be used as a tilt sensor.

The sensor is a surface micromachined polysilicon structure built on top of the silicon wafer. Polysilicon springs suspend the structure over the surface of the wafer and provide a resistance against acceleration-induced forces. Deflection of the structure is measured with a differential capacitor structure that consists of two independent fixed plates and a central plate attached to the moving mass. A 180° out-of-phase square wave drives the fixed plates. An acceleration causing the beam to deflect, will unbalance the differential capacitor resulting in an output square wave whose amplitude is proportional to acceleration. Phase sensitive demodulation techniques are then used to rectify the signal and determine the direction of the acceleration.

An uncommitted amplifier is supplied for setting the output scale factor, filtering and other analog signal processing.

A ratiometric voltage output temperature sensor measures the exact die temperature and can be used for optional calibration of the accelerometer over temperature.

V_{DD}

The ADXL105 has two power supply (V_{DD}) pins, 13 and 14. The two pins should be connected directly together. The output of the ADXL105 is ratiometric to the power supply. Therefore a 0.22 µF decoupling capacitor between V_{DD} and COM is required to reduce power supply noise. To further reduce noise, insert a resistor (and/or a ferrite bead) in series with the V_{DD} pin. See the EMC and Electrical Noise section for more details.

COM

The ADXL105 has two common (COM) pins, 4 and 7. These two pins should be connected directly together and Pin 7 grounded.

ST

The ST pin (Pin 6) controls the self-test feature. When this pin is set to V_{DD}, an electrostatic force is exerted on the beam of the accelerometer causing the beam to move. The change in output resulting from movement of the beam allows the user to test for mechanical and electrical functionality. This pin may be left open-circuit or connected to common in normal use. The self-test input is CMOS and TTL compatible.

A_{OUT}

The accelerometer output (Pin 8) is set to a nominal scale factor of 250 mV/*g* (for V_{DD} = 5 V). Note that A_{OUT} is guaranteed to source/sink a minimum of 50 µA (approximately 50 kΩ output impedance). So a buffer may be required between A_{OUT} and some A-to-D converter inputs.

V_{MID}

V_{MID} is nominally $V_{DD}/2$. It is primarily intended for use as a reference output for the on board uncommitted amplifier (UCA) as shown in Figures 14a and 14b. Its output impedance is approximately 10 kΩ.

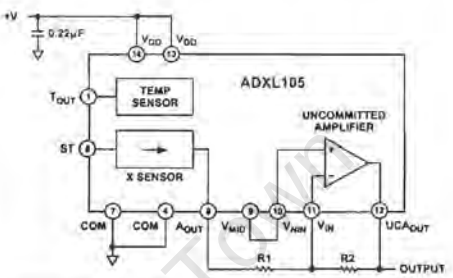

GAIN	SCALE – mV/g	R1	R2
1	250	50kΩ	50kΩ
2	500	50kΩ	100kΩ
3	750	50kΩ	150kΩ
4	1000	50kΩ	200kΩ

a. Using the UCA to Change the Scale Factor

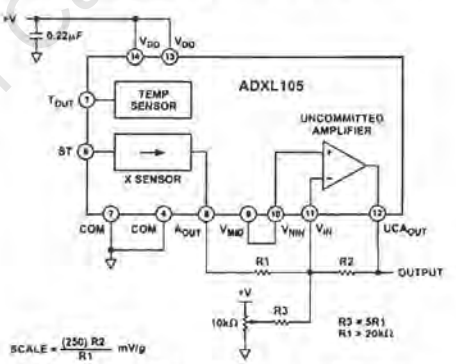

b. Using the UCA to Change the Scale Factor and Zero g Bias

Figure 14. Application Circuit for Increasing Scale Factor

T_{OUT}

The temperature sensor output is nominally 2.5 V at +25°C and typically changes 8 mV/°C, and is optimized for repeatability rather than accuracy. The output is ratiometric with supply voltage.

Uncommitted Amplifier (UCA)

The uncommitted amplifier has a low noise, low drift bipolar front end design. The UCA can be used to change the scale factor of the ADXL105 as shown in Figure 14. The UCA may also be used to add a 1- or 2-pole active filter as shown in Figures 15a through 15d.

Output Scaling

The acceleration output (A_{OUT}) of the ADXL105 is nominally 250 mV/*g*. This scale factor may not be appropriate for all applications. The UCA may be used to increase the scale factor. The simplest implementation would be as shown in Figure 14a. Since the 0 *g* offset of the ADXL105 is 2.5 V ± 625 mV, using a gain of greater than 4 could result in having the UCA output at 0 V or 5 V at 0 *g*. The solution is to add R3 and VR1, as shown in Figure 14b, turning the UCA into a summing amplifier. VR1 is adjusted such that the UCA output is $V_{DD}/2$ at 0 *g*.

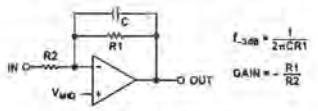

a. 1-Pole Low-Pass Filter

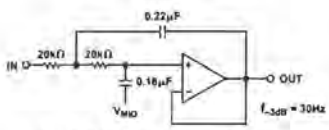

b. 2-Pole Bessel Low-Pass Filter

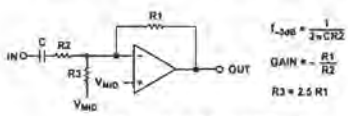

c. 1-Pole High-Pass Filter

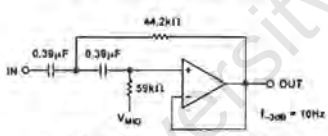

d. 2-Pole Bessel High-Pass Filter

*Figure 15. UCA Used as Active Filters**

Device Bandwidth vs. Resolution

In general the bandwidth selected will determine the noise floor and hence, the measurement resolution (smallest detectable acceleration) of the ADXL105. Since the noise of the ADXL105 has the characteristic of white Gaussian noise that contributes equally at all frequencies, the noise amplitude may be reduced by simply reducing the bandwidth. So the typical noise of the ADXL105 is:

$$Noise\ (rms) = (225\ \mu g/\sqrt{Hz}) \times (\sqrt{Bandwidth \times K})$$

Where

K = 1.6 for a single-pole filter

K = 1.4 for a 2-pole filter

So given a bandwidth of 1000 Hz, the typical rms noise floor of an ADLX105 will be:

Noise = $(225\ \mu g/\sqrt{Hz}) \times (\sqrt{1000 \times 1.6})$

= 9 mg rms for a single-pole filter

and

Noise = $(225\ \mu g/\sqrt{Hz}) \times (\sqrt{1000 \times 1.4})$

= 8.4 mg rms for 2-pole filter

Often the peak value of the noise is desired. Peak-to-peak noise can only be estimated by statistical means. Table I may be used for estimating the probabilities of exceeding various peak values given the rms value. The peak-to-peak noise value will give the best estimate of the uncertainty in a single measurement.

Table I. Estimation of Peak-to-Peak Noise

Nominal Peak-to-Peak Value	% of Time that Noise Will Exceed Peak-to-Peak Value
2 × rms	32%
3 × rms	13%
4 × rms	4.6%
5 × rms	1.2%
6 × rms	0.27%
7 × rms	0.047%
8 × rms	0.0063%

The UCA may be configured to act as an active filter with gain and 0 *g* offset control as shown in Figure 16.

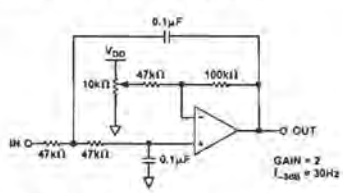

Figure 16. UCA Configured as an Active Low-Pass Filter with Gain and Offset

EMC and Electrical Noise

The design of the ADXL105 is such that EMI or magnetic fields do not normally affect it. Since the ADXL105 is ratiometric, conducted electrical noise on V_{DD} does affect the output. This is particularly true for noise at the ADXL105's internal clock frequency (200 kHz) and its odd harmonics. So maintaining a clean supply voltage is key in preserving the low noise and high resolution properties of the ADXL105.

One way to ensure that V_{DD} contains no high frequency noise is to add an R-C low-pass filter near the V_{DD} pin as shown in Figure 17. Using the component values shown in Figure 17, noise at 200 kHz is attenuated by approximately –23 dB. Assuming the ADXL105 consumes 2 mA, there will be a 100 mV drop across R1. This can be neglected simply by using the ADXL105's V_{DD} as the A-to-D converter's reference voltage as shown in Figure 17.

*For other corner frequencies, consult an active filter handbook.

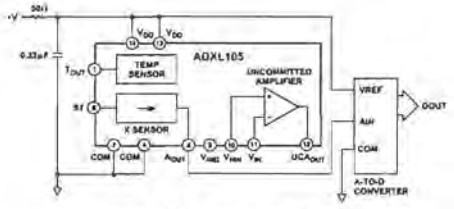

Figure 17. Reducing Noise on V_{DD}

Dynamic Operation
In applications where only dynamic accelerations (vibration) are of interest, it is often best to ac-couple the accelerometer output as shown in Figures 15c and 15d. The advantage of ac coupling is that 0g offset variability (part to part) and drifts are eliminated.

Low Power Operation
The most straightforward method of lowering the ADXL105's power consumption is to minimize its supply voltage. By lowering V_{DD} from 5 V to 2.7 V the power consumption goes from 9.5 mW to 3.5 mW. There may be reasons why lowering the supply voltage is impractical in many applications, in which case the best way to minimize power consumption is by power cycling.

The ADXL105 is capable of turning on and giving an accurate reading within 700 µs (see Figure 18). Most microcontrollers can perform an A-to-D conversion in under 25 µs. So it is practical to turn on the ADXL105 and take a reading in under 750 µs. Given a 100 Hz sample rate the average current required at 2.7 V would be:

$$100\ samples/s \times 750\ \mu s \times 1.3\ mA = 97.5\ \mu A$$

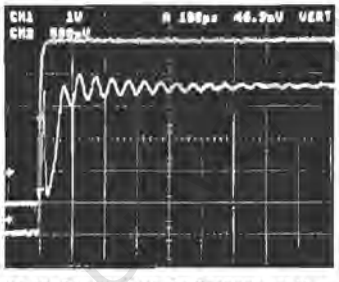

Figure 18. Typical Turn-On Response at V_{DD} = 5 V

Note that if a filter is used in the UCA, sufficient time must be allowed for the settling of the filter as well.

Broadband Operation
The ADXL105 has a number of characteristics that permits operation over a wide frequency range. Its frequency and phase response is essentially flat from dc to 10 kHz (see Figures 12 and 13). Its sensitivity is also constant over temperature (see Figure 3). In contrast, most accelerometers do not have linear response at low frequencies (in many cases, no response at very low frequencies or dc), and often have a large sensitivity temperature coefficient that must be compensated for. In addition, the ADXL105's noise floor is essentially flat from dc to 5 kHz where it gently rolls off (see Figure 7). The beam resonance at 16 kHz can be seen in Figure 7 where there is a small noise peak (+5 dB) at the beam's resonant frequency. There are no other significant noise peaks at any frequency.

The resonant frequency of the beam in the ADXL105 determines its high frequency limit. However the resonant frequency of the Cerpak package is typically around 7 kHz. As a result, it is not unusual to see 6 dB peaks occurring at the package resonant frequency (as shown in Figures 12 and 13). Indeed, the PCB will often have one or more resonant peaks well below 7 kHz. Therefore, if the application calls for accurate operation at or above 6 kHz the ADXL105 should be glued to the PCB in order to eliminate the amplitude response peak due to the package, and careful consideration should be given to the PCB mechanical design.

CALIBRATING THE ADXL105

The initial value of the offset and scale factor for the ADXL105 will require dc calibration for applications such as tilt measurement.

For low *g* applications, the force of gravity is the most stable, accurate and convenient acceleration reference available. An approximate reading of the 0 *g* point can be determined by orienting the device parallel to the Earth's surface and then reading the output. For high accuracy, a calibrated fixture must be used to ensure exact 90 degree orientation to the 1 *g* gravity signal.

An accurate sensitivity calibration method is to make a measurement at +1 *g* and −1 *g*. The sensitivity can be determined by the two measurements. This method has the advantage of being less sensitive to the alignment of the accelerometer because the on axis signal is proportional to the Cosine of the angle. For example, a 5° error in the orientation results in only a 0.4% error in the measurement.

To calibrate, the accelerometer measurement axis is pointed directly at the Earth. The 1 *g* reading is saved and the sensor is turned 180° to measure −1 *g*. Using the two readings and sensitivity is calculated:

$$Sensitivity = [1\ g\ Reading - (-1\ g\ Reading)]/2\ V/g$$

OUTLINE DIMENSIONS

Dimensions shown in inches and (mm).

14-Lead Cerpak
(QC-14)

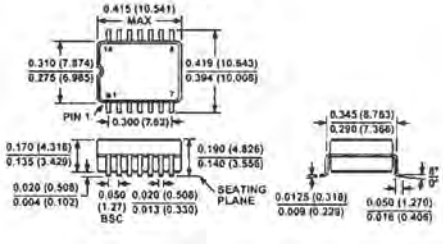

Appendix C

The EAGLE TECHNOLOGY ISA-Bus PC30FA Capture Card

ISA PC-30F/G

12bit Analog Inputs with DIO & D/A

PC-30F/G is an ISA-bus multi-function Analog & Digital I/O board. A variety of models with programmable gain, simultaneous sample and hold, and with or without DACs are available. 16 single ended inputs or 8 differential analog inputs are provided. Gains for each channel can be individually programmed in the board's memory (G, GA, F and FA models).

Programmable gain makes the PC- 30F/G board ideal for measuring low level signals. Throughputs in excess of 330KHz can be achieved using the FIFO buffer on the PC 30F models.Four 12 bit DACs are an optional feature.The PC 30F/G has uniquely flexible digital I/O capabilities consisting of 24 lines in three ports. Each port can be configured as inputs or outputs. Each PC 30F/G also includes a 16 bit Counter Timer used to generate or measure frequency and count events.

Features

- 100kHz or 330kHZ conversion rates
- 8 differential or 16 single-ended inputs
- 12 bit Analog resolution
- Programmable gain
- Simultaneous sample and hold option available
- 4x12-bit Analog outputs with flexible ranges
- 24 Digital I/O lines (3 ports)
- One 16-bit user Counter timer

ORDERING INFORMATION

330K A/D	100K A/D	
PC30FA (4 DACS)	PC30GA (4 DACS)	16 SE or 8 differential inputs
PC30F (no DACS)	PC30G (no DACS)	Gains: 1, 10, 100 and 1000
PC30FAS16 (4 DACS)	PC30GAS16 (4 DACS)	16 Simultaneously sampled
PC30FS16 (no DACS)	PC30GS16 (no DACS)	single ended inputs
PC30FAS4 (4 DACS)	PC30GAS4 (4 DACS)	4 Simultaneously sampled
PC30FS4 (no DACS)	PC30GS4 (no DACS)	and 12 normal SE inputs

Board supplied with: EDR Software, User Manual & PC30MIA or PC30MIA(1:1) (DB50 to IDC50 adaptor's)

Optional Accessories

Accessory Interconnectivity

- Screw Terminal Adaptors
- Application Modules
- Cabling

SPECIFICATIONS

ANALOG INPUTS (A/D)		
Input channels:	16 single-ended, 8 differential	
Resolution:	12bits (1 in 4096)	
Total Sys. Accuracy:	±1 LSB depending on environment	
Linearity	PC 30G	PC 30F
Differential:	±¼ LSB max	±¼ LSB max
Integral:	±0.05% FS	±0.05% FS
Input Ranges:	±5V, ±10V; 0 to 10V (G, GA)	
	±5V, ±10V (F, FA)	
	±5V (S Models)	
Acquisition Rates:	100kHz (G models)	
	330kHz [G<1000] (F models)	
	100kHz [G=1000] (F models)	
Input Impedance:	10GΩ/20pF (On chan)	
	10GΩ/100pF (Off chan)	
Offset voltage:	Adjustable to zero	
Input Gains	(G, GA, F and FA models only):	
Ranges:	1, 10, 100, 1000	
Error:	Adjustable to 0	
Gain Accuracy:	0.25% max, 0.05% typ	
CMRR:	1% max, 0.1% for G=1000	
Monotonicity:	0 to 70°C	
Temperature drift:	6ppm/°C (Full Scale)	
	1ppm/°C (Bipolar Zero)	
	±30ppm/°C(Gain)	
Overvoltage input:	±12V max	
A/D FIFO buffer:	16 samples	
Acquisition Modes:	Polled I/O, Interrupts, Single and Dual channel DMA	
ANALOG OUTPUTS		
No. of Channels:	4	
Resolution:	4 x 12bit	
Accuracy:	±1 LSB (12bit)	
Diff Non-linearity:	½ LSB max	
Output Ranges:	±5V, ±10V, 0 to 10V, 0 to 13V	
Throughput Rate:	100kHz	
Offset Error:	Unipolar: ¼ LSB typ, 1 LSB (max)	
	Bipolar: ½ LSB typ, 2 LSB (max)	
Gain ranges:	x1, x2	
Settling time:	10mS max in load 500pF, 2kΩ	
Max current output:	5mA	
DIGITAL I/O		
No of TTL I/O lines:	24 in 3 ports (8255 PPI)	
Counter/Timers		
Resolution:	16 bits	
Frequency:	2 or 8 MHz (for A/D)	
No of counters:	3 (2 used for A/D conversion)	
PC Interface		
Base Address:	0 to 1FE0h	
No of registers:	32x 8bit	
Interrupts:	IRQ2 to IRQ15	
DMA:	Dual DMA levels 5, 6 or 7	
Environmental / Physical		
Operating Temperature:	0 to 90°C	
Board Dimensions:	193mm x 111mm	
Power Requirements		
+5V:	500mA typ	
±12V:	100mA typ	

Appendix D

The MATLAB Accelerometer Data Analysis Code

```
% BEGIN PROGRAM
%%%%%%%%%%%%%%%%%%%%%%%%%%%%%%%%%%%%%%%%%%%%%%%%%%%%%%%%%%%%%%%%%%%%%%%%%%%%
clear all

% SET PRINTING PREFFERENCES
%%%%%%%%%%%%%%%%%%%%%%%%%%%%%%%%%%%%%%%%%%%%%%%%%%%%%%%%%%%%%%%%%%%%%%%%%%%%
set(0,'DefaultFigurePaperOrientation','landscape')
set(0,'DefaultFigurePaperUnits','centimeters')
set(0,'DefaultFigurePaperType','A4')

% LOAD CALIBRATION FILES
%%%%%%%%%%%%%%%%%%%%%%%%%%%%%%%%%%%%%%%%%%%%%%%%%%%%%%%%%%%%%%%%%%%%%%%%%%%%
load up.txt;
load down.txt;
posg = (up(:,1));
negg = (down(:,1));

% APPLY SCALE FACTOR
%%%%%%%%%%%%%%%%%%%%%%%%%%%%%%%%%%%%%%%%%%%%%%%%%%%%%%%%%%%%%%%%%%%%%%%%%%%%
scale = (-(mean(posg)-mean(negg))/2)/9.80665;

% LOAD CAPTURED DATA FILE
%%%%%%%%%%%%%%%%%%%%%%%%%%%%%%%%%%%%%%%%%%%%%%%%%%%%%%%%%%%%%%%%%%%%%%%%%%%%
temp = input('Enter DATA file name: ','s');
disp('loading DATA file...');
filename = load(temp);
sample_rate = 333333.344;
sample_time = 10;
no_of_samples = sample_rate * sample_time;
no_of_samples = round(no_of_samples);

acc = filename(:,1);
accM = mean(acc);
acceleration = (acc - accM)/scale;
```

```
% FILTER ACCELERATION
%%%%%%%%%%%%%%%%%%%%%%%%%%%%%%%%%%%%%%%%%%%%%%%%%%%%%%%%%%%%%%%%%%%%%%%%%%%%%%%%
disp('filtering...');
[b,a] = butter(5,150/(sample_rate/2),'low');
accF = filter(b, a, acc);
accFM = mean(accF);
accelerationF = (accF - accFM)/scale;

% CALCULATE VELOCITY BY INTEGRATION
%%%%%%%%%%%%%%%%%%%%%%%%%%%%%%%%%%%%%%%%%%%%%%%%%%%%%%%%%%%%%%%%%%%%%%%%%%%%%%%%
disp('calculating velocity...');
tempv = acceleration(2:no_of_samples);
diffv = tempv - acceleration(1:(no_of_samples - 1));
vel = (diffv./2 + acceleration(1:(no_of_samples - 1)))*(1/sample_rate);
old_velocity = cumsum(vel);
posv = [1:3:no_of_samples];%make the file smaller by taking every 3rd sample
velocity = old_velocity(posv,:);

% CALCULATE DISPLACEMENT BY INTEGRATION AGAIN
%%%%%%%%%%%%%%%%%%%%%%%%%%%%%%%%%%%%%%%%%%%%%%%%%%%%%%%%%%%%%%%%%%%%%%%%%%%%%%%%
disp('calculating displacement...');
tempd = old_velocity(2:no_of_samples - 1);
diffd = tempd - old_velocity(1:(no_of_samples - 2));
dis = (diffd./2 + old_velocity(1:(no_of_samples - 2)))*(1/sample_rate);
old_displacement = cumsum(dis);
posd = [1:3:no_of_samples];%make the file smaller by taking every 3rd sample
displacement = old_displacement(posd,:);

% CLEAR MEMORY
%%%%%%%%%%%%%%%%%%%%%%%%%%%%%%%%%%%%%%%%%%%%%%%%%%%%%%%%%%%%%%%%%%%%%%%%%%%%%%%%
disp('clearing memory...');
clear a
clear acc
clear accF
clear accFM
```

```
clear accM
clear b
clear diffd
clear diffv
clear dis
clear down
clear filename
clear negg
clear no_of_samples
clear old_displacement
clear old_velocity
clear posd
clear posg
clear posv
clear sample_rate
clear sample_time
clear scale
clear temp
clear tempd
clear tempv
clear up
clear vel
clear acceleration
clear accelerationF
disp('memory cleared!');

% PLOTTING
%%%%%%%%%%%%%%%%%%%%%%%%%%%%%%%%%%%%%%%%%%%%%%%%%%%%%%%%%%%%%%%%%%%%%%%%%%%%%%%
disp('plotting...')
figure;
plot(accelerationF)
figure;
plot(velocity)
figure;
plot(displacement)
```

```
% END PROGRAM
%%%%%%%%%%%%%%%%%%%%%%%%%%%%%%%%%%%%%%%%%%%%%%%%%%%%%%%%%%%%%%%%%%%%%%%%%%%%%%%%%%%
```

Appendix E

The LabVIEW Accelerometer Data Analysis Virtual Instrument (VI)

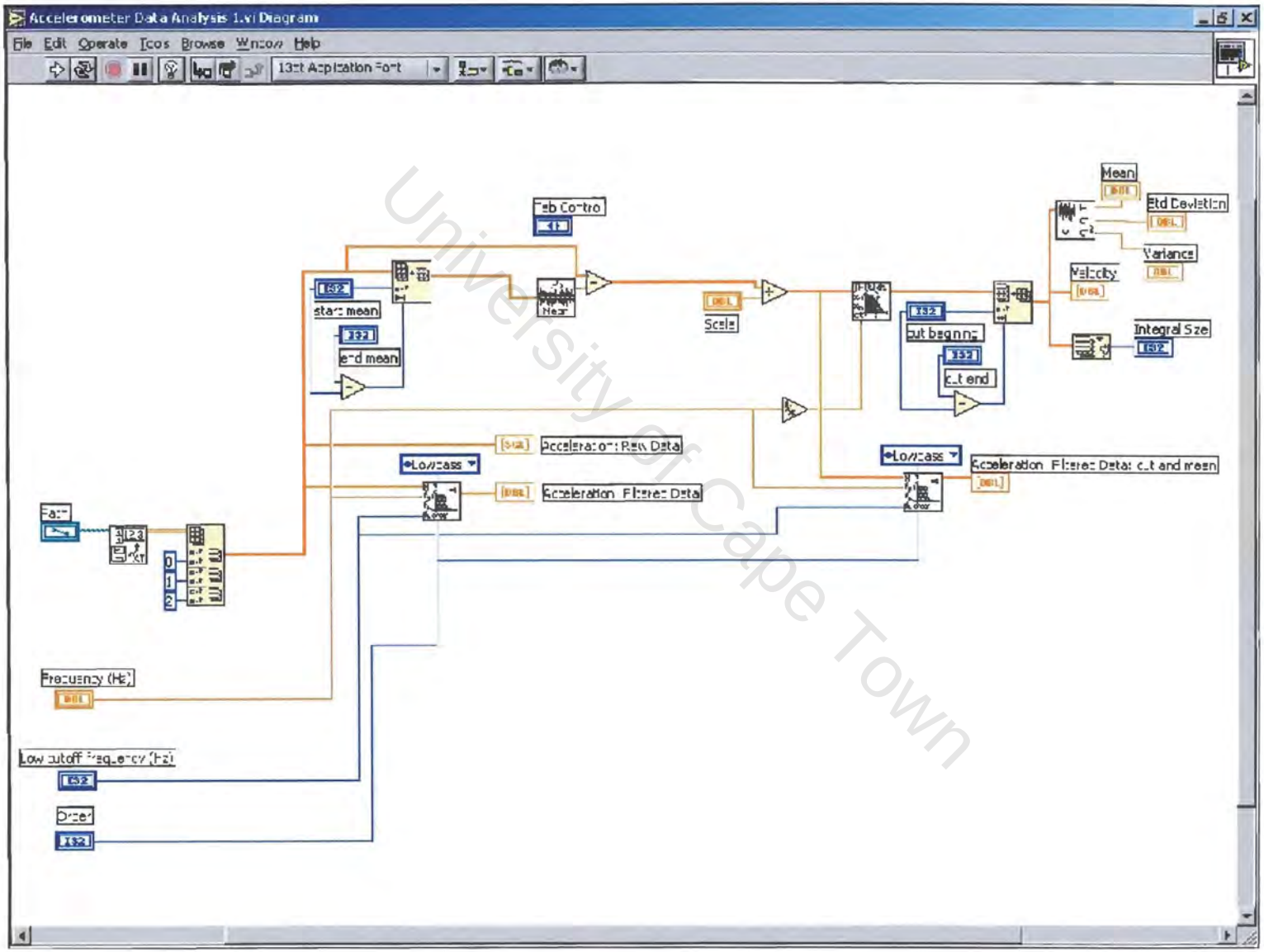

Figure E.1: The circuit diagram of the LABVIEW Accelerometer Data Analysis Virtual Instrument

Read From Spreadsheet File.vi

Reads a specified number of lines or rows from a numeric text file beginning at a specified character offset and converts the data to a 2D, single-precision array of numbers.

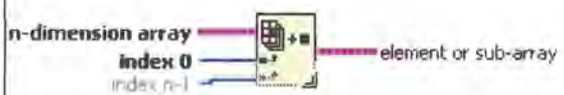

Index Array

Returns an element or subarray of array at index. Leaving an index unwired will slice out a cross-section of the array along that dimension.
The function will automatically resize to show one index per input array dimension, but you may resize by hand to show more outputs to access multiple elements in one operation. If all indices for the second or subsequent outputs are unwired, function will auto-increment the indices for the previous output in a sensible manner.

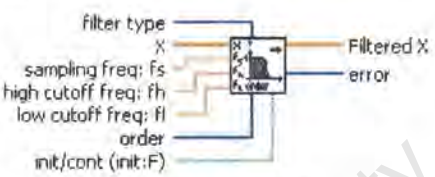

Butterworth Filter.vi

Generates a digital Butterworth filter using the **sampling frequency**, **low cutoff frequency**, **high cutoff frequency**, **order**, and **filter type** by calling the Butterworth Coefficients VI.

Integral x(t).vi

Performs the discrete integration of the sampled signal **X**.

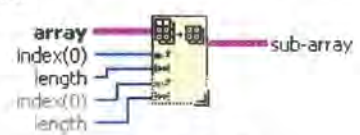

Array Subset

Returns a portion of array starting at index and containing length elements. Array can be an n-dimensional array of any type. Function will automatically resize to contain as many index/length inputs as dimensions in array.

Subtract

Computes the difference of the inputs. Works on numbers, arrays of numbers, clusters of numbers, arrays of clusters of numbers, and so on.

Divide

Computes the quotient of the inputs. Works on numbers, arrays of numbers, clusters of numbers, arrays of clusters of numbers, and so on.

Reciprocal

Divides 1 by the input value. Returns Infinity if x=0. Works on numbers, arrays of numbers, clusters of numbers, arrays of clusters of numbers, and so on.

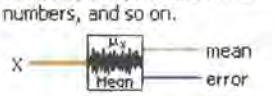

Mean.vi

Computes the mean (average) (μ) of the values in the input sequence **X**.

Array Size

Returns the number of elements in each dimension of input. Input can be an n-dimensional array of any type.

Standard Deviation and Variance [Std Deviation and Variance.vi]

Computes the **mean** value (mu), **standard deviation**, and **variance** of the values in the input sequence X. **Weighting** is used to specify whether X represents the entire population of data or only a sample. The values are computed using the following formulas:
mean = Sum (X[i])/n, where n is the number of elements in X.
variance = ((X[i] - mean)^2)/w where w is n for population and (n-1) for sample.
standard deviation = sqrt (variance).

Figure E.2: The legend for the LABVIEW Accelerometer Data Analysis Virtual Instrument

Appendix F

The Failure Modes, Effects & Criticality Analysis (FMECA) Conducted On The LODOX-LACT Machine

LODOX-LACT FAILURE MODES, EFFECTS \& CRITICALITY ANALYSIS

IDENT. No.	ITEM/ FUNCTIONAL IDENT.	FAILURE MODE	FAILURE CAUSE	FAILURE EFFECT	TARGET	RISK ASSESSMENT			ACTION REQUIRED/REMARKS
						SEV	PROB	Risk Code	
IC	**Image Capture**								
IC-01	*Patient Interface*								
IC-01-01	Trolley								
IC-01-01-01	Height Adjustable Frame	Clinician unable to raise the frame	Clinician not strong and/or tall enough	Require another taller/stronger person to assist	R	E	2		
		Release lever jammed	Mechanism seized or worn	Unable to perform Trendelenburg or lateral scans	R	E	4		
		Frame lowers erroneously with patient on it	Too low gas pressure in cylinder, seals worn, patient too heavy	Blurred image captured, patient would have to be rescanned	R P	E	4		
		Frame drops suddenly when release lever is pulled	Loss in gas pressure from cylinder, patient too heavy	Possible patient or clinician injury, equipment damage	P C M	C	4		
IC-01-01-02	Tabletop	Slips out of locating pockets	Rough handling during Trendelenburg procedure; excessive wear-and tear or loose locating bolts of the upright supports	Patient falls which may lead to injury	P	C	3		
IC-01-01-03	Mattress	Cracks/breaks/bends	Bad manufacturing; mishandeling	Possible injury to patient and/or clinician	P C	C	4		
		Patient uncomfortable	Mattress compressed from overuse	Possible patient movement during scan, hence possible bad image quality	P R	E	4		
		Mattress fabric tawn/cut	Wear and tear, carelessness	Fluid absorbed into mattress, possible cross-contamination	M P	E	3		
IC-01-02	Trolley Location (On ASP)								
IC-01-02-01	TLA Frame								
IC-01-02-02	Trolley Mechanical Location	Difficult to align trolley with TLA	If the arm of the TLA with the flat location point is docked first with the trolley, there can be misallignment for the other end	Only one position sensor detects the trolley, hence system inoperable	R	E	2		
IC-01-02-03	Trolley Clamping	Trolley does not clamp to TLA	Electromagnets not functioning, wiring, hardware problem	Position sensor does not detect trolley, hence system inoperable	R	E	4		
IC-01-02-04	CMC Feedback	Trolley is not detected when in correct position	Position sensor hardware or wiring problem	System inoperable	R	E	4		

Figure F.1: FMECA Of The Patient Interface Of The LODOX-LACT Machine

SEVERITY	
CODE	DESCRIPTION
A	Multiple Fatality and/or > R10 000 000
B	Fatality and/or R1 000 000 - R10 000 000
C	Reportable Injury and/or R100 000 - R1 000 000
D	Injury and/or R10 000 - R100 000
E	Minor Injury and/or < R10 000

PROBABILITY	
CODE	DESCRIPTION
1	Once per week
2	Once per month
3	Once per year
4	Once in 10 years
5	Once in 100 years

TARGET	
CODE	DESCRIPTION
P	Patient
C	Clinician/s
R	Productivity
M	Machine
E	Environment
D	Data

Figure F.2: Legend For The FMECA Of The LODOX-LACT Machine

Bibliography

Adler, J., Murphy, M., Chang, S., Hancock, S., 1999. Image-guided robotic radiosurgery. *Neurosurgery* 44 (6), 1299–1306.

American National Standards Institute/Robotic Industries Association, 1999. *Safety Requirements for Industrial Robots and Robot Systems*. R15.06 ed.

Asimov, I., 1942. Runaround. *Astounding Stories/Science Fiction* , 94–103.

Baowei, F., Ng, W., Chauhan, S., Kwoh, C., 2001. The safety issues of medical robotics. *Reliability Engineering and System Safety* 73, 183–192.

Busnel, M., Cammoun, R., 1999. The robotized workstation 'MASTER' for users with tetraplegia: Description and evaluation. *Journal of Rehabilitation Research & Development* 36 (3), 217–230.

Clarke, R., 1994. Asimov's Laws of Robotics, Implications for Information Technology: Part 2. *IEEE Computer* 27 (1), 57–66.

Davies, B., 2000. A review of robotics in surgery. *Proceedings of the Institute of Mechanical Engineering* 214 (1), 129–140.

DEBTECH, 2002. *Technical High Level Risk Assessment On Lodox X-ray Equipment*. Tech. Rep. Q02-200000-704, De Beers.

Deery, J., 1997. Courier robot keeps hospital staff 'on the job'. *Journal for healthcare quality : official publication of the National Association for Healthcare Quality* 19 (1), 22–23.

Dijkers, P., deBear, P., 1991. Patient and staff acceptance of robotic technology in occupational therapy: A pilot study. *Journal of Rehabilitation Research & Development* 28 (2), 33–45.

DULLIER, 2002. History of robotics and robots. Last accessed 21 February 2002.
URL http://www.geocities.com/Eureka/7331/hrorobot.htm

Fryman, J., 2002. New thinking in machinery sfeguarding strategy. Last accessed 19 February 2002.
URL http://www.roboticsonline.com/index.cfm?weburl=/public/articles/articledetails.cfm?id=666

Giakas, G., 2001. GGPSA–Automatic Filtering software. Last accessed 01 December 2001.
URL http://www.hop.man.ac.uk/satru/giannis/

Giakas, G., Baltzopoulos, V., 1997a. A comparison of automatic filtering techniques applied to biomedical walking data. *Journal of Biomechanics* 30 (8), 847–850.

Giakas, G., Baltzopoulos, V., 1997b. A comparison of automatic filtering techniques applied to biomedical walking data. *Journal of Biomechanics* 30 (8), 851–855.

Graves, S., Holman, B., Rossetti, M., Estey, C., Felder, R., 1998. Robotic automation of coagulation analysis. *Clinica Chimica Acta* 278, 269–279.

Hague, T., Marchant, J., Tillett, N., 2000. Ground based sensing systems for autonomous agricultural vehicles. *Computers and Electronics in Agriculture* 25, 11–28.

Hoffmann, G., 1998. Concepts for third generation of laboratory systems. *Clinica Chimica Acta* 278, 203–216.

IFR, 2001. Robots by type. Last accessed 19 October 2001.
URL http://prime.jsc.nasa.gov/ROV/history.html

Kassel, N., Graves, B., Downs, J., 1997. Telepresence in neurosurgery: the integrated remote neurosurgical system. *Studies in health technology and informatics* 39, 411–419.

Krebs, H., Volpe, B., Aisen, M., Hogan, N., 2000. Increasing productivity and quality of care: Robot-aided neuro-rehabilitation. *Journal of Rehabilitation Research & Development* 37 (6), 639–653.

Kwon, W., Roh, K., Baek, S., Lee, S., 2001. Robots for minimally invasive surgery: Review and new vision interface development. In: M. Mokhtari (Ed.), *Integration of*

Assistive Technology in the Information Age, IOS Press, vol. 9 of *Assistive Technology Research Series*, pp. 101–108.

Lob, W., 1990. Robotic transportation. *Clinical chemistry* 36 (9), 1544–1550.

Lueth, T., Bier, J., 1999. Robot assisted intervention in surgery. In: J. Gilsbach, H. Stiehl (Eds.), *Neuronavigation–Neurosurgical and Computer Scientific Aspects*, Springer–Verlag.

Mifflin, T., Estey, C., Felder, R., 2000. Robotic automation performs a nested RT-PCR analysis for HCV without introducing sample contamination. *Clinica Chimica Acta* 290, 199–211.

Mohr, R., 1994. *Failure Modes And Effects Analysis*. Tech. Rep. 8th Edition, Sverdrup.

Motoman, 1996. *ERC and MRC Controller–ROTSY User's Manual*. Motoman Inc, 805 Liberty Lane, West Carrollton, Ohio 45449.

Ng, W., Tan, C., 1996. On safety enhancements for medical robots. *Reliability Engineering and System Safety* 54, 35–45.

Pierrot, F., Dombre, E., Dégoulange, E., Urbain, L., Caron, P., Boudet, S., Gariépy, J., Mégnien, J., 1999. Hippocrate: a safe robot arm for medical applications with force feedback. *Medical Image Analysis* 3 (3), 285–300.

Prouskas, C., Oakman, A., 1996. Medical robotics. Last accessed 22 October 2001. URL `http://www.doc.ic.ac.uk/~nd/surprise_96/journal/vol4/ao2/report.html`

Quayle, C., 1996. Robot for hire. *Health Facilities Management* 9 (4), 18–24.

Regalbuto, M., Krouskop, T., 1992. Toward a practical mobile robotic aid system for people with severe physical disabilities. *Journal of Rehabilitation Research & Development* 29 (1), 19–27.

ROver Ranch, 2001. A short history of robots. Last accessed 19 October 2001. URL `http://prime.jsc.nasa.gov/ROV/history.html`

Schweikard, A., 1997. Resolution–complete inverse treatment planning in radiosurgery. In: H. Lemke, M. Vannier, K. Inamura (Eds.), *Proceedings of Computer Assisted Radiology*, Elsevier Science, Amsterdam.

Tsotsos, J., Verghese, G., Dickinson, S., Jenkin, M., Jepson, A., Milios, E., Nuflo, F., Stevenson, S., Black, M., Metaxas, D., Culhane, S., Ye, Y., Mann, R., 1998. A visually-guided robot for physically disabled children. *Image and Vision Computing* 16 (4), 275–292.

United States Coast Guard, 2002. *Failure Modes and Effects Analysis (FMEA)*, vol. 3 Procedures for Assessing Risks—Applying Risk Assessment Tools of *Risk-based Decision-making Guidelines*, chap. 9. Last accessed 27 January 2002.
URL `http://www.uscg.mil/hq/g-m/risk/e-guidelines/html/`

United States Department of Defense, 1980. *Military Standard Proceedures For Performing A Failure Mode, Effects And Criticality Analysis*. Washington DC, 20301, mil-std-1629a ed.

U.S. Department of Labor, Occupational Safety & Health Administration, 1981. *Occupational Safety and Health Standards, Electrical, General requirements. - 1910.303*. Occupational Safety & Health Administration, 200 Constitution Avenue, NW, Washington, DC 20210, 1910th ed.

Varley, P., 1999. Techniques for development of safety-related software for surgical robots. *IEEE Transcripts on Information Technology in Biomedicine* 3 (4), 261–270.